W-AM-Sym1 INTERACTIONS BETWEEN COMPONENTS IN THE PHOTOSYNTHETIC REACTION CENTER FROM RHODOPSEUDOMONAS VIRIDIS. H. Michel, J. Deisenhofer, K.A. Weyer, O. Epp, K. Miki and F. Lottspeich, Max-Planck-Institut für Biochemie, D-8033 Martinsried, West Germany

The photosynthetic reaction center from the purple bacterium Rhodopseudomonas viridis, a complex consisting of four protein subunits (H M, L and a cytochrome) and various pigments, has been crystallized (Michel, J. Mol. Biol. 158, 567-572 (1982)). The subsequent structure analysis yielded the arrangement of the chromophores (Deisenhofer et al., J. Mol. Biol. 180, 385-398 (1984)) and the folding of the protein subunits. The amino acid sequences of all four protein subunits have been determined and incorporated into the atomic model. The L- and M subunits form the central core of the reaction center. They possess five membrane spanning helices each and bind the photosynthetic pigments in a symmetric manner. The H subunit is anchored to the membrane by a membrane spanning aminoterminal helix. It possesses a globular domain at the cytoplasmic side and is bound to the L- and M subunits mainly by salt bridges and hydrogen bonds. The cytochrome is bound to the L-, M- and H subunitfrom the periplasmic side, again mainly by polar interactions. The bacteriochlorophylls and bacteriopheophytins fit tightly into hydrophobic pockets of the L- and M-subunits. Only a minor part of the oxygen atoms of the chlorophylls and pheophytins undergo hydrogen bonds with the protein. These however seem to be important for the energetics and direction of the electron flow.

W-AM-Sym2 PROTEIN/DNA INTERACTIONS IN THREE DIMENSIONS: CRYSTALLOGRAPHIC STUDIES OF REPRESSOR/OPERATOR COMPLEXES. S. C. Harrison, J. Anderson, C. Wolberger, and A. Aggarwal. Department of Biochemistry and Molecular Biology, Harvard University, Cambridge, MA 02138.

The crystal structure of a repressor protein bound to its operator DNA shows in detail the interactions that mediate sequence-specific binding (Anderson et al., 1984; Anderson et al., 1985). The protein is the amino-terminal domain of the repressor encoded by coliphage 434, and the DNA is a 14 base pair synthetic oligonucleotide with a sequence representing the consensus of six binding sites in the phage genome. The DNA comformation is B-like, with some deviation at the ends of the fragment. The repressor domain contains a helix-turn-helix structure, similar to the motif found in the repressor and cro proteins of phage λ and in the catobolite activator protein of E. coli. The second helix in this motif (α3) lies in the major groove of the DNA fragment, and the other helix (α2) lies across it. There are a number of important contacts between the repressor and the DNA backbone, as well as major-groove contacts between α3 side chains and DNA bases. Crystals of two related complexes (the amino terminal domain of 434 repressor with a variant DNA and the cro protein of phage 434 with the original 14 mer) are being studied to answer questions raised by the first structure. The presentation will focus on the basis of sequence-specific protein/DNA interactions, as revealed by the crystallographic results.

W-AM-Sym3 **THE THREE-DIMENSIONAL STRUCTURE OF ANTIBODIES,** Roberto J. Poljak
Département d'Immunologie, Institut Pasteur 75724 Paris Cedex 15, France.

X-ray diffraction studies of immunoglobulins, their light (L) chains and their fragments (Fab, Fc, pFc') have established that: 1) globular three-dimensional domains correspond to the homology regions of the amino acid (a.a.) sequences; 2) the folding of the polypeptide chain is basically repeated in each homology region or domain, a folding which appears to be shared by proteins such as the major histocompatibility antigens, the antigen receptor of T cells, and others; 3) there is intrasegmental flexibility in Fab fragments; 4) highly conserved a.a. residues account for the permuted associations of different L chains with different heavy (H) chains which contributes to antibody diversity; 5) hypervariable regions of L and H chains determine the conformation of the antigen combining site of antibodies, thus somatic recombination variable region gene segments maximize variation and functional diversity of antibodies.

The determination of the three-dimensional structure of a complex between the Fab fragment of a monoclonal anti-lysozyme antibody (D1.3) and its antigen, lysozyme (Amit et al., Nature 313, 156, 1985) has shown: 1) that the contacts between antigen and antibody take place over a large area involving the six complementarity determining regions of the antibody, and at least two segments of about 10 a.a. each which are in spatial proximity but not contiguous in the linear a.a. sequence of the antigen; 2) that no gross conformational changes are observed in the antigen and 3) that the model explains the failure of monoclonal antibody D1.3 to recognize and complex with related avian lysozymes in which a.a. variations occur at position 19, 21 and 121. Progress in the determination of the high resolution structure of this complex will be reviewed.

W-AM-Sym4 STRUCTURE, FUNCTION AND EVOLUTION OF HUMAN RHINOVIRUS 14. Michael G. Rossmann[1], Edward Arnold[1], James P. Griffith[1], Greg Kamer[1], Ming Luo[1], Anne G. Mosser[2], Ann C. Palmenberg[2], Roland R. Rueckert[2], Barbara Sherry[2] and Gerrit Vriend[1]. [1]Department of Biological Sciences, Purdue University, W. Lafayette, Indiana 47907 and [2]Biophysics Lab, University of Wisconsin, 1525 Linden Drive, Madison, Wisconsin 53706.

The structure of human rhinovirus 14 (HRV14) has been determined in three dimensions to atomic detail. The course of all four capsid polypeptides has been traced and correlated with the known amino acid sequences. The tertiary structures of the three larger proteins (VP1, VP2 and VP3) are each strikingly similar to those of the known icosahedral plant viruses, as is also their quaternary organization in the virus coat. Four neutralizing immunogenic regions have been identified by sequencing mutants selected for their ability to survive in the presence of neutralizing antibodies. The altered amino acids, as well as corresponding antigenic sequence in the homologous polio and foot-and-mouth disease viruses, reside on protrusions. A large cleft spanning the center of each icosahedral face, is most probably the host cell receptor binding site. The carboxy end of VP4 (the small internal coat protein) is very close to Ser 10 of VP2, providing the basis for the autocatalytic cleavage of VP0 during maturation of the virus. The intertwining of VP0, VP1 and VP3 shows the nature of the 6S and 12S protomeric assembly units and perhaps a basis for the steps in their post-translational cleavage. The evolution of picornaviruses and RNA viruses can be assessed on the basis of sequence and structural alignments. Conserved amino acids important in protein folding and viral function can be recognized.

W-AM-A1 INACTIVATION OF SODIUM CURRENTS IN BULLFROG SYMPATHETIC NEURONS. Stephen W. Jones, Department of Neurobiology and Behavior, SUNY at Stony Brook, Stony Brook, NY 11794.

Neurons dissociated from paravertebral sympathetic ganglia of bullfrogs have voltage-sensitive sodium currents similar to those of other preparations (e. g. squid and frog axons) except that activation and inactivation are shifted to positive potentials by ~30 mV (Soc. Neurosci. Abstr., 11:314,1985). The kinetics of inactivation of the sodium current have been investigated further, using a discontinuous single electrode voltage clamp, switching at 30-50 kHz, with 1-2 MΩ patch electrodes containing cesium, at room temperature.

Macroscopic inactivation, during maintained depolarizations or following prepulses, becomes more rapid with increasing depolarization above -20 mV. The time course of inactivation is not well fit by a single exponential; ½ inactivation times were ~10 msec at -20 mV and ~1 msec at +10.

Recovery from inactivation (see Fig.) becomes more rapid with hyperpolarization below -30 mV; ½ recovery requires ~10 msec at -30 mV and ~2 msec at -80 mV.

Long conditioning depolarizations reveal a very slow inactivation process, with ½ times for inactivation and recovery of several seconds.

Supported by NIH grants NS20751 to SWJ and NS18579 to Dr. Paul R. Adams.

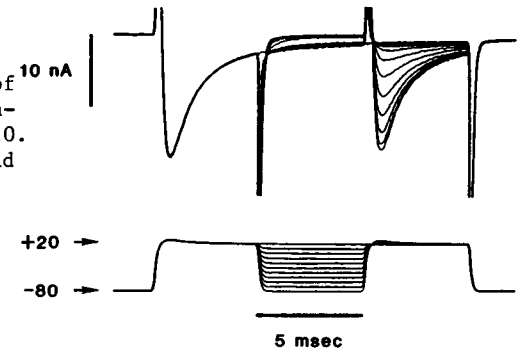

W-AM-A2 TEMPERATURE DEPENDENCE OF SODIUM CHANNEL KINETICS IN RABBIT AND FROG MUSCLE MEMBRANES. G. E. Kirsch and J. S. Sykes. Department of Biological Sciences, Rutgers University, New Brunswick, New Jersey 08903.

The effect of temperature (0 to 22 deg. C) on the kinetics of sodium (Na) channel conductance was determined in voltage-clamped rabbit and frog skeletal muscle fibers using the triple vaseline gap technique. The Hodgkin-Huxley model was used to extract kinetic parameters; the time course of the conductance change during step depolarization followed m^3h kinetics. Arrhenius plots of activation time constants (tau m), determined at both moderate (-10 to -20 mV) and high (+100 mV) depolarizations, were linear in both types of muscle. In rabbit muscle, Arrhenius plots of the inactivation time constant (tau h) were markedly non-linear at +100 mV, but much less so at -20 mV. The opposite effect was observed in frog muscle. The contrast between the highly non-linear Arrhenius plot of tau h at +100 mV in rabbit muscle compared with that of frog muscle, was interpreted as revealing an intrinsic non-linearity in the temperature dependence of mammalian muscle Na inactivation. These results are consistent with the notion that mammalian cell membranes undergo thermotropic membrane phase transitions which alter lipid-channel interactions in the 0 to 22 deg. C range. Furthermore, the observation that Na channel activation appears to be resistant to this effect suggests that the gating mechanisms which govern activation and inactivation reside in physically distinct regions of the channel. Supported by NIH NS17710.

W-AM-A3 SODIUM GATING CURRENTS WITHOUT RISING PHASE: EVIDENCE FROM POTASSIUM CURRENTS. Stimers, J. R., Bezanilla, F., Taylor, R. E., Webb, C. Dept. Physiology, University of California, Los Angeles, CA 90024 and Lab. Biophysics, NINCDS, NIH, Bethesda, MD 20205.

Internally perfused, voltage clamped squid axons from Loligo pealei were used to record both Na gating currents and K currents. We have previously shown that making the external solution hyperosmotic eliminates the rising phase of the Na gating currents and the slow component of the capacity transient (Biophys. J. 45:12a). We suggested that the hyperosmotic solution was expanding the Frankenhaeuser-Hodgkin (F-H) space. To test this, we looked at the accumulation and washout of K from the F-H space. The rate of washout of K was measured by first loading the space using a long prepulse to +50 mV. A test pulse was applied at various times after the prepulse and the tail currents were recorded at two potentials, -30 and -80 mV. From this data we could calculate the reversal potential for K as a function of time. We found that the reversal potential recovers with a time constant of 31±6 ms for normal solutions and 42±11 ms for hyperosmotic solution. From the intercepts of these data at time 0 we obtain a ratio of increase in the F-H space thickness by a factor of 2.5±0.6 in hyperosmotic solution. K accumulation was determined by measuring reversal potentials following a variable duration pulse to +50 mV. We found the accumulation of K was quite variable but was always much less in hyperosmotic solution. In these experiments we estimated that the F-H space thickness increased by a factor of 5±2 in hyperosmotic solution. From this we conclude that hyperosmotic solution increased the F-H space thickness and that the Na gating current rises in less than 10 μs. Research was supported by USPHS grant #GM30376 and NIH Fellowship to JRS.

W-AM-A4 **FURTHER CHARACTERIZATION OF THE KINETIC COMPONENTS OF SODIUM INACTIVATION IN CRAYFISH GIANT AXONS.** M. D. Rayner and J. G. Starkus. Department of Physiology and Bekesy Laboratory of Neurobiology, 1993 East West Rd., Honolulu, HI. 96822.

The enzymes pronase and trypsin, as well as the group specific protein reagent NBA, have classically been used to separate activation from fast inactivation. Although these agents remove fast inactivation, slow inactivation remains relatively unaffected. We have therefore used these agents to investigate the relationship between (a) the 4 kinetically-determinable components of inactivation in crayfish giant axons and (b) the enzymatically-separable fast and slow inactivation processes. Enzyme-insensitive reactions (i.e. slow inactivation) might be expected to become increasingly dominant in macroscopic sodium currents following exposure to such agents. By contrast enzyme-sensitive reactions (i.e. fast inactivation) would be expected to become less significant. Additionally the total number of available thermodynamic states, and hence the number of observed eigenvalues, might well be affected by enzyme action.

Our results demonstrate that the zero time intercepts of the two slower inactivation components are increased in a dose dependent manner by all three agents, while the intercepts of the two faster components are reduced. These results indicate that slow inactivation kinetics can be detected within individual sodium current transients.

Supported by NIH grants NS17202 and NS21151, Hawaii Heart Association, and BRSG.

W-AM-A5 DYNAMIC TRANSIENTS AND STEADY STATES OF GATING CURRENT. Adelman, W. J. and Fohlmeister, J. F., Lab. of Biophysics, NINCDS, NIH at the Marine Biological Lab, Woods Hole, MA 02543, and Lab of Neurophysiology, Univ. of Minnesota, Minneapolis, MN 55455.

Gating current records were obtained in sinusoidally driven dynamic steady states (c.f. Biophys. J. 48, pp. 375-390) and as dynamic transients for axons with intact sodium inactivation gating. The dominant non-linearity in dynamic steady state records is a bimodal distribution of the current within a single period of the command sine wave. The presence of inactivation gating selectively reduces the amplitude of one peak (previously associated with the so-called primary activation kinetics). The secondary activation kinetics are unaffected. The harmonic content is consistent with a mechanism of steric hindrance imposed by inactivation on specific kinetic transitions of the primary activation gating process.

Dynamic transients were measured as temporal changes in the harmonic content of the gating current records due to the developing inactivation that follows depolarizing voltage steps from a holding potential of -80 mV. The sine wave generator was triggered simultaneously with the depolarizing voltage step, and segments of the resulting gating current records of precisely one period of the command sinusoid in length were extracted with the starting point of consecutive segments advanced in time by 100 μs. The time dependence of the harmonic content given by these segments could be fit by exponentials with a single time constant, τ = 8 ms (8°C), that is independent of the mean depolarization. This value reflects the slowest transition rate involved in inactivation gating. Dynamic transients associated with inactivation gating were absent in protease treated axons.

W-AM-A6 A THIRD DIMENSION IN SODIUM CHANNEL GATING KINETICS. Fohlmeister, J. F. and Adelman, W. J., Lab of Neurophysiology, Univ. of Minnesota, Minneapolis, MN 55455, and Lab of Biophysics, NINCDS, NIH at the Marine Biological Lab, Woods Hole, MA 02543.

The principal consequence of our dynamic analysis of gating currents is the addition of a new dimension to the sodium channel gating process, namely that of the secondary activation gating. The figure gives the full gating kinetics as a three-dimensional diagram that satisfies the dynamic data and encompasses earlier results (Armstrong, Gilly, J. gen. Physiol. 74, 691). The three processes are mechanistically coupled with the secondary kinetics responding principally to a population shift between the two most distant primary kinetic states along the diagonal axis. Inactivation, and primary activation gating are coupled by a reciprocal steric hindrance mechanism. The secondary activation kinetics address a number of earlier difficulties with channel gating including the single channel flicker problem raised for K-channels (Conti and Neher, Nature 285, 140), and the suggestion (Armstrong, Physiol. Rev. 61, 644) that the transition to an open activation gate involves a greater charge movement than kinetic transitions among the closed activation gating states (Biophys.J. 48, 391). A molecular gating model based on the amino acid residue sequence (Noda et al, Nature 312, 121) has been constructed.

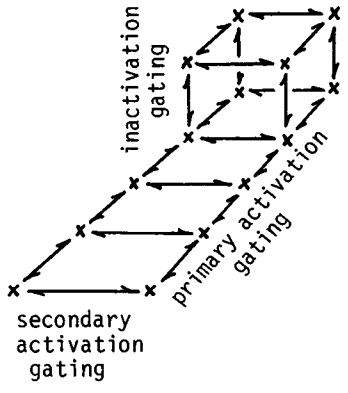

W-AM-A7 CONCENTRATION CHANGES AT SODIUM CHANNELS DUE TO OSCILLATING ELECTRIC FIELDS

M. BLANK and J.N. BLANK, Dept. of Physiology and Cellular Biophysics, Columbia University, 630 W. 168 St., New York, NY 10032

The Surface Compartment Model (SCM) of membrane transport, derived from first principles, takes into account ionic processes in the electrical double layers of membranes. A voltage gated channel is included as a voltage dependent permeability, and under voltage clamp, the SCM yields the currents shown by either sodium or potassium channels of squid axon. The SCM can account for the apparent selectivity of the two channels on the basis of the difference in the gating currents. We have applied oscillating voltages to the sodium channel model and obtained ion concentration changes that are frequency dependent. The greatest changes are in those concentrations that normally control the activity of the ion pump, internal sodium and external potassium, and the optimal frequency for a fast gating (sodium) channel is 200 Hz. These results indicate that:

(a) The ionic currents in excitable membranes can be described by electrodiffusion theory;
(b) the selectivity of an ionic channel is due to the kinetics of channel opening;
(c) the transient ion concentration changes due to oscillating electric fields provide the outline of a physical mechanism for the functioning of "ion pumps."

(Supported by ONR Contract N00014-83-K-0043).

W-AM-A8 MACROSCOPIC Na CURRENTS WITH GIGAOHM SEALS ON mRNA-INJECTED XENOPUS OOCYTES.

J. Leonard, T. Snutch, H. Lubbert, N. Davidson, and H. A. Lester, Divs. of Biology & Chemistry, Caltech, Pasadena 91125

Stage V and VI oocytes were removed from ovaries, then exposed to collagenase for 3 h which (a) removed the surrounding follicular cells and (b) improved sealing. After washing, some oocytes were injected with 70 nl (50 ng) poly-A^+ mRNA isolated from brains of 14-16 day old rats, then incubated for 2-3 days. Oocytes then were exposed to hypertonic saline for 30 min; the plasma membrane shrank away from the vitteline membrane, which was then manually stripped away. Large diameter patch pipettes (20-30 μm tip, ~250 kΩ) were fire polished, coated with Sylgard, and used to form gigaohm seals enclosing up to 600 μm^2 of the surface. A standard virtual-ground circuit was used for voltage-clamp studies on the fast inward Na current induced by brain RNA. The capacitance was fully charged within < 0.3 ms following a voltage jump. Maximal inward currents varied widely in amplitude among patches (0.1 to 3.4 $pA/\mu m^2$). The I-V curves usually peaked at -10 to 0 mV. h_{inf} curves showed 50% inactivation at -60 mV. The inward currents were not affected by Ca-free saline or by 100 μM Cd^{2+}. The transient inward currents were followed at more depolarized voltages by a long-lasting outward current of comparable amplitude. The outward currents are presumably carried by K^+ but are not completely blocked by tetraethylammonium and 3,4-diaminopyridine. RNA inducing the outward currents can be fractionated away from that inducing the Na currents. The "big patch" method should allow analysis of currents which are too fast to be resolved using the standard 2-electrode voltage-clamp of these very large (1 mm) cells. Supported by NS-11756, GM-10991, and fellowships from AHA and DFG.

W-AM-A9 STRUCTURAL MODEL OF THE SODIUM CHANNEL BASED ON ITS SEQUENCE

H. Robert Guy and P. Seetharamulu, Lab. Mathematical Biology, NCI,NIH, Bethesda MD 20892

Secondary and tertiary structural models of sodium channel transmembrane segments were developed from its recently determined primary sequence in Electrophorus electricus. The models have four homologous domains and each domain has eight homologous transmembrane segments, S1 through S8. In all models the first part of each domain contains three relatively apolar α helices (S1, S2, and S3) followed by a transmembrane α helix (S4) with positively charged residues, mainly arginines, at every third residue. These positively charged side chains form salt bridges with negatively charged side chains near the ends of S1 and S3 and with negatively charged segments (S7) that cross part of the membrane and are α helices in the first three domains and is a β strand in the last domain. The putative channel lining is formed by alternating positively charged S4 segments and negatively charged S7 segments. S7 segments are preceded by an apolar segment (S6) postulated to form short α helices in the first three domains and a β strand in the last domain. Each domain also contains two very apolar segments, S5 and S8 . Alternative models with different numbers of potential N-glycosylation sites on the extracellular surface can be constructed by giving these very apolar segments either transmembrane α helical or β hairpen conformations or by orienting the transmembrane segments different ways in different domains. Putative extracellular segments that contains five of the ten potential N-glycosylation sites link S5 to S6. An additional N-glycosylated transmembrane β hairpen may be formed by a segment near the COOH-terminal. Channel activation may involve a 'helical screw' mechanism in which S4 helices rotate around their axes as they move toward the extracellular surface.

W-AM-A10 THE SPATIAL DISTRIBUTION OF SODIUM CHANNELS IS ALTERED BY FERTILIZATION IN THE EGG OF THE ASCIDIAN Boltenia villosa. Rita E. Hice and William J. Moody, Department of Zoology, University of Washington, Seattle, Washington 98195.

Ion channel types are differentially distributed among developmentally-committed cell types. Ion channels can also have non-random spatial distributions within a single cell. To investigate when asymmetries in ion channel distributions arise during embryonic development, we examined the spatial distributions of voltage-sensitive ion channels in an ascidian egg before and after fertilization. In the ascidian egg, fertilization initiates a sequence of cortical contractions and cytoplasmic movements that segregate cell lineage determinates to specific regions of the uncleaved egg. Using the two-microelectrode voltage clamp technique, we have identified 3 major voltage-dependent currents in the Boltenia egg: a transient inward Na current (peak at -30mV), a transient inward Ca current (peak at +10mV), and an inwardly rectifying K current. Spatial distributions of these currents were examined by two-microelectrode voltage clamp of paired animal and vegetal half-cells (merogones) made surgically from both unfertilized and fertilized eggs. All currents are randomly distributed between the animal and vegetal hemispheres of the unfertilized egg. Na current density increased two-fold in the animal vs. the vegetal hemisphere within 30 min. after fertilization, while K and Ca current distributions along this axis remained random. Contained within the vegetal hemisphere of the fertilized egg is the presumptive muscle, a tissue which in the larva lacks Na channels. These results show that voltage-dependent ionic currents are randomly distributed in the mature oocyte and that Na current distribution is altered concurrently with an early stage of cytoplasmic segregation of cell lineage determinates in the fertilized Boltenia egg.

W-AM-A11 REGIONALIZATION AND LATERAL MOBILITY OF NA CHANNELS IN NERVE AND MUSCLE, Kimon Angelides, Department of Neuroscience, University of Florida, Gainesville, FL, 32610.

On cultured neurons Na+ channels are localized to morphologically distinct regions. Fluorescent neurotoxin probes specific for the Na+ channel stain the initial segment 10-times more intensely than the cell body and demonstrate punctate fluorescence confined to the hillock regions compared to the more diffuse labeling observed in the cell body. Using fluorescence recovery after photobleaching (FPR) we measured the lateral diffusion and mobile fraction of Na+ channels at specific regions of the neuron. We found that nearly all Na+ channels within the cell body are free to diffuse, while 80% of the channels located at the hillock and presynaptic terminal are immobile on the time-scale of the measurement. During the maturation of the neuron, the plasma membrane differentiates and segregates the Na+ channel into local compartments and maintains this localization by either direct cytoskeletal attachments or by segregation of the cytoskeletal framework of the axon.

We have used a laser microbeam and FPR to elucidate the topograhical distribution and lateral mobility of Na+ channels on myotubes and at specific sites on myotubes innervated by spinal cord neurons. On myotubes Na+ channels are dispersed and undergo rapid lateral diffusion. Mapping of Na+ channel topography on spinal cord/muscle co-cultures shows a very steep concentration gradient that decreases two-fold within 20μm of the endplate, and that Na+ channels co-localize with AchR. FRP measurements show that near the endplate all channels are immobile on the FPR timescale while 200 μm from the endplate the mobile fraction reaches 40%. During the events of muscle maturation and motoneuron innervation Na+ channels are segregated in the sarcolemma and may be trapped at the sites of nerve contact. Supported by the NIH (NS 18268).

W-AM-A12 **SELECTIVE DIFFERENTIATION OF MOUSE NEUROBLASTOMA CELLS CAN BE USED TO EXPRESS TWO DIFFERENT SUBTYPES OF SODIUM CHANNEL.** R.B. Rogart, E. Geller, and V.B. Sapirstein (Intro. by A. Scanu). Dept. of Neuroscience, Children's Hospital; Dept. of Medicine, Brigham and Women's Hospital; Dept. of Biochemistry, E.K. Shriver Center; Harvard Medical School, Boston, MA

The action potential (AP) in most excitable preparations is blocked by nM concentrations of the neurotoxins saxitoxin (STX) and tetrodotoxin (TTX). In some excitable tissues lacking mature innervation, a toxin-resistant Na dependent AP has been reported. We demonstrate here that NB2a neuroblastoma cells can selectively express Na channel(CH) subtypes with either "high-" or "low-affinity" ^{3}STX binding sites, depending upon conditions of differentiation.

We hypothesized that: (1) axonal processes should have "high-affinity" NaCH like most nerve; and (2) dendritic processes should have "low-affinity" NaCH, since dendrites (prior to synapse formation) are uninnervated post-synaptic membrane. Mouse NB2a cells were selected for development of neurites which morphologically appear as dendrites (DEN) or axons (AX), and binding of ^{3}H-STX was measured. Control NB2a cells showed a single specific "high-affinity" component of toxin uptake with Kd=0.2-0.3 nM, and maximum specific uptake (MH) of 5.0 fmole/mg wet. At 3-days, AX cells showed a specific "high-affinity" component of ^{3}H-STX binding with M_H=9.9 fmole/mg wet (2X control); DEN cells showed two specific components of ^{3}H-STX uptake: (1) one "high-affinity" component with M_H=5.0 fmole/mg wet; (2) a second "low-affinity" component with K_L=12 nM and M_H= 5.3 fmole/mg wet. These studies (1) indicate that NB2a cells selected for neurite growth can selectively express either NaCH with "high-affinity" or "low-affinity" ^{3}H-STX receptors. (2) pharmacologically confirm the morphological identification of axonal and dendritic neurites.

W-AM-B1 SHORTENING DEPENDENT DECLINE IN FORCE REDEVELOPMENT RATES OF SMOOTH MUSCLE. P.F. Dillon, Depts. of Physiology and Radiology, Michigan State Univ., E. Lansing, MI, 48823.

Maximum shortening velocities determined by an isometric release to zero load (Vus) assume a constant contractile velocity throughout the slack period. This assumption was tested by releasing strips of rabbit smooth muscle stimulated for 2 min with 1 micromolar carbachol from different lengths to a common length and allowing them to redevelop tension (ΔL = 2-10% Lo). At every tension common to separate redevelopments, the muscle which had the shorter release always had a higher rate of force redevelopment, despite having a common stimulus, duration of stimulus, length and tension. This dependence of rate on the magnitude of release and redevelopment time occured at lengths of 0.75, 1.0 and 1.2 Ls, the length where the passive tension reaches zero. It also occured when strips were released from a common length to different, shorter lengths. The slowing of force redevelopment may be due to transfer of phosphorylated crossbridges from detached positions, available for cycling, to attached, holding positions. Latchbridges responsible for maintaining isometric tension will be broken during filament translation, so that force maintained during translation must be the responsibility of phosporylated bridges. When rates decline at a common tension, there are fewer available cycling bridges and a lower force per attached bridge. If this occurs at zero load, the Vus will underestimate the true maximum velocity. Supported by NIH AM 34885.

W-AM-B2 THE EFFECT OF EXTRACELLULAR $[Ca^{2+}]_o$ ON SHORTENING VELOCITY IN SINGLE ISOLATED SMOOTH MUSCLE CELLS. David M. Warshaw, Physiology & Biophysics, Univ. of Vermont, Burlington, VT 05405

Correlation of smooth muscle shortening velocity (V) with myosin light chain phosphorylation (Murphy et al., 1983) and $[Ca^{2+}]_o$ (Siegman et al., 1984; Paul et al., 1983; Arner and Hellstrand, 1985) may reflect modulation of crossbridge cycling. These effects were observed in whole tissue and may be complicated by the multicellular interactions. Thus the effect of $[Ca^{2+}]_o$ (low (0.18mM) and normal (1.8mM)) on V was studied at the cellular level using single smooth muscle cells isolated from the toad (Bufo marinus) stomach muscularis. Cells were attached to a force transducer and length displacement device at 20°C. At the peak of isometric contraction (Fmax) cells were subjected to either a series of isotonic shortenings (0.05-0.90Fmax) to determine force:velocity relationships (F:V) or isometric releases in cell length (0.05-0.30Lcell) for slack test determinations of maximum V (Vmax). F:V data were analyzed using a linearized form of the Hill equation to estimate Vmax. Vmax from F:V data were 0.11 and 0.41Lcell/s in low and normal $[Ca^{2+}]_o$, respectively, although no differences in a/Fmax (0.29 vs. 0.21) were observed. These Vmax data agree with values determined by the slack test in both low (0.19+0.09(se)Lcell/s, n=4) and normal (0.39+0.11(se)Lcell/s, n=3) $[Ca^{2+}]_o$. Therefore a 10X increase in $[Ca^{2+}]_o$ results in a 2-4X increase in Vmax. Since Vmax may be rate limited by crossbridge detachment (Eisenberg et al., 1980), Ca^{2+} may exert its effect either directly or through a secondary biochemical modification of the crossbridge thus in turn affecting detachment. Alternatively, Ca^{2+} may affect the surrounding contractile protein environment thus creating an internal load. (Supported by NIH AM34872)

W-AM-B3 DETECTION OF MYOSIN ISOZYMES IN NON-PREGNANT AND PREGNANT HUMAN UTERINE SMOOTH MUSCLE AND COMPARISON OF THEIR SPEED OF SHORTENING. Lema MJ, Striz S, Ostheimer GW, Julian FJ. Brigham & Women's Hospital, Dept. Anesthesia Research Laboratories, Boston, MA.

Recent evidence suggests the existence of three myosin isozymes in embryonic chicken gizzard (Takano-Ohmuro et al., J. Biochem. 93:930, 1983) and two myosin isozymes in rabbit aorta, intestine, uterus, and human aorta, saphenous vein (Pagani et al. Biophys J. 47:301a, 1985, Lema et al., Circ Res. submitted). Since human uterus undergoes both hypertrophic and hyperplastic changes during pregnancy, studies were conducted on surgically obtained human non-pregnant and pregnant uterine smooth muscle to determine 1) if either or both contain myosin isozymes, 2) if any differences in isozymic patterns exist and 3) if there are any differences in their speed of shortening. Myosin extracts were prepared and analyzed by pyrophosphate gel electrophoresis (Pagani ED, Julian FJ; Circ. Res. 54:586, 1984). Both non-pregnant and pregnant uterine myosin displayed two bands. In all (6) non-pregnant uterine samples tested, the slower migrating isozyme (SM1) stained with greater intensity than the faster migrating isozyme (SM2), while in all (5) pregnant uterine samples the staining intensity of SM1 and SM2 appeared identical. Analysis of the the isozymes by SDS gel electrophoresis detected one heavy chain and two light chains (20,000 and 17,000 daltons). Smooth muscle bundles were dissected, connected to a force transducer and servo-motor and the velocity of shortening was measured. Data from 3 pregnant and 5 non-pregnant samples suggest that the extrapolated value for V_{max}, the unloaded speed of shortening, is greater for pregnant tissue which appears to correlate with the greater proportion of SM2 detected. Supported by the Parker B. Francis Investigatorship Award (MJL) and NIH grant HL35032 (FJJ).

W-AM-B4 DIFFERENT PHOSPHORYLATED FORMS OF MYOSIN IN CONTRACTING TRACHEAL SMOOTH MUSCLE. A. Persechini, K.E. Kamm, and J.T. Stull, Department of Pharmacology and Moss Heart Center, University of Texas Health Science Center at Dallas, Dallas, TX 75235.

A method for separating non-, mono-, and diphosphorylated myosins from smooth muscle tissue extracts has been developed and their relationship to contraction has been explored. Extracts of quick-frozen, electrically stimulated bovine trachealis strips were analyzed by nondenaturing PAGE in the presence of pyrophosphate. Three different myosin bands were visualized, designated M, MP, and MP2. Immunoblots showed that M, MP, and MP2 reacted with antisera against purified trachealis myosin P-light chain. An additional band which may be filamin (M_r = 240K by SDS-PAGE) did not react. The extent of P-light chain phosphorylation for each myosin band was estimated in gel slices by urea/glycerol PAGE, and values were 0.20 (M), 0.60 (MP), and 1.0 (MP2) mol phosphate/mol P-light chain. Values for P-light chain phosphorylation in tissue samples measured by urea/glycerol PAGE (Pmeas) were essentially identical to values calculated (Pcalc) from the relative amounts of M, MP, and MP2 which we have concluded are non-, mono-, and diphosphorylated myosin. After 2.5 sec of stimulation, Pmeas and MP2 were maximal at 0.63 ± 0.06 mol phosphate/mol P-light chain and 0.40 ± 0.06 mol MP2/mol myosin, respectively. Control strips had no detectible MP or MP2, and Pmeas was 0.02 ± 0.01 mol phosphate/mol P-light chain. The relationship between MP2 and Pmeas or Pcalc was consistent with a random phosphorylation mechanism. There was a linear correlation (r = 0.94) between the amount of MP2 and force measured at 1.0, 1.5, 2.0, and 2.5 sec. Thus, rapid, initial force development was associated with doubly phosphorylated myosin. (Supported, in part, by HL32607, HL26043, and HL07360)

W-AM-B5 **Mg^{2+} IS REQUIRED FOR MYOSIN LIGHT CHAIN KINASE (MLCK) ACTIVITY BUT NOT ACTIN-MYOSIN INTERACTION IN "CHEMICALLY SKINNED" GUINEA PIG TAENIA COLI SMOOTH MUSCLE.** **Richard J. Paul, John D. Strauss, Claudia Zeugner, and J. Caspar Rüegg, Depts. of Physiology, University of Cincinnati (45267-0576) and University of Heidelberg (FRG).**

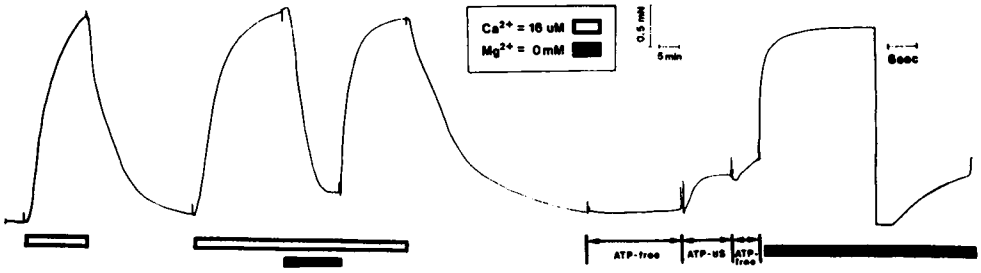

Solutions are described in Circ. Res. 53:342. Mg^{2+}-free solutions elicit a rapid relaxation in the presence of Ca^{2+}. Neither Ca^{2+} nor Mg^{2+} are required for contraction following thiophosphorylation. Far right side shows the force response to a rapid decrease in length (20%); note time scale change. Myosin phosphorylation was 53.1±6.5% (n=5) at the plateau of the Ca^{2+}-induced contraction in the presence of Mg^{2+} and declined to negligible levels after transfer to nominally Mg^{2+}-free solutions. These results indicate: (1) Mg^{2+} is required for MLCK but not actin-myosin interaction; (2) Mg^{2+} is not required for myosin phosphatase activity; (3) Any Ca^{2+}-regulatory mechanism(s) in addition to MLCK requires Mg^{2+}. Supported by NIH 22619, DAAD and AHA EI (RJP).

W-AM-B6 TWO-SITE PHOSPHORYLATION OF THE 20,000 DALTON MYOSIN LIGHT CHAIN OF GLYCERINATED PORCINE CAROTID ARTERY SMOOTH MUSCLE Joe R. Haeberle and Brett A. Trockman, Dept. of Physiology-Biophysics and Medicine, Indiana Univ. Sch. Med., Indianapolis, IN 46223

Two-site phosphorylation of isolated chicken gizzard myosin is now well documented. Nishikawa et al. (J.Biol.Chem., 259:8808, 1984) have reported that protein kinase C and myosin light chain kinase catalyze the phosphorylation of two unique sites on the 20,000-Da light chain of chicken gizzard HMM. More recently Perry et al. (FEBS lett., 180:165, 1985) have reported two-site phosphorylation of chicken gizzard myosin by endogenous kinase activity. The present study describes two-site phosphorylation of the 20,000-dalton myosin light chain (LC20) of glycerinated porcine carotid artery smooth muscle. Glycerinated porcine carotid artery strips were contracted for 10 min at 22°C in a buffered solution (pH 7.0) containing 30 uM free calcium, 10 uM calmodulin, 6 mM Mg[γ-^{32}P]ATP (or thio-ATP), 1 mM free Mg^{2+} and 1 mM DTT with the ionic strength adjusted to 0.15 M with potassium gluconate. Phosphorylation was monitored by glycerol-urea gel electrophoresis followed by radioimmunoblotting. In the presence of ATP, two phosphoprotein bands were present, LC20-P1 and LC20-P2. The fastest migrating phosphoprotein band (LC20-P2) was not present when muscles were phosphorylated exclusively with thio-ATP. The specific activity of radiolabeled LC20-P2 was 1.8 times that of LC20-P1 suggesting that LC20-P2 was diphosphorylated. The presence of two distinct phosphorylation sites was confirmed by peptide mapping of LC20-P2. LC20-P2 was excised from urea-glycerol gels and digested with TPCK-treated trypsin. The phosphopeptides were resolved using electrophoresis at 10°C and 1000 V for 60 min in a buffer of acetic acid:formic acid:H_2O (15:5:80, pH 1.9) in the first dimension followed by ascending chromatography in n-butanol:pyridine:acetic acid:H_2O (32.5:25:5:20) at 25°C in the second dimension. Two major phosphopeptides were resolved. These data demonstrate that LC20 of glycerinated porcine carotid artery smooth muscle can be phosphorylated at two distinct sites by endogenous calcium dependent protein kinase activity. The inability of thio-ATP to serve as a substrate for second-site phosphorylation suggests that a myosin kinase, different from myosin light chain kinase, is present in glycerinated carotid artery smooth muscle. This work was supported by grants from the NIH (R23 AM 35822-1); the American Heart Association, Indiana Affiliate; and the Herman C. Krannert Fund.

W-AM-B7 EFFECTS OF PHOSPHORYLATION AT A SECOND LIGHT CHAIN SITE ON CONFORMATION AND ENZYMATIC ACTIVITY OF SMOOTH MUSCLE MYOSIN. M. Ikebe, D. Hartshorne, & M. Elzinga*, Muscle Biol. Grp., Univ. of Ariz., Tucson, AZ 85721, *Dept. of Biol., Brookhaven Natn. Lab, Upton, N.Y. 11983.

Previously it has been shown that smooth muscle myosin can be phosphorylated by myosin light chain kinase at a second light chain site. (Ikebe and Hartshorne, J. Biol. Chem. 260, 10027 (1985)). The second phosphorylation site is threonine 18 (Ikebe, Hartshorne and Elzinga, J. Biol. Chem. in press). Phosphorylation of both light chain sites (4 mol P/mol myosin) enhances actin-activated ATPase activity and superprecipitation response, compared to phosphorylation at only 1 site (i.e., 2 mol P/mol myosin). The effects of phosphorylation at thr 18 and ser 19 on myosin conformation and filament formation was studied. The conformational transition, 6S to 10S, was monitored by viscosity and sedimentation velocity measurements. For myosin phosphorylated at ser 19 (2 mol P/mol myosin) its relative viscosity (in 1 mM $MgCl_2$, 1 mol ATP) decreased at ionic strengths below 0.2 M KCl and this is paralleled by a reduction of Mg^{2+}-ATPase activity. In contrast, myosin phosphorylated at both thr 18 and ser 19 exhibited neither a reduction in viscosity nor ATPase activity on decreasing ionic strength. Sedimentation patterns of myosin phosphorylated at ser 19 indicate that the reduction in viscosity observed on decreasing ionic strength is due to the transition of 6S to 10S myosin and possibly also to the formation of relatively small myosin polymers (3-5 molecules). For the doubly-phosphorylated myosin (4 mol P/mol myosin) the transition to 10S is not observed, and at low ionic strength ($<$125 mM KCl) larger myosin aggregates are formed. These results suggest that the phosphorylation of thr 18, in addition to ser 19, favors the 6S conformation and also filament formation. Supported by HL 23615 and HL 20984 from the NIH.

W-AM-B8 MODULATION OF ACTIN-ACTIVATED ATPASE ACTIVITY OF PHOSPHORYLATED GIZZARD MYOSIN BY TROPOMYOSIN, CA^{2+} AND MG^{2+}. William S. Fillers* and Samuel K. Chacko, Department of Pathobiology, University of Pennsylvania, Philadelphia, PA 19104.

Fully phosphorylated myosin was reconstituted with gizzard actin (molar ratio of M:A = 1:20) which was mixed with varying ratios of tropomyosin to actin. The ATPase activity of reconstituted actomyosin at free Mg^{2+} concentrations <3 mM continued to increase on raising the free Ca^{2+} concentration (up to pCa 3). At pCa 4.0 and 2 mM free Mg^{2+}, a 40-50% Ca^{2+}-sensitivity was observed; it was increased to 80-90% at pCa 3. At low free Ca^{2+} concentration (pCa >4), μ moles P_i released per mg myosin increased at a fast rate for 2-3 min after the initiation of the ATPase assay, this was followed by a slow rate which was continued during the rest of the assay (up to 30 min). Unlike the activity at low free Ca^{2+} concentration, the rate of ATP hydrolysis at pCa between 3.5 and 2.5 showed only the fast rate. The non-linearity of ATP hydrolysis was unaffected by the molar ratio of tropomyosin to actin; however, the activity increased as a function of tropomyosin concentration until the molar ratios of myosin to actin and tropomyosin to actin reached 1:20 and 1:3, respectively. High concentration (>4 mM) of free Mg^{2+} could not completely replace Ca^{2+} in maintaining the ATP hydrolysis at the faster rate. The data from these experiments reveals that (1) the actin-activated ATP hydrolysis of phosphorylated myosin at physiological range of free Ca^{2+} shows an initial fast rate followed by a slow rate at all molar ratios of myosin:actin and actin:tropomyosin, and (2) the initial fast rate observed in the physiological range of Ca^{2+} concentrations is sustained at Ca^{2+} concentrations higher than the physiological range. Supported by grants from NIH and NSF.

W-AM-B9 EFFECTS OF CALDESMON ON SMOOTH MUSCLE ACTO-HMM ATPase ACTIVITY AND BINDING OF HMM TO ACTIN. J.A. Lash, J.R. Sellers and D.R. Hathaway, Dept. of Medicine and Krannert Inst. of Cardiology, Indiana Univ. Sch. of Medicine, Indianapolis, IN and Laboratory of Molecular Cardiology, NHLBI, NIH, Bethesda, MD.

The in vitro interaction of myosin subfragments and actin has proven useful in the analysis of both thin filament and myosin-based regulation of the actomyosin ATPase cycle. Caldesmon, a major actin and Ca^{2+}-calmodulin (Ca^{2+}-CAM) binding protein of smooth muscle has been shown to localize to thin filaments of smooth muscle and to inhibit actin-activated ATPase of smooth muscle myosin. We have used smooth muscle heavy meromyosin (HMM) and subfragment 1 (S1) to define the effects of caldesmon on actomyosin ATPase. Caldesmon was purified to homogeneity from avian gizzard and bovine aortic smooth muscle (gizzard Mr-140,000;aortic Mr-145,000) and shown to be a dimer. Maximal inhibition of acto-HMM and acto-S1 ATPase was observed at a molar ratio of caldesmon(dimer) to actin of 1:20. However, saturation binding of caldesmon to actin was significantly higher at a ratio of 1:14 under similar conditions. The ATPase inhibition and binding of caldesmon to actin were partially reversible by addition of Ca^{2+}-CAM. By light microscopy there was no apparent bundling of actin by caldesmon at a ratio of 1:20. The binding of phosphorylated and unphosphorylated HMM to actin in the presence of ATP was observed to markedly increase in the presence of caldesmon. In a similar manner, S1 binding to actin was also increased. The binding constants of phosphorylated and unphosphorylated HMM for actin were 33.4 uM and 170 uM respectively. Addition of caldesmon to actin at a ratio of 1:20 resulted in an approximate 40-fold increase in affinity of both phosphorylated and unphosphorylated HMM for actin (K_D-0.9 uM and 4.2 uM respectively). Addition of Ca^{2+}-CAM significantly reversed the caldesmon mediated enhancement of HMM binding to actin. Our data suggest that caldesmon may serve as a thin filament regulator of actomyosin ATPase. Moreover, caldesmon may serve to reversibly modulate crossbridge affinity in smooth muscle by trapping the actomyosin ATPase cycle in a relatively high affinity state.

W-AM-B10 THE INHIBITION OF ACTIN-ACTIVATED ATPASE ACTIVITY OF PHOSPHORYLATED GIZZARD MYOSIN BY A PARTIALLY PURIFIED PREPARATION OF MYOSIN LIGHT CHAIN KINASE. Sumitra Nag, Jan Sosinski and John C. Seidel, Department of Muscle Research, Boston Biomedical Research Institute, Boston, MA 02114

We previously observed that limited chymotryptic digestion of phosphorylated gizzard myosin (PGM) produced a loss of Ca^{2+} dependence of its actin-activated ATPase activity. This loss of Ca^{2+} dependence was not associated with dephosphorylation, raising the possibility that PGM might contain a Ca^{2+} sensitizing factor. A soluble fraction extracted from chicken gizzard with a solution of low ionic strength and purified by ammonium sulfate fractionation (35-55%) and isoelectric precipitation at pH 4.9, that has been used to phosphorylate gizzard myosin, inhibits the actin-activated ATPase activity of PGM in the absence but not in the presence of Ca^{2+}, the inhibition being reversed upon addition of Ca^{2+}. Two proteins present in this fraction, having molecular weights between 70,000 and 90,000, bind to skeletal muscle actin but not to gizzard myosin. When activity is measured at Mg^{2+} concentrations of 2 mM or below there is no detectable dephosphorylation of the 20 kDa light chain during the ATPase assay, as judged by urea gel electrphoresis in 6 M urea. The inhibition is relatively independent of ionic strength, temperature and the presence of tropomyosin, and is lost upon digesting the active preparation with chymotrypsin. Trifluoperazine inhibits ATPase activity in the presence but not in the absence of Ca^{2+}, suggesting the possible involvement of calmodulin. The crude preparation has been partially resolved on a DEAE-Sephacel column and the active fraction contains the two actin-binding proteins.

W-AM-C FORUM
Muscle Contraction Frontiers & Controversies

Moderator Gerald H. Pollack, University of Washington at Seattle
Speaker: Haruo Sugi, University of Tokyo, Japan
Series elasticity: Is It in the Crossbridges?
Speaker: Charles Trombitas, University of Washington at Seattle. Thick Filaments Shortening in Vertebrate Striated Muscle
Speaker: Mark Sharnoff, University of Delaware at Newark. Does Activation Occur in Patterns?
Speaker: Tatsuo Iwazumi, University of Calgary at Alberta, Canada. Single Myofibril Experiments Reveal Many Wonders About Sarcomere Mechanics
Speaker: Tsukasa Tameyasu, St. Marianna University, Kawasaki, Japan. Shortening in Single Cardiac Cells Is Interrupted by One or More Pauses

W-AM-D1 ANTIPHOSPHOLIPID ANTIBODIES DISTINGUISH BETWEEN DIFFERENT POLYMORPHIC FORMS OF THE SAME PHOSPHOLIPID A.S. Janoff[1], P.R. Cullis[2], C.P.S. Tilcock[2], M.J. Hope[2], M. Tannenbaum[3], H. Tannenbaum[3], & J. Rauch[3]. [1]The Liposome Company, Inc., 1 Research Way, Princeton, NJ 08540; [2]Department of Biochemistry, University of British Columbia, Vancouver, B.C. V6T1W5; [3]Montreal General Hospital Research Institute, McGill University, Montreal, Canada H3G1A4

Antibodies to phospholipids represent a unique set of poorly characterized antibodies important in a variety of autoimmune disorders. One possible mechanism for the induction and/or pathogenesis of these antibodies involves alterations in the normal molecular architecture of the cell membrane. Such a mechanism seems plausible in light of the ability of membrane lipids to assume a variety of structures in addition to the bilayer phase. We have shown that certain monoclonal and polyclonal antiphospholipid antibodies associated with pathological conditions react with non-bilayer but not with bilayer phase phosphatidylethanolamine. This reactivity is presumed to be specific for the altered packing properties of the monolayer of phospholipid surrounding hexagonal (II) phase phosphatidylethanolamine and cannot be influenced by the phase behavior of bilayer phosphatidylethanolamine. Thus these antibodies are capable of distinguishing between lipid on purely structural criteria. Insofar as we are aware, this is the first demonstration that antiphospholipid antibodies are able to distinguish between different structural arrangements of the same phospholipid and may have important implications regarding the immunoregulation of autoimmunity.

W-AM-D2 MEMBRANE LIPIDS OF ALKALOPHILIC BACTERIA. Sanda Clejan, Terry A. Krulwich, Katherine R. Mondrus and Donna Seto-Young, Depts. of Pathology and Biochemistry, Mount Sinai School of Medicine, New York, N.Y. 10029.

The unusual bioenergetic properties of obligately alkalophilic Bacillus firmus RAB and Bacillus alcalophilus and the apparent loss of cellular integrity by these organisms at moderately acidic pH has prompted a study of their membrane lipids. For comparative purposes, several newly isolated facultative alkalophiles (Bacillus OF1 and OF3) that grow well both at pH 10.5 and at near neutral pH were included. The alkalophiles have high contents of total lipids, with the two obligately alkalophilic species having the especially high levels of 1.22-1.35 mg total lipid/mg of membrane protein. The two obligate alkalophiles also exhibit high proportions of neutral lipids, with neutral lipid/polar lipid ratios of 45/55. The main nonpolar lipids are diacylglycerols, squalene, dihydrosqualene, and C_{40} carotenoids. The proportion of the neutral lipid that is present as C_{40} carotenoids is high in the obligate alkalophiles (18%), whereas in the two facultative strains, OF1 and OF3, is 7% and 1% respectively. There are also differences in the polar lipids: the obligate alkalophiles have higher proportions of phosphatidylethanolamine and cardiolipin, whereas the facultative strains have a greater proportion of phosphatidylglycerol and phosphatidic acid. The kinetics of efflux of trapped markers from small unilamellar vesicles prepared from the extracted lipids indicate interesting effects of pH and of neutral lipid on the barrier properties of the vesicles.

W-AM-D3 MEMBRANE LIPIDS REVEAL THE METASTATIC POTENTIAL OF HUMAN TUMOURS VIA 1-H NMR.

Ian C.P. Smith, John K. Saunders, J. Robin Barr, Philip A. Williams, and Carolyn E. Mountford, National Research Council, Ottawa, Canada K1A 0R6, Ottawa Civic Hospital, Ottawa K1Y 4E9, and Ludwig Institute for Cancer Research, Sydney, Australia.

Tumours from human patients yield high resolution proton nuclear magnetic resonance spectra. Primary tumours from forty patients with cancer of the ovary or colon have been examined. The relaxation parameters obtained for the visible methylene protons were within the range of those measured previously for three experimental tumour models. Primary tumours, with metastases already identified, gave T_2 values greater than 350 ms. In contrast, primary tumours with no apparent metastases at the time of excision gave a range of T_2 values from 180 to 800 ms. The experimental laboratory models have shown that those cells with T_2 values less than 200 ms do not have the capacity to metastasise at the time of excision. Thus, the human data are similar to those recorded for the experimental cancer metastasis models, and are consistent with the premise that T_2 values are indicative of the metastatic potential of a tumour. As such they may provide very valuable information about human tumour behaviour.

W-AM-D4 CHARACTERIZATION OF A SECRETORY GRANULE MEMBRANE. A. Pande, A.U. Freiburghaus, G. Gantenbein, R. Ammann, and *J. Pande. Dept. of Medicine, University Hospital Zürich, and *Biochemistry Dept., University of Zürich, Zürich, Switzerland.

Membranes of the secretory granules play a central role in exocytosis. Physico-chemical characterization of these membranes would hopefully lead to a better understanding of this process.

Porcine pancreatic zymogen granules were isolated by repeated Percoll density gradient centrifugation and the membranes were obtained by lysis, followed by sucrose step-density-gradient centrifugation. Quantitative phospholipid analysis of the membrane shows phosphatidylcholine, phosphatidylethanolamine and lysophosphatidylcholine as major phospholipids. Gel-permeation chromatography of the membrane proteins in sodium dodecyl sulfate yields five major fractions, ranging in molecular weight (M.W.) from approximately 10,000 to 80,000. The largest (M.W. 80,000) protein, rich in serine, glutamic acid and glycine, appears similar to GP-2, a major protein component of these membranes in several other mammalian species. Biophysical techniques employed to study the thermotropic behavior of the membrane show a transition temperature of about 30° C for the gel to liquid crystalline phase change.

An unrelated secretory granule, namely the adrenal chromaffin granule, is known to have a similar lipid composition and thermotropic properties, but quite different membrane proteins. Thus it appears that the phospholipid composition largely determines the membrane structure and organization in the secretory granules.

W-AM-D5 COMPLEMENTARY PARTICLES AND PITS IN FREEZE-FRACTURE EM OF Na,K-ATPase MEMBRANES. H.P. Ting-Beall, Florence Burgess Stubbs and J. David Robertson. Dept. of Anatomy, Duke Univ. Med. Ctr. Durham, N.C. 27710.

High resolution electron microscopic images of complementary membrane surface replicas of purified microsomal vesicles of pig kidney outer medulla containing Na,K-ATPase have been obtained. This is accomplished by ultra-rapid freezing of a membrane suspension followed by fracturing and replicating of the liquid helium cooled specimen under ultra-high vacuum conditions, free of hydrocarbon contaminants as measured with a VG Supavac mass spectrometer. The protoplasmic fracture faces are populated with intramembrane particles (IMPs) while the external fracture faces reveal complementary pits. This is the first demonstration of precise and extensive matching of randomly dispersed IMPs and corresponding pits on the complementary fractured faces of biological membrane containing transmembrane proteins. Failure in demonstrating this complementarity has in the past persistently confused interpretations of the molecular organization of biological membranes. We show in this presentation that this failure is attributable to technical factors that can be controlled. The results further confirm the hypothesis that the majority of the mass of Na,K-ATPase is located at the protoplasmic half of the membrane and that fracture planes do not break polypeptide chains of transverse membrane proteins. (Supported by NIH grant GM 27804 and a gift from R.J. Reynolds Industries.)

W-AM-D6 CALORIMETRIC STUDIES OF THE THERMOTROPIC PHASE BEHAVIOR OF FATTY ACID-HOMOGENEOUS *ACHOLEPLASMA LAIDLAWII* B CELLS, MEMBRANES AND MEMBRANE LIPID DISPERSIONS. Charles Seguin and Ronald N. McElhaney, Department of Biochemistry, University of Alberta, Edmonton, Alberta, Canada

Acholeplasma laidlawii B is a simple, cell wall-less procaryotic microorganism whose membrane lipid fatty acid composition and cholesterol content can be dramatically altered by manipulation of the composition of its growth medium. Previous studies of the thermotropic phase behavior of exogenous fatty acid-enriched whole cells, isolated plasma membranes and total membrane lipids of this organism by conventional differential scanning calorimetry (DSC) were repeated using a high-sensitivity calorimeter (the Microcal MC-2) and fatty acid-homogeneous *A. laidlawii* cells, which exhibit considerably more cooperative lipid phase transitions. These new studies reveal subtle but significant differences in the enthalpy and in the cooperativity of the lipid gel to liquid-crystalline phase transition in intact cells, isolated membranes and membrane lipid dispersions. In particular, the gel to liquid-crystalline phase transitions of the lipid dispersions, although having similar midpoint temperatures, exhibit higher enthalpies but considerably reduced cooperativities in comparison to whole cells and isolated membranes, which behave essentially identically. However, the thermal denaturation of the proteins of intact cells or isolated membranes has no effect on lipid thermotropic phase behavior. These results imply that, in contrast to previous interpretations, the organization of lipids is not completely identical in intact cells or isolated membranes and membrane lipid dispersions, probably due at least in part to the influence of membrane proteins. (Supported by the Medical Research Council of Canada and the Alberta Heritage Foundation for Medical Research)

W-AM-D7 NONBILAYER STRUCTURES STIMULATE LIPID EXCHANGE KINETICS IN MYCOPLASMA CAPRICOLUM MEMBRANES. Robert Bittman and Sanda Clejan, Department of Chemistry, Queens College of The City University of New York, Flushing, NY 11367, and Sek Wen Hui, Biophysics Department, Roswell Park Memorial Institute, Buffalo, NY 14263.

The effects of nonbilayer structures in Mycoplasma capricolum membranes on the kinetics of [^{14}C] cholesterol and protein-mediated ^{14}C- labeled phospholipid exchange between the membranes and small unilamellar vesicles were studied. The growth medium was supplemented with phosphatidylcholine (PC), which results in an increase in cardiolipin/phosphatidylglycerol ratio in the membrane, and/or with Ca^{2+}. The formation of nonbilayer structures was examined at 37°C in trypsin-treated mycoplasma membranes and in aqueous suspensions of the extracted lipids by freeze-fracture electron microscopy and by ^{31}P nmr spectroscopy. Lipidic particles were observed in trypsin-treated membranes containing Ca^{2+} and PC, and the hexagonal-II phase appeared in membranes containing Ca^{2+} but not PC. Under the conditions in which these nonbilayer structures appeared, the rates of exchange of cholesterol and phospholipids (in the presence of transfer protein from rat liver) between membranes and vesicles were facilitated. The rate enchancements are considered to result from structural defects, which are associated with bilayer disruption sites when lipidic particles and other transitional states between the lamellar and hexagonal-II phases are present. [Supported by NIH Grants HL16660 and GM28120.]

W-AM-D8 CYTOCHROME C BINDS TO LIPID REGIONS IN PERIODIC ARRAYS OF THE OUTER MITOCHONDRIAL MEMBRANE PORE-PROTEIN, VDAC. C.A. Mannella, A. Ribeiro and J. Frank, Wadsworth Center for Laboratories and Research, New York State Department of Health, Albany, NY 12201 and State Univ. of New York, Albany, NY 12222.

The first step in uptake of cytoplasmically synthesized polypeptides by mitochondria involves binding of the polypeptides to as yet unidentified receptors on the mitochondrial outer membrane (OM). The concentrations of receptors for apocytochrome c (apocyt c) have been calculated from binding experiments with Neurospora mitochondria (Hennig et al. 1983 PNAS 80:4963). The only protein component of the OM known to be present at these concentrations is the pore-former, VDAC. We have analyzed negative-stain electron microscopic images of Neurospora OMs containing periodic arrays of VDAC after incubation of the membranes with apo- and holocyt c (+/- glutaraldehyde). The largest differences between images of these specimens and of controls (no cyt c) occur immediately adjacent to the channels, at loci known (from images of unstained, ice-embedded VDAC arrays) to be composed of lipid. These 2-4-nm-dia lipid patches stain lightly with uranyl and decrease in size when the arrays are treated with phospholipase A_2, indicating that phospholipids are a significant component. Interestingly, the affinity constants of apocyt c for mitochondria reported by Hennig et al. (ca. 10^7 M^{-1}) are in the range of values observed for cyt c binding to asolectin (Cannon and Erman 1980 BBA 600:19). These findings raise two possibilities: either (1) under low-salt conditions (used in both the binding and electron microscopic studies), nonspecific binding of cyt c to phospholipids may mask specific receptor binding, or (2) certain groups or classes of lipids in the OM may actually be physiological receptors for cyt c. (Supported by NSF grant PCM 83-15666.)

W-AM-D9 ULTRASTRUCTURE OF FROZEN SUSPENSIONS OF PROTEOLIPOSOMES. M.J. Costello, J. Escaig†, K. Matsushita, N. Carrasco, D. Menick and H.R. Kaback. Department of Anatomy, Duke University Medical Center, Durham, NC 27710; †CNRS, Laboratoire de Technologie a la Microscopie Electronic, 105 Boulevard Raspail, 75006 Paris, France and Department of Biochemistry, Roche Institute of Molecular Biology, Nutley, N.J. 07110

Freeze-fracture images of proteoliposomes reconstituted with purified lac permease and cytochrome o oxidase from Escherichia coli plasma membranes display the enzyme functional units as intramembrane particles (IMPs). Lac permease protein (46.5k dal) catalyzes the β-galactoside:H^+ symport driven by a proton electrochemical gradient and cytochrome o oxidase (140k dal) establishes a proton electrochemical gradient during turnover. Reconstitution with E. coli phospholipid by the octyl glucoside dilution method was followed by freeze-thaw/sonication. Proteoliposome suspensions were ultra-rapidly frozen and fractured using a double replica device. As described previously (J. Biol. Chem. 259, 15579, 1984; Biochem. 23, 4703, 1984), IMPs were randomly distributed on convex and concave fracture faces in the presence of protein. Lac permease and cytochrome o oxidase produced 7.0 nm and 8.5-9.0 nm diameter IMPs, respectively, in platinum/carbon replicas. Reexamination of these specimens using 0.6 nm tantalum replicas gave IMP diameters about 10-15% smaller and IMP substructure was visible. In platinum/carbon replicas of mixed proteoliposomes, IMPs corresponding to cytochrome o oxidase appear larger in diameter and extend further above the fracture face than those of lac permease, and only cytochrome o oxidase IMPs have matching pits in complementary images. Based on the size of the IMPs and the relationship of IMP density to composition, it appears that both enzymes reconstitute as monomers.

W-AM-D10 SURFACE PROPERTIES OF 1,2-DIPALMITOYL-3-ACYL-sn-GLYCEROLS: CHAINS LYING FLAT AND THEN FLIPPING INTO OR OUT OF WATER.

D.A. Fahey, D. Kodali and D.M. Small
Biophysics Institute, Boston University School of Medicine, Boston, MA 02118.

Stereospecific 1,2-dipalmitoyl-3-acyl-sn-glycerols (TGs) were synthesized with 3-acyl chains of 2-6 and 8 carbons in length. Pressure-area isotherms (27°C), surface melting temperatures (T_s), and equilibrium spreading pressures (esp) at the bulk melting temperature (T_f) were obtained for each TG and for dipalmitin. Whereas dipalmitin and the 3-acetyl TG condense directly to an expanded mesomorphous state (30-33Å^2/chain at the vapor pressure, π_v), the 3-propionyl through 3-octanoyl TGs show an area at π_v which increases linearly from 105-130Å^2/molecule (slope=5Å^2/CH_2). This slope suggests that the 3-acyl chains are lying flat on the water at the end of the gas-liquid transition. Before solidification at 42-47Å^2/molecule, the 3-propionyl through 3-hexanoyl TGs show a first order transition corresponding to the flipping of the 3-acyl chain into the water. The pressure at the transition, π_{tr}, vs. 3-acyl carbon number is linear and indicates a chain flipping energy of 512 cal-mole^{-1} per CH_2. T_s decreases with increasing chain length from 68-25°C, but the 3-octanoyl monolayer does not solidify even at 5°C because the unflipped octanoyl chains fluidize the palmitoyl chains. The esp (at T_f) drops from 40 mNm^{-1} for dipalmitin to 25.4 mNm^{-1} for the 3-acetyl TG whereas further sn-3 chain lengthening to 8 carbons depresses the esp by only 8 mNm^{-1}. In summary, increasing the length of the shorter 3-acyl chain of these di-acid TGs decreases the T_s and the esp. In monolayers, the shorter 3-acyl chains, lying flat on the surface at π_v, either submerge if π_{tr} < esp or stand up and fluidize the monolayer if π_{tr} > esp.

W-AM-E1 DIRECT MEASUREMENT OF K CURRENT ACROSS THE BASOLATERAL MEMBRANE OF FROG SKIN. Thomas C. Cox. Dept. of Physiology, Southern Illinois University, Carbondale IL 62901.

In previous studies of K transport across the basolateral membrane of the frog skin, direct measurements of K flux have not been possible because of a lack of knowledge of the specific activity of tracer in the K transport pool. Specific activity cannot be determined by loading the tissues with ^{42}K and then measuring tissue CPM and total tissue K because there are two pools, one of which is not readily exchangeable. I present here a method to directly measure the specific activity of ^{42}K as it leaves the K transport pool of the cells. Isolated epithelia of frog skin (R. pipiens) were loaded with ^{42}K for 2-3 hours. The tissue was then rinsed in tracer-free Ringer and mounted in a flux chamber. After ouabain treatment (K-free Ringer on both sides), K exiting the cells into the basolateral solution was collected at 2-4 minute intervals and compared with the short circuit current (Isc) averaged over the same time interval. ^{42}K flux was plotted against K flux. There was a strong correlation with $r = 0.951 \pm 0.014$ (9). The specific activity of K in the transport pool (slope of this plot) was used to calculate the unidirectional K efflux when the tissue was bathed with 2.4 mM K Ringer. The post ouabain Isc and the calculated K flux (corrected for neutral K flux) were 14.7 ± 1.8 and 14.2 ± 1.8 $\mu A/cm^2$ (9), respectively. Just prior to ouabain treatment, K current was calculated to be 11.6 ± 1.9 while Isc was 20.5 ± 2.6 $\mu A/cm^2$ (9). If you assume that the K current is equal to K uptake by the pump and that Isc underestimated Na flux through the pump by about 3.5 $\mu A/cm^2$ due to Na recycling, the pump stoichiometry can be estimated to be about 2.0. Support from AHA.

W-AM-E2 MEMBRANE POTENTIAL AND SODIUM DEPENDENCE OF PHLORIZIN BINDING TO ISOLATED ENTEROCYTES. Diego Restrepo and George Kimmich, Intr. by David A. Goldstein, Department of Radiation Biology and Biophysics, University of Rochester, Rochester, NY 14642.

The absorption of sugars in small intestine is mediated by a sodium-dependent sugar transport system. We have measured steady-state phlorizin binding [37°C] to ATP-depleted isolated intestinal cells of the chick. Carrier specific phlorizin binding was defined as D-glucose (90 mM) inhibitable binding. The dependence of carrier specific phlorizin binding on phlorizin concentration at fixed $\Delta\psi$ and sodium concentration follows simple saturation kinetics indicating the presence of a single binding site. Sodium concentration and $\Delta\psi$ modify the binding affinity but not the maximum number of binding sites. In contrast, at constant phlorizin, binding is a sigmoid function of sodium concentration and the phlorizin binding level at saturating sodium concentrations is phlorizin dependent. The rates of association and dissociation were measured at 1-2°C. Phlorizin association is both $\Delta\psi$ and sodium concentration dependent. Dissociation is sodium concentration dependent, but not $\Delta\psi$ dependent. Theoretical analysis indicates that the order of sodium and phlorizin binding is random, with preferred sodium first association and dissociation. In addition, the data suggest a stoichiometry of 2 sodiums to 1 phlorizin. The $\Delta\psi$ dependence can be explained by two models: either translocation is $\Delta\psi$-dependent and the free carrier is anionic, or sodium binding is the $\Delta\psi$ dependent step. (Supported by NIH AM15365.)

W-AM-E3 REGULATION OF TRANSEPITHELIAL Na^+ TRANSPORT BY RECRUITMENT THEN ALTERATION OF CONDUCTIVE SITES. Richard S. Fisher and Jerry W. Lockard, Walter Reed Army Institute of Research, Washington, D.C. 20307.

When toad urinary bladder (TB) or frog skin (FS) epithelia are treated with amiloride (10^{-4}M), short-circuit current (Isc), which represents the net, active transepithelial Na^+ transport rate from the apical to basolateral surface, decreases within 2 sec to about 20% (TB) and 40% (FS) of control values and then slowly over several minutes continues falling toward zero. This latter phase of the decline is attributed to recruitment of Na^+ conductive channels in the apical membranes of these cells which initially may be insensitive to amiloride. Tissues were pre-incubated in zero-Na^+ Ringer solution on the apical surface for 30 min and then were returned to control Na^+ Ringer. Transient increases of Isc above control values averaging 25% (TB) and 60% (FS) were observed. Tissues were re-exposed to amiloride near the peak Isc response, and Isc decreased to values near zero within seconds. This substantially reduced or eliminated the secondary, slow decline. Neither colchicine nor cytochalasin B affected the response of Isc to amiloride for either control or zero-Na^+ pre-incubated tissues indicating that the integrity of the cytoskeleton is not required for this response. We conclude that inhibition of Na^+ transport activates Na^+ conductive pathways which slowly either change affinity for amiloride or become more accessible to amiloride possibly by migrating to more superficially located sites in the apical cell membrane.

W-AM-E4 THE AMILORIDE-BINDING PROTEIN FROM CULTURED A6 EPITHELIAL CELLS: PARTIAL PURIFICATION AND CHARACTERIZATION. S. Sariban-Sohraby* and D.J. Benos, Department of Medicine, Brigham and Women's Hospital, Boston, MA 02115, and Department of Physiology and Biophysics, University of Alabama Medical Center, Birmingham, AL 35294.
The amiloride-binding component of the epithelial Na^+ transport protein has been purified to a specific activity of 159 pmoles/mg protein which represents a 910-fold enrichment of amiloride binding sites relative to cell homogenate. Cultured A6 toad kidney cells grown on porous supports were used as starting material. The purification protocol included 1) the preparation of a crude apical plasma membrane fraction (V_1) by $CaCl_2$ precipitation and differential centrifugations; 2) detergent solubilization of V_1 using CHAPS; 3) affinity chromotography of solubilized V_1 on agarose-immobilized wheat germ agglutinin (WGA); and 4) gel filtration of WGA by size exclusion high performance liquid chromatography (HPLC). The extent of purification was assessed by enrichment in [^{3}H]-methylbromoamiloride ([^{3}H]-CH_3BrA) specific binding. Average protein yields and [^{3}H]-CH_3BrA specific binding activities were as follows (starting with 40, 14 cm diameter filters): cell homogenate (H):480 mg, 0.5 pmole/mg; V_1:9.6 mg, 4 pmoles/mg; WGA: 30 µg, 49 pmoles/mg. These values correspond to binding enrichment relative to their corresponding H of 9.8±1.9-fold for V_1 and 95±11-fold for WGA. Scatchard analysis of [^{3}H]-CH_3BrA binding to V_1 and WGA revealed a single class of binding sites with a K_D~130 nM. This K_D value coincides with the apparent K_D determined from $^{22}Na^+$ influxes in both intact A6 epithelia and V_1, and from amiloride inhibition of Na^+ conductance in single A6 Na^+ channels incorporated into planar lipid bilayers. HPLC separation of WGA samples yielded 5 peaks, only one of which displayed specific [^{3}H]-CH_3BrA binding. The protein yield after HPLC was 170 ng and the specific activity 159 pmoles/mg. Thus, our purification scheme resulted in a 910-fold enrichment of the epithelial amiloride binding protein. Supported by N.I.H. Grant No. AM 37206.

W-AM-E5 EFFECT OF INHIBITORS ON RESISTANCE AND POTENTIAL OF GASTRIC FUNDUS OF RANA PIPIENS IN Cl MEDIA. W. S. Rehm, G. Carrasquer and M. Schwartz. Departments of Medicine and Physics, University of Louisville, Louisville, KY 40292.
Is the gastric proton pump in the intact fundus neutral (NP) or electrogenic (EP)? The gastric K-H ATPase pump in the form of vesicles is NP, but evidence supports the EP concept in intact fundi. SCN inhibits secretion and generally increases PD and resistance (R)--predicted by EP concept. We found that the increase in R is less with a hypertonic than with a normotonic secretory. Hersey et al using a hypertonic secretory confirmed an increase in R due to SCN but the increase was small with omeprazole (OME). They argue that the latter supports the NP concept. We find that SCN added to the nutrient rapidly changes PD, R, and H^+ rate -- R peaks and then decreases. In contrast, OME produces a slow inhibition and a slow increase in PD and R with no peak in R. There were no differences in the steady state levels between SCN and OME. Ba (1 mM) in nutrient increases R in highly secreting fundi from about 100 to 800 ohm cm^2 and then with Ba present SCN, OME and cimetidine decrease R from about 800 to 400 ohm cm^2. This decrease in R results primarily from a decrease in resistance of the nutrient membrane of the tubular cells. We postulate 1) that the peak SCN increase in R is due to the increase in resistance of the secretory membrane which is followed by a decrease in resistance of the nutrient membrane and 2) the increase in R wiith OME which occurs with the slow decrease in H^+ rate results from a concurrent change in the resistance of the two opposing membranes. The peak increase due to SCN is the best value for the increase in resistance of the secretory membrane due to acid inhibition.

W-AM-E6 IDENTIFICATION OF SEPARATE CELLS FOR Cl^- AND Na^+ TRANSPORT IN GASTRIC MUCOSA. J.R.Demarest, C.Scheffey* and T.E.Machen. Dept.of Physiol/Anat,Univ. of CA,Berkeley,CA 94720;*Natl. Vibrating Probe Facil.,MBL,Woods Hole,MA.
The short circuit current (Isc) of resting gastric mucosa can be attributed to the algebraic sum of the net Cl-secretion (JCl) and amiloride inhibitable net Na+ absorption. We have attempted to identify the cell types (surface epithelial cells, SECs, or oxyntic cells, OCs) responsible for the transport of these ions in Necturus gastric mucosa using microelectrode impalements under open circuit conditions and vibrating probe measurements under short circuit conditions. Mucosae were mounted horizontally in an open-topped chamber either serosal side up for basolateral impalements of OCs, or mucosal side up for apical impalements of SECs and vibrating probe measurements. Impalements of OCs indicated that neither their apical to basolateral membrane resistance ratio (Ra/Rb=1.3±.2)nor their cell membrane potentials were affected by 10^{-6}M mucosal amiloride.In contrast,impalements of SECs indicated that amiloride increased their Ra/Rb from 3.5±.2 to 15.6±1.8 and hyperpolarized both cell membrane potentials by>20 mV. In the presence of amiloride,when Isc=J^{Cl}, vibrating probe measurements showed that the current density over the opening to the gastric glands which contain the OCs was 374±67 µA/cm^2,while that over the SECs was 0.09±.05 µA/cm^2. We conclude that Na+ is transported exclusively by SECs and OCs account for J^{Cl}. (Supported by NIH AM17328).

W-AM-E7 SOME ZWITTERIONIC ORGANIC COMPOUNDS INTERACT WITH THE SALT TASTE MECHANISM

Krishna C. Persaud, Gerard L. Heck and John A. DeSimone
Dept. of Physiology and Biophysics, Medical College of Virginia, Virginia Commonwealth University, Richmond, Va 23298, USA

Zwitterions such as 2-(N-Morpholino)ethanesulfonic acid (MES) N,N-bis(2-hydroxyethyl)-2-aminoethanesulfonic acid (BES), N-Tris (hydroxymethyl)methyl-2-aminoethanesulfonic acid (TES) and the dipeptide lysine-taurine have complex tastes, but are predominantly salty. The transepithelial currents and potentials induced by these compounds when they interact with the rat lingual epithelium has been investigated using both in vitro and in vivo voltage or current clamped lingual epithelia. In the latter case, simultaneous recording of the integrated chorda tympani neural response was performed to insure correlation with an objective measure of gustation. These compounds all induce inward positive transepithelial currents at low concentrations (<10 mM). When presented in concentrations between 0.1 mM to 50 mM in 0.5 M NaCl, MES, BES and TES act as competitive inhibitors of the transepithelial current induced by 0.5M NaCl. However, in low concentrations of NaCl (30 mM), 200 mM MES produces a neural response of about the same magnitude as 150 mM NaCl, and induces an inward transepithelial current. These large organic compounds may act by facilitating proton transport through sodium channels in the lingual epithelium.

Supported by NIH Grant NS 13767 and the Campbell Insitute for Research and Technology.

W-AM-E8 PASSIVE IONIC PROPERTIES OF THE BOVINE RETINAL PIGMENT EPITHELIUM. Daniel Joseph and Sheldon Miller. School of Optometry, U.C. Berkeley, Berkeley Ca. 94720.

The relative ionic conductances of bovine retinal pigment epithelium (RPE) have been estimated in microelectrode ion-replacement studies. The mean apical membrane potential (V_a) is -61.5 mV (s.d. = ± 9.8 mV). The transepithelial potential (TEP) and transepithelial resistance (R_t) are 5.6 ± 2.1 mV and 138 ± 45 Ωcm^2 (mean ± s.d.), respectively. The apparent ratio of apical to basal membrane resistances (a) is 0.20 ± 0.16. Apical membrane conductance properties are dominated by the presence of Ba^{++}-sensitive K^+ channels. A decrease in the apical solution K^+ concentration elicited a response that has three phases. The first phase is an apical membrane hyperpolarization of 20 ± 7.5 mV (mean ± s.d.) and is consistent with a K^+ diffusion potential. The basal membrane hyperpolarizes during the second phase and cannot be explained on the basis of passive shunting of current from the apical membrane. The third phase is an apical membrane depolarization. Elevating $[K^+]_o$ from 5mM to either 20mM or 50mM depolarizes the apical membrane by 27 ± 3.2 mV and 30 ± 7.0 mV (mean ± s.d.) respectively. The K^+-induced voltage changes were blocked by 1mM Ba^{++} in the apical solution. When bicarbonate and CO_2 were removed from the apical solution, V_a depolarized by 5.1 ± 1.7 mV. This response is not blocked by barium in the apical solution. When 0.1 mM ouabain is added to the apical solution V_a depolarizes at an initial rate of 12.5 mV/min. After 1 minute the depolarization is slowed to 4 mV/min. The ouabain-induced depolarization of V_a can be used to calculate the resistances of the apical and basal membranes (R_a and R_b, respectively) and the shunt resistance, R_s. It is found that R_s = 2550 ± 600 Ω, R_a = 3190 ± 1130 Ω, and R_b = 17,920 ± 7710 Ω (mean ± s.d.). (Support: EY02205, EY00242 (SM); GM07379 (DJ)).

W-AM-E9 HIGH CHLORIDE CONDUCTANCE IN HUMAN ECCRINE SWEAT DUCTS. P.M. Quinton. Division of Biomedical Sciences, University of California, Riverside, CA. 92521.

The electrical conductance of isolated, microperfused segments of human eccrine sweat ducts was determined by cable analysis. Short segments of ducts (300-500 μ) were cannulated at each end and perfused with defined solutions. Each cannulating pipette served as a luminal electrode. Perfusion was conducted through a double barrel pipette so that a 3 second constant current pulse of 100 nA/20 sec could be passed into the lumen through one barrel while the luminal potential was monitored through the other barrel. The resistance of the duct was calculated from cable equations using the measured length of the duct and the changes in the input voltage at the perfusion end and output voltage at the collection end of the duct during the current pulses. When Cl was present in both the luminal and bath solutions, the average conductance was 8 ± 3 Ω $-cm^2$ (n=5). When gluconate replaced Cl first in the lumen and then also in the bath, the resistance rose to 47 ± 11 and then to 58 ± 8 Ω $-cm^2$ (n=4), respectively. Addition of amiloride (0.1 mM) to luminal perfusate also increased the resistance to 25 ± 5 Ω $-cm^2$. In a single duct from a subject with the genetic disease cystic fibrosis, the specific resistance was 56 Ω $-cm^2$ with Cl replete media, and rose to 131 Ω $-cm^2$ when amiloride was included in the luminal perfusate. But when Cl was removed from both bath and luminal fluids, the resistance only increased to 88 Ω $-cm^2$. The data show that the sweat duct is a low resistance epithelium whose conductance is constituted primarily by a high Cl dependent electrodiffusive pathway and that this pathway is absent or poorly functional in this tissue in cystic fibrosis.

W-AM-E10 TACHYKININS ON THE ISOLATED CANINE TRACHEAL EPITHELIUM: AN ANALYSIS OF THE "DIP". P.K. Rangachari, D. McWade [Dept. Medicine, Intestinal Disease Research Unit, McMaster University, Hamilton, Ont., Canada L8N 3Z5].

Luminal addition of substance P (SP) and other tachykinins to the open-circuited trachea produces a biphasic change in P.D.--a rapid, transient dip, followed by a rise (Refs. 1,2). The dip could arise from either an anion moving from lumen to serosa or cation from serosa to lumen or a combination of both. The dip bore a linear relation (r^2=0.94, 7 expts) to the open-circuit P.D. and could be either exaggerated, minimised or reversed by artificially altering the P.D. (see Fig). Total or partial Na^+ replacement with N-methyl-D-glucamine failed to affect significantly the dip, whereas luminal Cl^- replacement with isethionate did. Partial substitution of luminal Cl^- preserved the linear relation between the dip and P.D. but significantly shifted the intercept to more negative values. The intercepts observed were however significantly different from those predicted by the Nernst relation for Cl^- alone. Several possible explanations can be given for this deviation. Nevertheless, these studies clearly show that the peptides open anion-selective channels in the apical surface of the epithelium, perhaps in the tight junctions.

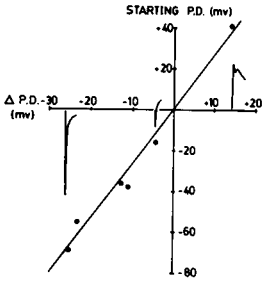

References: 1) Biophy.J. (1985), 47, 11a. 2) Regulatory Peptides (1985)12:9-19.

Supported by Canadian Cystic Fibrosis Foundation.

W-AM-E11 ROLE OF BRUSH BORDER CARBONIC ANHYDRASE IN NET ACID TRANSPORT BY RABBIT RENAL PROXIMAL TUBULES. J.L. Garvin, M.A. Knepper, R. Star and M.B. Burg. NHLBI, Bethesda, MD 20892.

Brush border carbonic anhydrase (BCA) catalyzes the dehydration of luminal H_2CO_3 formed by reaction of secreted H with HCO_3. BCA is present in the middle part (P2), but not in the last part (P3) of renal proximal tubules. In order to determine the role of BCA in net acid transport, we studied total ammonia (Tamm) and total CO_2 (TCO_2) transport in isolated, perfused P2 and P3.

P2: With 1mM Tamm and 26mM TCO_2 in both perfusate and bath the net fluxes were TCO_2 = 48 ±5 and Tamm = -1.3 ±0.4 pmol/mm/min (- = secretion). Addition of 10^{-4}M acetazolamide (to inhibit BCA) decreased TCO_2 flux to 8.6 ±1.5 without significant change in Tamm flux which was -3.2 ±1.5. With acetazolamide, equilibrium pH calculated from collected TCO_2 and bath [CO_2] exceeded the pH calculated from collected Tamm and bath [NH_3], indicating an acidic pH disequilibrium due to accumulation of H_2CO_3.

P3: With 4.0 mM Tamm and 27 mM TCO_2 in both perfusate and bath and perfusion rate of 2 nl/mm/min the collected fluid contained 5.0 mM Tamm and 28 mM TCO_2. The rise in luminal Tamm without a fall in TCO_2 is consistent with a luminal acidic disequilibrium. Addition of 0.1mg/ml carbonic anhydrase to the perfusate (to eliminate the disequilibrium) decreased Tamm significantly to 4.0 mM, but did not change TCO_2.

Conclusions: 1) The normal presence of BCA in P2 segments facilitates HCO_3 absorption by enhancing H_2CO_3 dehydration. 2) The normal absence of BCA in P3 segments facilitates ammonia secretion by allowing an acidic pH disequilibrium.

W-AM-E12 RESPONSE OF RABBIT CORTICAL COLLECTING TUBULE (CCT) TO CHANGES IN LUMINAL OSMOLALITY. Kevin Strange and Kenneth R. Spring, N.H.L.B.I., Bethesda, MD 20892.

We measured apical and basolateral water permeability (Posm) in individual cells of isolated perfused CCT using a high resolution video-optical system. Water flow across the basolateral membrane of both principal (PC) and intercalated (IC) cells was a linear function of the imposed osmotic gradient. Mean basolateral Posm values corrected for all surface area amplification in PC and IC were 66 μm/sec and 62.3 μm/sec, respectively. ADH did not alter the permeability of the basolateral membrane. Because of high total basolateral surface area and water flow it was necessary to measure apical Posm in tubules perfused under a small drop of silicone oil. Apical membrane Posm values corrected for surface area amplification were 19.2 μm/sec and 25 μm/sec for PC and IC, respectively, in the absence of ADH. PC and IC responded to ADH by increasing apical Posm to 92.2 μm/sec and 86.2 μm/sec, respectively. Our results indicate that previous cell morphology changes which suggested significant cell swelling and osmotic dilution induced by ADH and luminal hypotonicity in rabbit CCT have been misinterpreted. If CCT are exposed for 30 min to a supramaximal dose of ADH and then perfused with a 150 mOsm solution, our Posm measurements demonstrate that PC volume should be increased by at most 6%. In situ it is highly unlikely that CCT ever undergo any significant cytoplasmic dilution. The large apparent cell swellings observed by others are due to interspace distension with subsequent generation of a lateral hydrostatic pressure on the epithelial cells causing them to bulge prominently out into the tubule lumen. CCT cells prevent cytoplasmic dilution during ADH-induced water flow simply by having a highly water permeable basolateral membrane with a suface area 8-10 fold greater than that of the apical membrane.

W-AM-F1 MEMBRANE CURRENTS DURING DRUG-INDUCED AUTOMATICITY IN WELL-POLARIZED CAT VENTRICULAR MUSCLE.

Mario Delmar and Jose Jalife. SUNY/Upstate Medical Center, Syracuse, NY. 13210

A number of drugs are known to induce pacemaker activity in ventricular muscle at well-polarized maximum diastolic potentials (MDP). The mechanisms of this activity were studied in cat papillary muscle-sucrose gap preparations under current or voltage clamp conditions, during superfusion of $BaCl_2$. When $[Ba]_o$ was $\leq$ 0.2 mM, pacemaker activity developed at MDP's of -80 mV or greater. Hyperpolarizing current pulses prolonged, whereas depolarizing pulses abbreviated the spontaneous cycle in a voltage-dependent manner. With 2 mM Ba, the preparation depolarized to about -50 mV and spontaneous activity increased. However, hyperpolarization to -65 mV or greater abolished the activity. In the presence of 0.2 mM Ba, voltage clamping at the MDP (-85 mV), revealed an inwardly directed time and voltage dependent current. Hyperpolarizing pulses from a holding potential of -50 mV showed that this current was maximal at -70 mV and diminished with larger hyperpolarizations. The Ba-induced current was insensitive to TTX (10 μg/ml) or $CoCl_2$ (1 mM) and was reduced by $CsCl_2$ (2.5 mM). However, it was almost completely abolished by increasing $[Ba]_o$ to 2 mM. This paradoxical effect, together with the voltage dependency of the current, suggest that spontaneous activity is not the result of unmasking an already present i_f-like current. Instead, our data suggest that Ba-induced automaticity in well-polarized ventricular muscle results primarily from a time dependent blockade of the inward rectifying potassium current.

W-AM-F2 INTRACELLULAR CLOFILIUM REDUCES iK IN ISOLATED ADULT CARDIAC MYOCYTES.

D.J. Snyders and B.G. Katzung, Dept Pharmacology, UC San Francisco, CA 94143

Clofilium is a quaternary ammonium derivative that prolongs action potential duration in Purkinje fibers and refractoriness in arrhythmia models. We studied the effects of external and internal application of the drug using the whole cell clamp technique on enzymatically isolated ventricular myocytes of the guinea pig. Extracellular clofilium (10 - 100 μM) reduced the slope of the steady-state I-V relation at positive potentials, the amount of activated outward current during a clamp pulse, and the amplitude of the steady-state activation curve as measured from tails at -50 mV. The effect was slow in onset, and no reversal was observed after washout. Intracellular application (by adding the drug to the filling solution of the electrode, 10 and 50 μM) produced a fast reduction of the amount of activated current to 21 $\pm$ 8 % (50 μM, n=3) of controls after correction for apparent cylindrical surface area. (Controls were cells from the same batch). The tail current amplitude was reduced to 34 $\pm$ 13 %. No significant effect of either external or internal clofilium was observed on the resting potential or on the inward current through iK1. In addition extracellular clofilium reduced the slow inward current, whereas this was not significant in the intracellular studies, indicating a probable extracellular effect. These results suggest that clofilium acts on iK from the inside, but do not rule out an additional effect on outward iK1.

W-AM-F3 IONIC BASIS OF RYANODINE SENSITIVE CURRENTS IN CARDIAC PURKINJE FIBERS.

J.L. Kenyon and J.L. Sutko. Departments of Pharmacology, Physiology, and Internal Medicine. University of Texas Health Science Center, Dallas, TX 75235

As ryanodine abolishes the Purkinje fiber twitch it has complex effects on net membrane currents. At early times (0-20ms) the current is less outward while at later times (100-250ms) the current is more outward. The early effect presumably reflects the loss of a Ca-gated outward current component (Siegelbaum and Tsien, J. Physiol. 299:485 1980) but the basis for the later effect is unclear. We investigated the ionic bases of these effects using the two microelectrode voltage clamp technique to record membrane currents and isometric force from shortened calf Purkinje fibers. 250ms depolarizations from about -55mV activated currents and contractions. Perfusates contained 50μM 3,4-diaminopyridine. We found that in low Na perfusates (NaCl replaced by LiCl, CsCl, or choline Cl; $NaHCO_3$ retained), 1μM ryanodine abolished the twitch, reduced the early outward current, but did not increase the late outward current. This suggests that ryanodine affects two separate current components and that it might increase the late outward current by decreasing a component of inward current. We tested this possibility by stepping the membrane potential to about +15mV for 125ms and then to test potentials up to +79mV (i.e. positive to E_{Na} and the reversal potential for I_{Ca}) in normal perfusates. At all test potentials ryanodine caused an increase in net outward current, implying that it increased a component of outward current. In low Cl perfusates (NaCl and KCl replaced by Na isethionate and K methanesulfonate) ryanodine effects on force and currents resembled those in normal solutions. We conclude that ryanodine affects at least two components of membrane current that are outward at potentials positive to -20mV, they are not Cl currents, one is sensitive to Na, and one is reduced while the other is increased. NIH HL26528, HL17669, NSF 8402100.

W-AM-F4 RESTING PUMP CURRENT AND THE DOSE-RESPONSE RELATIONSHIP FOR DIHYDRO-OUABAIN IN ISOLATED CANINE CARDIAC PURKINJE MYOCYTES. N.K. Mulrine, +P. Pennefather, I.S. Cohen, G.A. Gintant and N.B. Datyner. Physiology & Biophysics, SUNY Stony Brook and +University of Toronto.

Canine Purkinje myocytes were obtained from Purkinje strands by gentle trituration and exposure to collagenase. The isolated myocytes were studied in Tyrode's solution (8mM K^+, 2mM Ca^{2+}) at 37°C. The effects of dihydro-ouabain (DHO) were assessed by voltage clamping the myocytes (-20 to -60mV) with a single microelectrode switch clamp and measuring the change in current induced by various concentrations of DHO. We obtained a K_D of 3.7±1.1μM (n=14) for the inhibition of pump current (I_p) by DHO. The resting pump current measured by adding 10^{-4}M DHO to the perfusing Tyrode was 0.28±.03 μA/μF (n=22).

We also examined the effects of changing $[K^+]_o$ from 8 to 1 mM on the resting pump current. In the first 5 minutes following reduction of $[K^+]_o$, I_p was reduced by more than 50%. However for long-term exposures t≥30 min, the resting pump current approached its original value in 8mM $[K^+]_o$. This suggests that $[Na^+]_i$ rises with time in 1mM $[K^+]_o$ and that as previously assumed in cardiac Na/K pump models, the inward background current is not markedly dependent on $[K^+]_o$ in this range of external $[K^+]$'s. Supported by HL20558, HL28958, and an NRSA and AHA to G.G.; P.P. is a Career Scientist of the O.M.H.

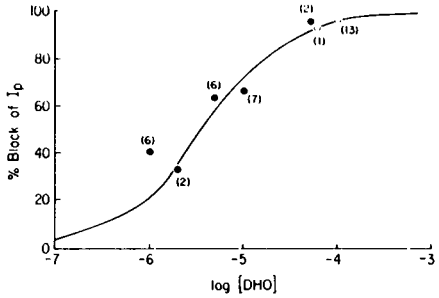

W-AM-F5 EXTERNAL ATP-ACTIVATED CURRENTS IN CARDIAC ATRIAL CELLS. David D. Friel and Bruce P. Bean, Department of Neurobiology, Harvard Medical School, Boston, MA 02115

We used whole-cell recording to study background currents activated by ATP in single atrial cells isolated from calf and bullfrog hearts. The external solution was a Tyrode's solution containing 4 mM K, and the internal solution was a K glutamate solution containing 10 mM EGTA and (sometimes) 5 mM ATP and 1 mM GTP. External ATP (1-200 uM) elicited an inwardly-rectifying current which activated within seconds and then underwent a slow decay in the continued presence of ATP (half-time about 4 sec. in frog cells, about 30 sec. in calf cells). The reversal potential of the ATP-induced current varied considerably from cell to cell. In calf cells, it was most often very near the calculated K equilibrium potential (-92 mV), but in a few cells was near -60 mV (mean -83 mV ± 3 mV SEM); in frog cells, the reversal potential was more consistently positive to E_K (-73 ± 3 mV). In contrast, the current elicited by ACh or carbachol consistently reversed near E_K. In frog cells, either raising [K]out to 50 mM or removing it entirely shifted the reversal potential for ATP-induced current in the depolarizing direction. Clear inward currents were seen with no external K, and ATP elicited sizeable currents even when all external and internal monovalent cations were replaced with Cs, suggesting that the ATP-induced current is not a simple K current like that activated by ACh. However, in some (but not all) cells, pretreatment with ATP substantially reduced the current elicited by a saturating concentration of carbachol, suggesting that the channels activated by ATP and ACh are not completely independent. Supported by grants from the NIH (HL 35034) and the American Heart Association.

W-AM-F6 USE OF DIACETYL MONOXIME (DAM) IN ISOLATING CARDIAC MYOCYTES AND ITS EFFECT ON THE SLOW INWARD CURRENT. Tung Li, Nicholas Sperelakis, Dept. Physiol. & Biophys., University of Cincinnati, OH 45267

DAM is a negative inotropic agent due to several actions: (1) a direct inhibition at the myofibril level (J. Pharmacol. Exp. Ther. 232:688, 1985) and (2) depression of Ca^{++} influx in some species. We found that DAM was also useful in isolating Ca^{++}-tolerant cardiac myocytes from guinea-pigs. The following sequence of Langendorff perfusion solutions were used to disperse the ventricular cells: normal Ca^{++} (1.8 mM) → 0 Ca → 0Ca/collagenase → 0 Ca. If DAM, 10 - 20 mM, was included in the final 0Ca perfusion and in the normal-Ca^{++} Tyrode's solution in which the dispersed cells were suspended, a significantly greater yield of rod-shaped myocytes was obtained. The effect of DAM is highly reversible, and can be readily washed out. Cells suspended in DAM-containing Tyrode's solution and stored in the refrigerator for up to 48 hr showed normal action potentials (APs) upon electrical stimulation, and are thus suitable for electrophysiological studies. The "patch-clamp" method in the whole-cell configuration was used to identify the effect of DAM on the electrical properties of the myocytes. At room temperature, voltage steps from -40 to 0 mV elicited slow inward currents (I_{si}) of 0.5-3 nA (1.8 Ca_o). DAM (10 - 20 mM) decreased I_{si} to about 50%, and decreased AP duration. The beneficial effect of DAM on myocyte isolation may be due to the prevention of contracture during the isolation procedure. (Supported by Grant HL-31942.)

W-AM-F7 ACTION POTENTIAL ALTERATIONS IN RESPONSE TO CHANGES IN RATE IN THE ISOLATED VENTRICULAR AND PURKINJE MYOCYTE. Penelope Boyden and Richard B. Robinson, Dept. of Pharmacology, Columbia University, College of Physicians and Surgeons, New York, New York.

The transmembrane potentials of dog Purkinje fiber (PF) strands or ventricular (VM) preparations are altered by the rate of stimulation. Frequency-dependent variations in $[K]_o$ in the restricted clefts of these multicellular preparations are expected to influence this electrical activity. To avoid the consequences of frequency-dependent accumulation of $[K]_o$, we studied potential changes in isolated VM and PF myocyte. Careful placement of an extracellular K^+-sensitive electrode near a myocyte during these protocols showed that there was neither beat-to-beat nor slow change in $[K]_o$ during drive. Consistent with the $[K]_o$ measurements, there was no change in resting potential (RP) with change in stimulation rate. However, there were alterations in action potential duration (APD). In both the PF and VM myocyte, when the rate of stimulation was increased, there was a decrease in APD with an approximate time constant (τ)= 60 sec. Electrical restitution (ER) of APD was also determined in myocytes by measuring APD_{-60mv} of single test pulses (S_2) delivered at various intervals after every 10th basic pulse (S_1)(S_1-S_1=500 msec). Similar to multicellular preparations, the kinetics of ER were best fit by a double exponential; for PF average τ_1=200 msec, τ_2=3100 msec; for VM average τ_1=120 msec, τ_2= 7700msec. Therefore, extracellular K+ ion accumulation and depletion effects, and concomitant changes in RP, may not be a prerequisite for either component of ER. (Supported by NIH PPG HL 30557 and HL 34470).

W-AM-F8 EVIDENCE FOR Na^+-Li^+ EXCHANGE IN HUMAN HEART.
Helge Rasmussen, Robert TenEick, Robert Harvey, Donald Singer (Introd. by R.F. Novak)
Depts. of Pharmacology & Medicine, Northwestern University, Chicago, IL 60611

During exposure of cardiac cells to Li^+ the intracellular Li^+ concentration is considerably lower than expected if Li^+ were passively distributed, yet Li^+ is apparently not pumped by the sarcolemmal Na pump. To investigate the mechanism of Li^+ extrusion human atrial tissue was incubated at 2-3° in Li^+ substituted (for Na^+) Tyrode's solution for 90 min. When rewarmed to 30° in normal Na^+ Tyrode's containing 20 mM K^+ and 0.5 mM Ba^{2+}, the resting potential (RP) transiently hyperpolarized to a maximum (RP_{max}) of -58.4±1.4 mV (mean±SD, n=5) 10 min after the onset of rewarming. When RP was at RP_{max}, acetylcholine caused depolarization indicating that RP was negative to E_K. RP_{max} during exposure to 500 nM acetylstrophanthidin was less negative than RP_{max} during control (-42.3±4.0 mV, n=6 vs. -58.4±1.4 mV, n=5, $p<0.001$) suggesting that the hyperpolarization was due to electrogenic pumping of an intracellular Na^+ load. RP_{max} was -68.0 ±2.1 mV (n=3) with 0.01 mM tetrodotoxin and was similar to control with 25 mM Li^+ in the Tyrode's solution, indicating that hyperpolarization was not due to outward diffusion of Li^+ through ionic channels. RP_{max} during rewarming in TEA-Tyrode's containing 25 mM Na^+ was -60.3±3.1 mV(n=4). However, hyperpolarization during rewarming in TEA- Tyrode's containing 25 mM Na^+ was inhibited when 25 mM Li^+ was also present suggesting that Na and Li compete for a binding site. These results suggest that a Na^+-Li^+ exchange occurs in human heart and may account for intracellular Li^+ concentration being lower than predicted for purely passive distribution.

W-AM-F9 ISOLATION OF SODIUM-CALCIUM EXCHANGE CURRENT IN SINGLE VENTRICULAR CELLS OF GUINEA PIG. A. Noma, J. Kimura and H. Irisawa. National Institute for Physiological Sciences, Myodaiji, Okazaki, 444 Japan (Intr. by D.C. Gadsby)

Control of the intracellular ion concentration is an essential step to isolate a current generated by the electrogenic Na-Ca exchange. We applied the gigaohm-seal patch electrode to collagenase-treated ventricular cells and varied the Na^+ and Ca^{2+} concentrations within the pipette using the intrapipette perfusion device during the whole cell current recordings. The composition of the bath and pipette solutions was designed to reduce the membrane conductance and to buffer the intracellular free Ca^{2+} as follows. The bath solution contained in mM; NaCl 140, CsCl 2, $MgCl_2$ 2, $BaCl_2$ 2, D 600 0.001 and ouabain 0.02, while the pipette solution; aspartate 42, EGTA 42-$CaCl_2$ 21 (pCa=7.1), MgATP 10, creatine phosphate 5, TEA-Cl 20, Hepes 5 and was titrated to pH 7.4 with CsOH. Neither application of 1 mM Ca outside or 30 mM Na^+ inside the cell produced large change in the I-V relation. However, the application of Ca^{2+} following the internal application of Na^+ induced a marked outward current, which increased exponentially with depolarization (0.5 nA at 0 mV) from a nearly 0 current at around -110 mV. The current was blocked by La, Cd, Ni and partly by amiloride. When the internal solution contained no Ca^{2+} (42 EGTA), the current was not induced. These characteristics suggest that the dissected current is generated by the Na-Ca exchanger.

W-AM-G1 STRUCTURAL STUDIES OF PROTEINS AND NUCLEIC ACIDS BY TWO-DIMENSIONAL NUCLEAR MAGNETIC RESONANCE. A. Pardi, A.C. Bach II, C. Wang and X.L. Zhang, Department of Chemistry, Rutgers, The State University of New Jersey, New Brunswick, N.J. 08903.

The three-dimensional structures of several biomolecules in solution are being investigated by high resolution nuclear magnetic resonance experiments. Resonance assignments in the molecule are made using a variety of two-dimensional (2D) NMR techniques and then structural information is obtained from 2D nuclear Overhauser effect (nOe) experiments. The 2D nOe experiment provides a generally applicable method for obtaining proton-proton internuclear distances less than 4.5A. Three-dimensional structures are generated from these proton-proton distances using interactive graphics or distance geometry techniques. The DNA decamers d(GCGAATTCGC) and d(CGCCTAATCG) have been studied by these methods to search for correlations between base sequence and local variations in the structure of the DNA in solution. The dynamics of DNA in solution has also been studied using hydrogen exchange experiments of the imino and amino protons. We are also studying the neutrophil cationic protein NP2 by 2D NMR. NP2 is a naturally occurring broad-spectrum antimicrobial agent. Preliminary results on the determination of the solution structure of this protein will be presented.

W-AM-G2 SECONDARY STRUCTURE OF SEA ANEMONE TOXIN RP II. N. V. Kumar, D. E. Wemmer[1], R. Metrione[2], H. Schweitz[3], M. Lazdunski[3] and N. R. Kallenbach, Department of Biology, University of Pennsylvania, Philadelphia, PA 19104. 1 Department of Chemistry, University of California, Berkeley; 2 Department of Biochemistry, University of Washington, Seattle; 3 Centre de Biochimie du CNRS, Universitat de Nice, Parc Valrose.

RP II toxin from the sea anemone Radianthus Paumotensis binds to sodium channels and slows down the inactivation process. It consists of 48 amino acid residues with 3 disulfide bonds. Its amino acid sequence, ^{1}A S C K C D D D G ^{10}P D V R S A T F T G ^{20}T V D F W N C N E G ^{30}W E K C T A V Y T P ^{40}V A S C C R K K ^{48}K, shows significant homology in the N-terminus region with 3 other neurotoxins from sea anemone Anemonia Sulcata. We have determined the structure of RPII in solution at pH 4.6 by high resolution ^{1}H 2D-NMR spectroscopy at 500MHz. We have completed the sequential resonance assignments combining the results of homonuclear correlated spectroscopy (COSY), relayed coherence transfer spectroscopy (RCT) and phase sensitive nuclear Overhauser enhancement spectroscopy (NOESY) in D_2O and H_2O solutions. Contiguous stretches of NOEs between the amide NH and α protons of neighboring residues indicate that RPII is a stable β-protein in solution. The extended structural elements are connected by the 4 tight turns. Conspicous absence of NOEs between the amide protons of adjacent residues further show that RPII does not have any α-helical segment in its structure. A low resolution structure has been presented on the basis of distance constraints from the NOEs between non-neighboring residues. Inter-strand NOEs between the α and amide protons show that the C-terminus forms an anti-parallel β - sheet with residues 30-33 of RPII protein. (This work has been supported by grant PHS-CA-24101-07 from NIH)

W-AM-G3 HIGH RESOLUTION SOLUTION NMR STUDIES OF THE MEMBRANE-BOUND FORM OF THE fd AND Pfl COAT PROTEINS M.J. Bogusky, R.A. Schiksnis, and S.J. Opella (Intr. by P. Lu)

High resolution NMR studies of the filamentous bacteriophage fd and Pfl coat proteins in micelles are being conducted to characterize the structure and dynamics of the membrane-form of the protein as well as the viral infection and assembly processes. The coat proteins are found to exist in the bacterial host cell membrane during infection and assembly and are thus ideally suited as model membrane systems to study membrane-protein interactions and macromolecular assembly.

Two-dimensional homonuclear and heteronuclear correlation experiments are being used to assign the backbone and sidechain resonances and provide means for structural elucidation of the protein by distance constraints consistant with the NMR data. The dynamics of the coat protein are characterized by NOE measurements, proton-exchange and relaxation measurements. These results indicate two distinct motional domains present in the fd and Pfl backbone which contrasts with the results found for globular proteins where the entire polypeptide backgone is generally found to be rigid. Similar results have been found for the coat protein in bilayers as studied by solid-state NMR. Amide-proton exchange experiments have been used to examine structural transitions occuring in the coat proteins during infection and assembly. These data demonstrate the existence of a structured region of the backbone which is conserved during the infection process, where the coat protein is inserted into the bacterial cell membrane. The secondary structure of this region has been characterized by 2D-NOE methods. Comparisons of the micelle and bilayer forms of the coat protein with the structural form found in the intact virus reflect the structural and dynamical transitions associated with the viral infection and assembly processes.

W-AM-G4 STRUCTURAL CHARACTERIZATION OF α, β AND γ FORMS OF EPIDERMAL GROWTH FACTOR.
K.H.Mayo, A. DeMarco, B.H. Yoo, and C. Burke. Dept. of Chemistry, Temple University, Philadelphia, PA 19122, USA & Istituto di Chimica delle Macromolecole, CNR, Milan, Italy.

Mouse epidermal growth factor (mEGF) is a protein hormone effector molecule that regulates cellular development and division. When purified by HPLC methods, mEGF is found to be composed of three different forms of the protein (i.e.α, β, and γ). Structural aspects of each of these forms have been investigated by HPLC, NMR and photo-CIDNP methods under a variety of solvent conditions. Proton-NMR results at 500 MHz suggest that only the N-terminal structural domain of the protein (Mayo, K.H. (1984) Biochemistry 23, 3960-3973) is responsible for these differing forms. When comparing NMR spectra of the three forms, chemical shifts of proton resonances assigned to the His-22, Tyr-10, Tyr-13, and Ile-23 residues demonstrate differences between 0.02 and 0.05 ppm while other resonances are unshifted. Photo-CIDNP results indicate that both tryptophans and four out of the five tyrosines are solvent exposed and suggest that some structural differences involving these aromatic residues exist among the different forms of the protein. Chemical reduction of the three disulfide bridges in all forms results in significantly longer retention times by RP-HPLC with greatly altered elution profiles. NMR and photo-CIDNP results on the reduced forms suggest that their gross conformations are only slightly altered when compared to the native proteins. These results are discussed in relationship to the possible biological significance of α, β, and γ mEGFs.

This work was supported by NIH grant (GM-34662) and a generous gift from the Glenmede Trust Fund (to K.H.M.) and by a NATO research grant (RG.85/0424) (to K.H.M. & A.D.).

W-AM-G5 DETERMINATION OF PEPTIDE AND PROTEIN CONFORMATION BY FUNDAMENTAL AND OVERTONE ^{14}N NMR
P.L. Stewart, R. Tycko, and S.J. Opella

The orientations of the peptide planes in single crystals of peptides have been determined unambiguously and with high precision solely on the basis of fundamental and overtone ^{14}N NMR experiments. The experimentally determined orientations are relative to the direction of the applied magnetic field and are described by the polar angles which relate the molecular axis system to the field direction. These angles can be related to the Φ, Ψ torsion angles which describe the orientation of two peptide planes joined at an α carbon. The relative peptide plane orientations determined by ^{14}N NMR are in excellent agreement with those obtained by X-ray diffraction.

The use of ^{14}N NMR means that no isotopic labelling is required. Since ^{14}N is a spin S=1 nucleus, two fundamental transitions are observed near the Larmor frequency. Angular information is obtained by measuring the quadrupole and N-H dipole splittings. The overtone transition near twice the Larmor frequency can also be directly detected. The second order shift of the overtone frequency, the N-H dipole splitting, and the effective nutation frequency all have characteristic angular dependences. Combined with standard bond lengths and geometries, this angular information fully describes the secondary and tertiary structure of proteins.

W-AM-G6 CHANGES IN THE COAT PROTEIN OF fd BACTERIOPHAGE DURING THE VIRAL LIFECYCLE
K.G. Valentine, D.M. Schneider, G.C. Leo, L.A. Colnago and S.J. Opella

The major coat protein of the bacteriophage fd undergoes a significant structural transition during the infection and assembly processes. The coat protein is stored in the bacterial membrane following infection and prior to assembly when newly formed virus particles are extruded from the bacteria. The properties of the membrane bound and structural forms of the coat protein can be compared with solid state NMR experiments. Specific ^{15}N and ^{2}H labelled amino acids can be selectively incorporated into the 50 amino acid coat protein biosynthetically. It is possible to map out regions of the protein which exhibit mobile or static behavior based on the assignments of the labelled sites.

The structural form of the coat protein in the virus contains four mobile residues at the amino terminus. The remaining residues are rigid on the 10^{-3} Hz time scale. The membrane bound form of the coat protein has a more extensive mobile region at the amino terminus and a few mobile residues near the carboxy terminus. The central hydrophobic core of the protein remains immobile. These data suggest that the protein spans the bilayer with immobile internal residues and two highly mobile end domains outside the bilayer boundries. Spectra of side chain ^{2}H labelled protein indicates limited motion of aliphatic sidechains within the bilayer boundries that isotropic averaging of the sidechains on residues at the two ends of the protein extending beyond the bilayer. The model of the structural form of the coat protein in the intact virus describes a highly rigid structure for 90% of the protein residues in an α-helix with only the amino terminal residues exhibiting substantial motion.

W-AM-G7 CONFORMATIONAL ENERGY CALCULATIONS AND ^{1}H NUCLEAR OVERHAUSER ENHANCEMENTS REVEAL A UNIQUE CONFORMATION FOR BLOOD GROUP A OLIGOSACCHARIDES. C. Allen Bush, Zhen-Yi Yan and B. N. Narasinga Rao, Dept. of Chemistry, Illinois Institute of Technology, Chicago, IL 60616 U.S.A.

The ^{1}H NMR spectra of a series of blood group A active oligosaccharides containing from four to ten sugar residues have been completely assigned and quantitative nuclear Overhauser enhancements (n.O.e.) measured between protons separated by known distances within the pyranoside ring. The observation of n.O.e. between anomeric protons and those of the aglycone sugar as well as small effects between protons of distant rings suggests that the oligosaccharides have well defined conformations. Conformational energy calculations using three different potential energy functions which have been widely used in peptides and carbohydrates give several distinct minimum energy conformations. In complete n.O.e. calculations for each of the low energy conformations, the rotational correlation time was adjusted to fit T1's and intra-ring n.O.e. Comparison of the effects predicted for each low energy conformation with experimenatal values implies that the oligosaccharides adopt single rigid conformations which do not change with temperature. Since the glycosidic linkage of galNAc (α1$\rightarrow$3)gal-β adopts an unusual conformation in which the anomeric proton is closer to gal H4 than it is to gal H3, some caution should be used in the application of recently proposed 2-d NMR methods which use n.O.e. to determine the positions of intersaccharide linkage in oligosaccharides. While the results of the conformational energy calculations are very sensitive to the details of the non-bonded interactions, the influence of electrostatics, hydrogen bonding and torsional potentials is minimal.

W-AM-G8 The Structure of Glycopeptides and their Complexes with Putative Cell Wall Precursors

L. Mueller, S.L. Heald and P.W. Jeffs
Smith, Kline & French Laboratories, Mail Code F90, 1500 Spring Garden Street
Philadelphia, PA 19101

Glycopeptide antibiotics of the vancomycin class may serve as excellent models for the study of drug receptor bindings. The entire peptide core of these molecules forms a binding pocket for putative cell wall precursors L-Lys-D-Ala-D-Ala of Gram-positive bacteria. Furthermore, the structure of these compounds is highly rigid due to numerous cross-links between the sidechains of amino acid residues in the peptide core. This rigidity makes these systems suitable for testing new methods of structure elucidation.

We have elucidated the 3d-structures of several novel glycopeptide antibiotics utilizing two-dimensional NMR methods and computer-assisted molecular modeling. 3d-Structures of complexes between glycopeptides and putative cell wall precursors L-Lys-D-Ala-D-Ala were investigated by standard two-dimensional NMR methods as well as by a novel technique of proton observed ^{15}N NMR. We found that ^{15}N chemical shifts may serve as a monitor of interpeptide hydrogen bond formation.

W-AM-G9 ^{31}P NMR HIGH RESOLUATION AND SURFACE COIL STUDIES ON AVIAN EGGS. C. Tyler Burt, Lisa M. Jeffreys, and Robert E. London, Laboratory of Molecular Biophysics, National Institute of Environmental Health Sciences, PO Box 12233, Research Triangle Park, NC 27709.

Eggs represent a good system for NMR studies because 1. they can be used to investigate environmental factors in embryonic development; 2. there exist several different compartments that allow spatial resolution techniques to be tested; 3. they have a range of interesting compounds in them; and 4. they come in convenient sizes. By examining separate components we corrobrate classical studies that hen egg white (albumin) contains 2 phosphate resonances from ovalbumin, a phospholipid resonance and a further two probably due to uridine diphospho-N-acetylgalactosamine. The albumin is considerably alkaline with a pH greater than 8. The yolk on the other hand is very acidic (pH 6) and contains a broad resonance due to phospholipid and a sharper one from inorganic phsophate. The resonance due to phosvitin is not present at a level which would be expected. This apparently is due to a pH mediated exchange phenomena since yolk at the more alkaline pH's does show a prominent phosphoprotein peak. Surface coil studies show spectra that are combinations of egg white and eggs yolk whose proportional contribution depend on orientation. Peaks were assigned by comparison with known chemical shift values for reported metabolites, pH titration curves and extractibility.

W-AM-G10 HIGH RESOLUTION PROTON NMR SPECTROSCOPY OF METABOLITES IN BODY FLUIDS WITH THE WATER PEAK SUPPRESSED

Thomas M. Eads* & Robert G. Bryant, Dept. Radiology, Univ. Rochester Med. Ctr., Rochester, NY 14642 (*present address: Kraft, Inc. R&D, Basic Food Science Laboratory, 801 Waukegan Rd., Glenview, IL 60025).

Natural aqueous fluids are analyzed by high resolution proton nuclear magnetic resonance spectroscopy using a method which suppresses the water proton peak by at least 10E-4. The method exploits the increase of water proton transverse relaxation rate (1/T2) induced by a paramagnetic reagent added at low (few tenths mM) concentration. A spectrum is acquired after allowing H2O magnetization to decay in the transverse plane during application of the CPMG spin echo pulse train (Bryant & Eads, J. Magn. Res. *in press* (1985)). Experiments are done on FT nmr spectrometers on normal size samples with little or no modification of hardware or software. We demonstrate facile detection of glucose and other solutes at their naturally low concentrations (a few to tens mM) in human cerebrospinal fluid, blood plasma and urine. The method is less suitable for observation of solutes with naturally short T2's. However, the extent to which those signals decay can be controlled in the CPMG spin echo pulse sequence, for the purpose of spectral editing on the basis of T2. Since sample preparation is trivial and nmr methods are straightforward, the method lends itself to automation. Chemistry and reaction kinetics in aqueous solutions may be studied. The method has also been extended to semisolids and slurries such as intact and minced brain tissue.

W-AM-G11 Formation of Superoxide and Hydroxyl Radicals in the Mouse Central Nervous System: Effect of Electroconvulsive Shock. M.S. Darsillo, E.J. Essman, W.B. Essman, H.D. Gafney, Queens College of the City University New York, Flushing, N.Y., 11369. C.E. Swenberg, Div. of Molecular Radiobiology, Armed Forces Radiobiological Research Institute, Bethesda, MD, 20814-5145.

The detection of superoxide and hydroxyl radicals in biological tissues has been demonstrated through the use of EPR spectroscopy. These studies employed such methodology to assess the effect of electroconvulsive shock (ECS), known to alter central nervous system (CNS) chemistry upon the production of superoxide and hydroxyl radicals. The high reactivity of these radicals in cells and tissues has accounted for cytotoxic effects including membrane damage, mitochondrial alterations, and nuclear damage. In vitro studies with purified presynaptic membranes (PSM) from mouse cerebral cortex and cerebellum were conducted using a hyxanthine-xanthine oxidase generating system in which superoxide and hydroxyl radicals were trapped with 5,5-dimethyl-1-pyrroline-1-oxide (DMPO). No resonances were detected for PSM from the cerebral cortex, however, the spectra for PSM from the cerebellum revealed the presence of both superoxide and hydroxylnitrone spin adducts. EPR spectra recorded for PSM from the cerebral cortex following ECS revealed significant superoxide and hydroxyl radical formation. EPR spectra for PSM from cerebellum were essentially unchanged after ECS. In vivo investigations of superoxide and hydroxyl radical formation in cerebrospinal fluid (CSF) were conducted with DMPO as a spin trap. Recovery and stability of DMPO in CSF was measured using UV spectroscopy. Results suggest that tissue diffusion of the nitrone spin trap was attenuated by ECS. Convulsions modified superoxide and hydroxyl radical formation in CSF. The data indicate that electrically-induced convulsions alter the status of free radical formation in the mouse CNS.

W-AM-G12 **MOLECULAR DYNAMICS OF SICKLE HEMOGLOBIN POLYMERS: AN ELECTRON-SPIN-ECHO STUDY**

LEELA KAR[†], MICHAEL K. BOWMAN[§] AND MICHAEL E. JOHNSON[†]

[†]Department of Medicinal Chemistry, College of Pharmacy, P.O.Box 6998, University of Illinois at Chicago, Illinois 60680, and [§]Chemistry Division, Argonne National Laboratory, Illinois 60439.

Electron-spin-echo (ESE) spectroscopy has been used to make the first direct measurements of relaxation times of a spin-labeled protein at physiological temperatures. Two-dimensional ESE (2D-ESE) experiments have been performed using the ESE spectrometer at the Chemistry Division of Argonne National Laboratory. Experiments using maleimide labeled deoxy hemoglobin (dHb) from individuals homozygous for sickle cell anemia (dHbS) have been compared with control experiments using dHb from normal adults (dHbA). Hb 'immobilized' by ammonium sulfate precipitation and by polymer entrapment have been studied for a suitable 'rigid' reference. The two-dimensional contour plots show that 2D-ESE is sensitive enough to detect the slow motion of dHbS polymers and to differentiate it from both that of 'immobilized' Hb and of dHbA molecules in solution at the same temperature and concentration. Computer simulations using current slow motional theories have been done to obtain information regarding motional anisotropy - with the purpose of identifying strong intermolecular contact sites in the dHbS polymer. The considerable potential of 2D-ESE spectroscopy in the study of macromolecular motion is illustrated by comparing the results of these experiments with previous studies using saturation transfer electron paramagnetic resonance.

W-PM-Min1 GATING AND CONDUCTION IN THE LIGHT-SENSITIVE CHANNELS OF RETINAL RODS. A.L. Zimmerman and D.A. Baylor, Neurobiology Department, Stanford Medical School, Stanford, CA 94305.

Excised patches from the outer segments of retinal rods show a cyclic GMP-sensitive cation conductance (1, 2). We have studied the properties of the light-sensitive conductance and the cGMP-sensitive conductance of salamander rods and find several features consistent with the notion that the two conductances are identical: a) The outer segment conductance is composed almost exclusively of light-sensitive channels, and excised outer segment patches rarely show evidence of channels other than those activated by cGMP. b) The effects of internally applied cGMP analogs on whole cell currents are consistent with their potency in activating the conductance of excised patches (3). c) Both conductances show outward-going rectification and have similar reversal potentials. d) Channel density estimates from whole cell and excised patch experiments are similar. e) At physiological ionic concentrations, both show a very small apparent single channel conductance compatible with either a pore or carrier mechanism of conduction. In the absence of added divalent cations, the cGMP-activated conductance of excised patches becomes very large, and single channel currents are measurable. The apparent unitary conductance is about 16 pS, indicating conduction by a pore. The burst-like form of the single channel currents and the prominent noise in the macroscopic current at saturating agonist concentrations suggest that a channel with bound agonist undergoes a rapid gating or blocking process. Activation of the channel shows a Hill coefficient of 3 and is increased by depolarization.

References: 1) Fesenko et al., (1985) Nature 313: 310-313. 2) Nakatani & Yau (1985) Biophys. J. 47: 356a. 3) Zimmerman et al., (1985) PNAS (in press).

W-PM-Min2 **A CRITIQUE OF SOME MODELS FOR INTRACELLULAR TRANSMISSION IN RODS AND CONES** **W.A. Hagins & S. Yoshikami. Lab. of Chemical Physics, NIADDK, N.I.H., Bethesda, MD 20892**

Both cytoplasmic free cGMP and free Ca^{++} have been proposed as light-controlled regulators of the dark current conductance of rod and cone plasma membranes. New experiments with thermochemical detectors and with new intracellular Ca^{++} buffers have led to challenges of simple forms of both the cGMP and Ca^{++} models. Some new critical tests of these models will be considered in the light of recent work from several laboratories.

W-PM-Min3 ROLES OF CALCIUM AND CYCLIC GMP IN VISUAL TRANSDUCTION IN RETINAL RODS. King-Wai Yau, Dept. Physiol. Biophys., Univ. Texas Medical Branch, Galveston, TX 77550.

We have recently performed some experiments to study the roles of Ca^{++} and cGMP in visual transduction in rods. We found that the rate of Ca^{++} efflux from a rod outer segment decreased rapidly in the light; this suggested that free Ca^{++} in the outer segment decreased rather than increased during illumination. In other experiments we found that internal Ca^{++} also did not appear to block the light-sensitive conductance directly. These results indicate that intracellular Ca^{++} does not mediate visual excitation.

In separate experiments on excised patches, we found, as did Fesenko et al[1], that cGMP activated an ionic conductance in rod membrane which resembled the light-sensitive conductance in its electrical properties. The activation of the conductance appeared to result from a direct agonistic effect of cGMP rather than to involve a protein kinase. Using a truncated, dialyzed rod outer segment preparation we were also able to verify that this cGMP-activated conductance was present in the plasma membrane of the rod outer segment, and that in the presence of GTP the conductance could be suppressed by light. We conclude that cGMP is the internal transmitter for phototransduction.

Since internal free Ca^{++} decreases during illumination, and since others have found that Ca^{++} tends to suppress the cGMP content in the rod outer segment, we think Ca^{++} most probably has a role in light adaptation.

[1] Fesenko, E.E., Kolesnikov, S.S. and Lyubarsky, A.L. Nature 313, 310-313 (1985).

W-PM-Min4 CALCIUM AND LIGHT-ADAPTATION IN RETINAL ROD PHOTORECEPTORS. T.D. Lamb, H.R. Matthews and V. Torre (Intr. by D.A. Baylor). Physiological Laboratory, University of Cambridge, Cambridge CB2 3EG, U.K., and Dipartimento di Fisica, Universita di Genova, Italy.

In order to examine the role of cytoplasmic calcium in phototransduction we have attempted to minimize the rate of change of Ca_i by trapping calcium buffer in the rod cytoplasm. A suction pipet monitors the outer segment photocurrent while a patch pipet is used to introduce the calcium buffer BAPTA (Tsien, Biochemistry **19**, 2396 (1980)). Subsequently the patch pipet is gently withdrawn and the plasma membrane reseals, leaving the buffer trapped within the rod.

With approx. 10 mM BAPTA trapped in the cytoplasm the rising phase of the light response is essentially unaltered, indicating that closure of the "light-sensitive" channels does not require a change in Ca_i. However, the turn-off phase of the light response is substantially retarded, and the time taken to reach a steady level of light-adaptation is substantially slowed. We interpret the results to indicate that the normal light-induced reduction in Ca_i plays an important role in terminating the light response and in adjusting the gain in the light-adapted state.

Ca_i presumably acts via the rod's cyclic nucleotide metabolism. During incorporation of exogenous cyclic GMP the elevated dark current and elevated Ca_i are accompanied by a pronounced increase in the duration of the light response. We interpret this to indicate a powerful effect of Ca_i on the phosphodiesterase, either directly or indirectly. Our results do not indicate whether Ca_i also acts on the guanylate cyclase, as suggested by others (Lolley & Racz, Vision Res. **22**, 1481 (1982); Hodgkin et al., J. Physiol. **358**, 447 (1985)).

W-PM-A1 RELATIONSHIP BETWEEN STATISTICAL PROPERTIES OF NOISE AND THE THERMODYNAMIC STATE OF THE NOISE-GENERATING SYSTEM. Izchak Z. Steinberg, Chemical Physics Department, Weizmann Institute of Science, Rehovot 76100, Israel

Noise in a measured signal can often be traced to fluctuations in the physical system which produces the signal. Even if the noise-generating system is at steady state, it may or may not be at thermodynamic equilibrium. If it is, detailed balance must prevail, i.e., the ongoing mutual interconversions between pairs of states in the system are individually balanced for every pair. This leads to the result that at thermodynamic equilibrium the probability $p(j/i;\tau)$ for a system which is presently in state i to be transformed into state j during the next time interval τ is equal to the probability $p(j/i;-\tau)$ that a system which is presently in state i was τ units of time earlier in state j. The equality $p(j/i;\tau)=p(j/i;-\tau)$ at equilibrium dictates that a noise signal generated by a system which is at thermodynamic equilibrium has the same statistical properties when run forward or backward in time.

To observe the time-reversal properties of noise, autocorrelation functions or power spectra are not useful since they are always the same for any signal and for its time-reverse. However, a generalized form, $G^{\alpha,\beta}(\tau)$, of the autocorrelation function of the noise signal f(t) may be used, where $G^{\alpha,\beta}(\tau)=\langle f^{\alpha}(t)f^{\beta}(t+\tau)\rangle$ and the powers α and β are chosen not to be the same. If $G^{\alpha,\beta}(\tau)$ is found to be different for a noise trace and for its time-reverse, violation of detailed balance is demonstrated, and the noise-generating system is not at thermodynamic equilibrium. This has been illustrated by some computed examples of noise produced by stationary and non-stationary systems. The time-reversal properties of noise signals might be useful for gaining information about the thermodynamic state of noise-generating systems, such as ionic channels in biological membranes.

W-PM-A2 A FERROELECTRIC ELECTRODIFFUSION MODEL FOR CHANNELS OF EXCITABLE CELLS. H. Richard Leuchtag, Department of Biological Sciences, Texas Southern University, Houston, TX 77004.

Although membrane channels of excitable cells have been studied extensively, the physical basis of their behavior remains unknown. A physical approach to excitability is electrodiffusion, but this has been inadequate when analyses are based on constant parameters. Allowing one of the parameters, the dielectric permittivity, to vary as a nonlinear function of the electric field gives rise to a new model, encompassing the properties of ferroelectricity. Ferroelectric materials possess, in some temperature range, an electric polarization in the absence of an electric field, which may be reversed by the application of an electric field. The literature shows that excitable membranes exhibit properties that are also shared by ferroelectrics, including evidence of piezoelectricity, pyroelectricity, transition temperatures, hysteresis loops and voltage-dependent birefringence. The spontaneous electrical pulses observed in single-channel preparations bear similarities to the Barkhausen pulses observed in ferroelectric materials. The hypothesis that excitable channels contain ferroelectric transmembrane units may be tested by a ferroelectric electrodiffusion model. In this model the nonlinear dielectric properties of the hypothesized ferroelectric channel unit are modeled by a polynomial (Devonshire) equation of state. This, together with Gauss's law and the Nernst-Planck and continuity equations, forms a differential equation system that may be solved for waves of electric displacement transverse to the membrane. Such a wave may be interpreted as a propagating phase transition, accompanied by the movement of ionic charges.

W-PM-A3 AN INTERMEDIATE STEP IN THE DIMERIZATION OF GRAMICIDIN A. S. Shenkel and F. J. Sigworth, Dept. of Physiology, Yale School of Medicine, New Haven CT 06510.

In high-resolution recordings of channel currents from Gramicidin A (GA) and its N-acetyl desformyl derivative (NAG) we observe brief gaps of durations ~100μs - 1ms, many of which do not represent complete interruptions of the ion flow. Furthermore, the initial openings and final closings in a burst of channel activity show similarly brief sojourns at a low but nonzero current level. The trace below shows such sojourns (arrows) in a recording from NAG channels at 200 mV in symmetrical 1 M KCl solutions; similar events are seen in GA channels, except that the frequency of gaps is ~2 orders of magnitude lower. The observed behavior is consistent with the presence of an intermediate with low conductance that may occur in the formation and dissociation of the channel dimer, such as the structure with four H-bonds proposed by Venkatachalam and Urry (J. Comput. Chem. 4:461, 1983).

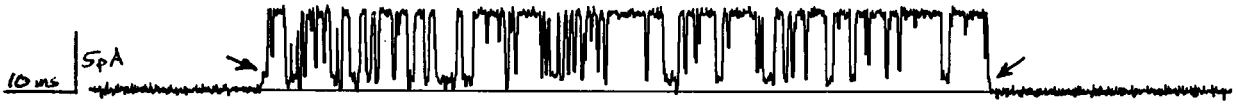

W-PM-A4 ISOLATION OF THE cDNA CODING FOR THE VOLTAGE-DEPENDENT ANION CHANNEL OF THE OUTER MITOCHONDRIAL MEMBRANE OF YEAST

Michael Forte and H. Robert Guy (intr. by Carol M. Liedpki), Department of Biology, Case Western Reserve University Cleveland, OH 44106 and Lab. Mathematical Biology, NCI NIH, Bethesda MD 20892.

The voltage-dependent anion channel (VDAC) of the outer mitochondrial membrane of yeast provides a model system in which the combined approaches of molecular genetics and biophysics can be applied to the general question of the voltage gating of ion flow through membrane channels. We have purified VDAC to virtual homogeneity from the outer mitochondrial membrane of S. cerevisae, characterized some of its molecular properties and examined its biohysical properties following incorporation into planar lipid bilayers. Using antibodies raised to the purified protein we have screened yeast genomic libraries constructed in the expression vector λgt 11. DNA sequences from phages expressing VDAC antigenic determinants were then used to screen yeast cDNA libraries. Plasmids carrying the yeast VDAC gene were identified by hybrid-select translation and immunoprecipitation. The largest cDNA insert was then sequenced by standard dideoxy techniques. The sequence contains one open reading frame producing a protein of 283 amino acids with a molecular weight of 29883. This is in good agreement with a value determined for purified yeast VDAC by SDS-polyacrylamide. Computer analysis of the VDAC amino acid sequence suggests that most of the molecule is in a β sheet conformation. By postulating approximately 18 transmembrane β strands a "β barrell" type structure can be derived which has pore dimensions consistent with those determined by biophysical analysis and electron microscopy of other VDAC molecules.

W-PM-A5 THE GENERATION OF ULTRA-STEEP VOLTAGE DEPENDENCE IN VDAC CHANNELS.

Patrick S. Mangan and Marco Colombini, Laboratories of Cell Biology, Department of Zoology, University of Maryland, College Park, MD 20742

Channels with an extremely high voltage-dependence have been generated. The addition of dextran sulfate to the medium resulted in channels whose conductance changed e-fold for a 0.5 mV change in transmembrane potential. These observations were made on the mitochondrial channel, VDAC, inserted into planar phospholipid membranes. The voltage dependence, as measured by the parameter n, increased in a concentration-dependent manner from 3.8 (no dextran sulfate) to approximately 50 (200 mg/ml dextran sulfate 8000). This is the equivalent of 50 charges moving through the entire electric field. Simultaneously, V_o, the voltage at which half the channels are closed, decreased from 22 mV to less than 2 mV. Thus the voltage independent conformational energy of the channels, nFV_o, remained rather constant. As little as 10 ug/ml increases the voltage dependence by 50%. This effect is not induced uniquely by dextran sulfate. Essentially the same results were obtained with polyaspartic acid indicating that it is the polyvalent anionic nature of the substances that induces the ultra-steep voltage dependence. Several lines of evidence support a model in which dextran sulfate accumulates at the mouth of the pore in a voltage-dependent manner. The negative charges on the polymer may interact electrostatically with the positive gating charges on VDAC and stabilize the closed state. These results represent a novel mechanism for controlling voltage-gated channels. It remains to be determined whether this phenomenon has general applicability or biological relevance.

Supported by NIH grant GM 28450 and ONR grant N00014-85-K-0651

W-PM-A6 ACTION OF COLICIN E1 ON LIPOSOMAL MEMBRANES: DETECTION BY THE EFFLUX OF CARBOXYFLUORESCEIN AND CALCEIN, AND THE INFLUX OF THALLIUM.

C. Kayalar, E. Bruggemann and N. Düzgüneş, Dept. of Chemistry, Univ. of California, Berkeley, CA 94720 and Cancer Research Inst. Univ. of California, San Francisco, CA 94143

The membrane action of colicin E1 was investigated in large unilamellar liposomes by two fluorescence assays. Colicin E1 induced the efflux of carboxyfluorescein (M_r:378) and calcein (M_r:622) from liposomes whose phospholipid composition is similar to that of E. coli. This colicin action takes place at protein to liposome ratios and within pH ranges that are physiologically meaningful. Colicin-induced permeability of carboxyfluorescein is not limited to the initial phase of colicin-membrane interaction but is sustained thereafter. These results support our earlier conclusions that colicin E1 increases membrane permeability to relatively large molecules, in addition to small ions.

Colicin E1-induced thallium influx was measured by the quenching of liposome-entrapped aminonaphthalenetrisulphonate fluorescence in a stopped-flow spectrofluorometer. The dependence of the influx rate on the colicin concentration in a log-log plot (i.e., molecularity) was found to be 0.94. This is consistent with a single colicin molecule forming the functional channel. The same technique determined the molecularities of valinomycin and gramicidin to be 1.02 and 1.97, respectively, in accordance with their known mode of action as a monomeric carrier and a dimeric channel.

W-PM-A7 SITE-DIRECTED MUTAGENESIS OF THE STRUCTURAL GENE FOR COLICIN E1. Crozel, V., Liu, Q.-R., Levinthal, C. Department of Biological Sciences, Columbia Univ., NY, NY 10027

We have continued our studies of the structure-function relationship of the ion channel produced by the bacterial toxin colicin E1 in two directions. Molecular model building of barrels made of anti-parallel twisted β-sheets and α-helices are being built and analyzed by computational methods (Fine, R., and Levinthal, C., in preparation). In attempts to evaluate these models experimentally, we have used site-directed mutagenesis with chemically synthesized oligonucleotides to determine the minimum length of the peptide fragment which shows channel activity. In addition, reactive sites are being inserted so that various chemical groups can be attached at sequential positions along the peptide chain in such a way that they can act as indicators of which residues are pointing into the lumen, which are in the lipid and which are in the aqueous phase on one side or the other of the membrane.

The active peptide has no methionine residues and new mets are inserted to provide cleavage sites for CNBr. There is only one cysteine residue in the protein and it has now been altered to valine. The mutant protein is still able to form an ion channel and kill sensitive cells. New cys codons have been substituted for codons along the chain in order to provide sulfhydril groups to which chemical attachments can be made. These mutants have all been made and present evidence indicates that a peptide which is not longer than 130 amino acids can still make an active channel. The effect on channel turn-on rate and single channel conductance of all of the mutations and the chemical attachment to the sulfhydril group of the cys will be reported.

W-PM-A8 GATING OF A MULTI-STATE, VOLTAGE-DEPENDENT ION CHANNEL: COLICIN E1. Stephen Slatin and Alan Finkelstein, Albert Einstein College of Medicine, Bronx, N.Y. 10461.

The E1 group of colicins are bacterial proteins that form voltage-dependent ion channels in membranes. Colicins E1, A and Ib are among the few protein channels which have been cloned and sequenced. We have been using colicin E1, and various chemical and genetic variants of it, to study gating. We had previously found that the channel could be destroyed by the protease pepsin from the cis side only when it was closed. This and other evidence led us to surmise that the channel opened by a voltage-driven insertion mechanism. The situation is complicated by the fact that the channel has several states, including at least 2 closed states. Under certain conditions, it is possible to cleanly resolve these 2 states, by their characteristic kinetics. The channel first closes to a shallow closed state (C_s) with a rate constant of about 20 ms, and then passes into a deeper closed state (C_d) with a rate constant of a few seconds. By alternately turning a population of channels off and on with appropriately timed voltage pulses the channels can be forced to spend essentially all of their closed time in C_s. We find that C_s and C_d are both vulnerable to cis pepsin. A possible explanation for this is that gating is a multi-step process involving the sequnetial insertion of 2 or more protein segments or monomers; if any one "de-inserts" the channel closes and the protein is exposed to the enzyme. Supported by grant GM29210 from NIH.

W-PM-A9 A VOLTAGE-DEPENDENT CHLORIDE CURRENT IN HIPPOCAMPAL PYRAMIDAL CELLS IS BLOCKED BY PHORBOL ESTERS. D.V. Madison, R.C. Malenka, & R.A. Nicoll, Dept.'s of Pharmacology & Physiology, University of California, San Francisco, CA. 94143. (Intr. by K. Miller)

Using the hippocampal slice preparation and a single-electrode voltage clamp we have identified in pyramidal cells a voltage-dependent current which is activated by hyperpolarization with an apparent time constant of 0.5 sec. This current is voltage-sensitive over a wide range. It is completely inactive at potentials positive to zero, is largely active at resting potential, and appears to be fully activated at potentials negative to -90 mV. The blockade of K^+ currents either by extracellular tetraethylammonium and/or intracellular Cs was necessary for its detection suggesting that this current is localized at a site remote from the somatic recording site. In Cl^- loaded cells depolarizing steps turn off this current resulting in an outward current relaxation which reverses at approximately +5 mV. When recording with electrodes containing the impermeant anion, methylsulfate, the reversal potential was shifted to approximately -70 mV. These data suggest that this current is carried primarily by Cl^- ions. This Cl^- current is completely blocked by phorbol esters which in other systems have been shown to activate protein kinase C. Evidence will be presented that blockade of this Cl^- current may increase electrical coupling between dendrites and soma.

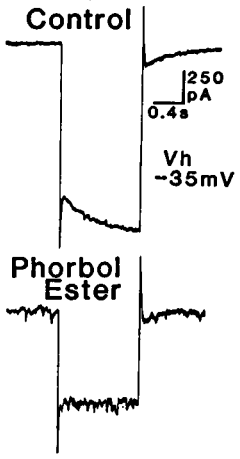

W-PM-A10 DIRECT DEMONSTRATION THAT CHLORIDE IONS ARE NOT PASSIVELY DISTRIBUTED ACROSS THE MEMBRANE OF DORSAL ROOT GANGLION CELLS OF THE FROG: PRELIMINARY STUDIES ON THE NATURE OF THE CHLORIDE PUMP. F.J. Alvarez-Leefmans, S.M. Gamiño and F. Giraldez. Laboratory of Neurobiology. Department of Pharmacology, CINVESTAV-IPN. Apdo. Postal 14-740, México 07000, D.F.

The cell bodies of sensory neurons of vertebrate dorsal root ganglia (DRG) are depolarized by GABA, and constitute a suitable model for studying the mechanisms underlying presynaptic inhibition. The GABA effect is due to an efflux of Cl^- resulting from chemical activation of a Cl^- permeability that transiently drives the membrane potential (Em) towards the Cl^- equilibrium potential (E_{Cl^-}). This implies that the intracellular free chloride concentration, $[Cl^-]_i$, must be higher than predicted from a passive distribution and an inwardly directed Cl^- pump must exist. Hitherto there is no direct evidence backing this hypothesis. We measured $[Cl^-]_i$, in frog (R. pipiens) DRG cells and studied the effect of external ions on $[Cl^-]_i$. Double barrelled Cl^- sensitive microelectrodes were used. The selective barrel contained Corning 477913 liquid sensor. The reference barrel was filled with 3M KCl or 4M K-acetate. No significant differences were found in $[Cl^-]_i$ measured with either type of filling solution. In 38 neurons (10 animals) having Em > -50 mV ($\bar{X}$ ± S.E.; 54.0 ± 0.6 mV) the apparent $[Cl^-]_i$ was 35.6 ± 0.9 mM, which is about 20 mM higher than expected for a passive distribution. The mean of the difference $Em-E_{Cl^-}$ was 23.1 ± 0.9 mV and Em vs E_{Cl^-} were uncorrelated. Replacement of external Na^+ for glucamine led to a decrease in $[Cl^-]_i$ with little change in Em. The steady state $[Cl^-]_i$ after 60 min in 0 Na^+ was 15.1 ± 4.4 mM (n=5 cells), $Em-E_{Cl^-}$ was -1.8 ± 5.3 mV, and the relation between Em vs E_{Cl^-} became linear with a slope of one. It is concluded that Cl^- is normally accumulated inside DRG cells and that this "uphill" movement of Cl^- is dependent on external Na^+. (Supported by CONACyT, Mexico).

W-PM-A11 CHLORIDE CHANNELS IN ADULT FROG SKELETAL MUSCLE. Karl H. Woll, Mark D. Leibowitz, Bertil Hille, Physiol. & Biophys., Univ. of Washington, Seattle, WA 98195 (Intr. by C.E. Stirling).

In excised, inside-out patches from Rana pipiens toe muscle, anion channels with complex gating kinetics were observed in symmetrical NaCl or tetraethylammonium-Cl solutions (110 mM). Immediately after excision many patches are silent; channels become active following depolarizations to E_m > 20 mV. Active periods are complex, characterized by a spectrum of lifetimes and multiple current levels. Channel gating is voltage dependent and graded. Channels are open at 0 mV; and closed at E_m < -90 mV. At potentials > -20 mV, complex active periods last from seconds to minutes. From histograms of currents in symmetrical NaCl (110 mM), conductance levels of 70, 260, and 320 pS were calculated. These may represent different channels or substates of a single macromolecule. Raising the NaCl concentration at the sarcoplasmic side (inside) 5-fold to 500 mM gave a reversal potential between 35 and 40 mV, indicating no permeability for Na^+. Substitution of Cl^- by $citrate^{-3}$ or $glucuronate^-$ inside did not reveal a highly specific selectivity against these anions. The permeability sequence is $P_{glucu} < P_{citr} \simeq P_{Cl}$. When applied inside, the membrane-impermeant amino group reagent DIDS (2 mM) did not remove chloride currents. The crosslinking reagent tannic acid irreversibly inhibits currents (50 µM inside); "aged" solutions of gallic or tannic acid reversibly inhibit. Exposing the inside to 110 mM NaCl + 10 mM $ZnCl_2$ reversibly inhibits Cl influx and has little effect on Cl efflux, suggesting a voltage-dependent block caused by zinc. We favor the idea that the chloride conductance described here comes from a dynamic molecule able to assume many conductance substates and with a relatively wide pore size. Supported by NIH grants NS08174, NS07097, RR00374 and Deutsche Forschungsgemeinschaft W0338/1-2.

W-PM-A12 CHLORIDE CHANNELS IN NEOPLASTIC B LYMPHOCYTES

Martha M. Bosma, Dept. Physiology, UCLA, Los Angeles, CA 90024

Ca and K channels similar to those found in nerve and muscle have recently been shown to be important in immune cell function. Using the tight seal patch recording technique on cells from a B lymphocyte line which actively secretes antibodies, I have found an anion-selective channel which is voltage-sensitive. In cell-attached membrane patches, the channel had a single 30 pS conducting level at the resting potential of the cell. There was inward rectification at potentials more negative than rest (max. g = 40 pS), and channel activity was seen in a range of +/- 100 mV relative to rest. Upon excision of the membrane patch, marked changes were observed in channel gating and conductance. Multiple conductance levels were seen in addition to the 30 pS state, predominantly a 400 pS (the largest state) and a 200 pS state. Channel opening occurred between -50 and +60 mV (symmetrical 165 Cl^-) and there was no rectification with that range. The channel tended to enter a closed state at the extremes of the voltage range. No dependence of open or closed times on internal or external Ca was seen. The channel was anion selective, and had the conduction sequence: Cl=Br (1.0)› I (.89)› glucuronate (.45). Cytoplasmic application of SITS blocked the channel: at 20 uM the closed time probability was increased, while at 200 uM high frequency flicker was seen. Application of artificial internal solutions to the cytoplasmic side of the membrane containing MgATP, cAMP, theophylline and variable Ca levels did not return the large channel to the smaller state seen in the on-cell configuration. Since it is known that the only other ion channel in these cells is a voltage-gated Ca channel (Fukushima and Hagiwara, J.Physiol. 358:255, 1985), the maintenance of the resting potential is probably an important function of the Cl channel.

W-PM-A13 MULTIPLE SUBCONDUCTANCE STATES OF A LARGE CONDUCTANCE CHLORIDE CHANNEL IN PYRAMIDAL CELLS DISSOCIATED FROM RAT HIPPOCAMPUS. P.W. Gage, A.J. Gibb & M.E. Krouse (Intr. by D.G. Stephenson), Dept. of Physiology, JCSMR, ANU, Canberra, ACT 2601, Australia.

The patch clamp technique was used to record currents from pyramidal cells mechanically dissociated (without use of enzymes) from adult rat hippocampal slices. Cells were in a solution containing (mM) CsCl, 140; HEPES, 10; $CaCl_2$, 2; $MgCl_2$ 1 (temp. 22°C, pH 7.4). The pipette solution contained 140mM NaCl instead of 140mM CsCl. A high conductance (>300pS) ion channel was observed in 8 out of 56 patches. Single channel currents reversed close to 0mV indicating that the channel is chloride selective. Channel opening probability was greatest around 0mV and decreased with polarisation in either direction. Thus the channel appears similar to the high conductance chloride channel seen in a variety of cultured cells. In 2 of the 8 patches, the channel was active in the cell-attached recording mode while in the others, activity appeared only after the patch was excised. Channel activity seemed to be unaffected by calcium concentration. In excised patches, fully open channel conductance was 577±113pS (mean ± s.e. n=6). Several "subconductance" levels were evident, the smallest being 1/12th of the maximum level and others appearing to be integer multiples of the 1/12th level. There were two types of transition between levels (bandwidth 4kHz): 1) steps of 1/12 of the maximum conductance between adjacent levels and 2) steps between non-adjacent levels, the majority of which were between the closed and fully open states. The behaviour cannot be attributed to 12 independent channels but is consistent with a channel containing 12 conducting pathways in parallel (cochannels) with a shared "gate" that can occlude some or all of the cochannels simultaneously. We propose that the properties of a variety of other channels (e.g. subconductance states) can be explained by a similar mechanism.

W-PM-A14 PERMEABILITY OF ANION CHANNELS IN RAT HIPPOCAMPAL NEURONS. F. Franciolini and W. Nonner, Dept. of Physiology and Biophysics, Univ. of Miami, Miami, FL 33101.

Excised patches taken from neurons after 8 to 24 days in culture consistently reveal spontaneous openings of low-conductance anion channels (30 pS in symmetrical 150 mM NaCl saline). The channels do not require intracellular Ca ion to open and are active at potentials between -80 and +60 mV. We have exploited these convenient properties to study ion permeation in a small anion channel. The excised patches (mostly inside-out) were stimulated with staircase voltage patterns for measuring single-channel current-voltage relations. Conductance was found to increase in approximate proportion to salt concentration in symmetrical NaCl (11, 30, 65, 130 pS for 75, 150, 300, 1000 mM). Complete substitution of Cl ion by F, Br, I, or nitrate ion shifted the reversal potential to -15.7, +8.25, +15, or +19 mV, indicating a moderate distinction between these small anions (P_X/P_{Cl}=0.54, 1.39, 1.82 or 2.12, if cation permeability is neglected). Unilateral variation of NaCl concentration (and osmolarity) consistently shifted the reversal potential into the direction expected for an anion-preferring channel; these shifts, however were smaller than expected for perfect anion selectivity (e.g. -37 mV with 75 mM internal and 1000 mM external NaCl). In order to test whether co-transport of water was contributing to this result, osmolarity was changed by neutral solutes (urea, gycerol, glucose); the resulting shifts of reversal potential were consistent with a co-transport of about 10 water molecules per unit charge. Supported by NIH grant GM30377.

W-PM-A15 SELF-REPLICATION OF A CHANNEL-FORMING PROTEIN IN VITRO. Azer Lektin and Millie Osmol, Institüt für Drükwerker in Biophysik, Ratekonstanz, FRG.

Recently, Lektin and co-workers reported that consciousness could be incorporated into planar lipid bilayers following the addition of a channel-forming protein obtained from the brains of human volunteers (1). Here, we report that when consciousness-activating factor from male (Cm) and female (Cf) donors were added simultaneously to the bath, unusual channel behavior was observed which resembled that described previously (2). Addition of the proteins was followed by a period of normal activity in which Cm and Cf channel kinetics were independent. Simultaneous channel openings were often followed by a period of rhythmic bursting activity which gradually rose to a crescendo and then abruptly descended into a period of quiescence. Typically the nonrandom superposition of channel openings occurred with Cf on top 67% of the time. This behavior has been designated as F-kinetics. Interburst duration and number of bursts per experiment varied among preparations, but was weakly correlated with age of Cm preparation. It was found that the latency to onset of F-kinetics was highly variable but could be significantly shortened by adding nonelectrolytes (eg., ethanol) and by dimming the laboratory lights. Occasionally the quiescent period was followed by the appearance of "baby" channels which resembled the originals in all parameters except that they had a smaller conductance.

1. Lektin et al., Consciousness reconstituted into planar bilayers, in Membranes: a Series of Setbacks, 1985.

2. Sex and the Single Channel, I.M. Hornie and R.U. Tu.

W-PM-B1 IDENTIFICATION OF THE FLAGELLAR MOTOR BY FREEZE-FRACTURE.

Shahid Khan, John Walrond and T.S Reese.
Laboratory of Neurobiology, NINCDS, NIH at MBL, Woods Hole, MA 02543.

The rotation of bacterial flagella is powered by a transmembrane proton potential. Thus basal flagellar structures associated with the cytoplasmic membrane are of special interest. However, basal discs isolated from solubilized membranes are devoid of the force-generation machinery (J Bact,161:836,1984). We are, therefore, using freeze-fracture to visualize the basal structures in situ. Freeze-fracture examination of the polarly tufted bacterium, A.Serpens (J Bact,136:1037,1978) had previously revealed putative motor structures. Of special interest were circlets of intramembrane particles concentrically arrayed around a central plug (presumably the flagellar rod) and depression (presumably the basal discs). We now report similar structures in two peritrichously flagellated species; the gram negative E.Coli AW405 and the gram positive Streptococcus V4051. Their occurrence per unit area of membrane, about one per two um^2, corresponds to the density expected for flagella, and they are also absent in membranes of mutants lacking flagella. These findings support the earlier conclusion that these structures correspond to flagellar motors. The structures were observed when whole cells were fast frozen, but not when cells were frozen slowly (Murray; pers comm). This discrepancy is consistent with steadily accumulating evidence that the force-generation machinery is labile (J Mol Biol, 184:645,1985; Nature,309:470,1984) and, in particular, that it is abruptly disabled at low temperatures (Cell,32:913,1983). In both species, there are approximately 16 particles in the circlet around the central plug, similar to the number observed in A.Serpens. The generality of this motif indicates that it has an important role in motor function. This deployment of particles makes them prime candidates for the transmembrane proton channels. Analysis of mutants is underway to determine what gene products correspond to the intramembrane structures seen with freeze-fracture.

W-PM-B2 PROPERTIES OF KINESIN-DRIVEN MICROTUBULE MOVEMENT.*#

Shahid Khan#, Bruce J.Schnapp# and Michael P.Sheetz*.
#Laboratory of Neurobiology, NINCDS, NIH at MBL, Woods Hole, MA 02543.
*Department of Cell Biology and Physiology, Washington University School of Medicine, St Louis, MO 63110.

A soluble protein, kinesin, which mediates the movement of beads and organelles along microtubules as well as microtubules along glass has recently been purified from squid neural tissue (Cell,42:39,1985). Kinesin-driven microtubule movement can now be examined as a function of kinesin and ATP concentrations. Movement of microtubules is assayed by video light microscopy (Cell,40:449,1985). In excess ATP and kinesin, microtubules move at a constant rate of about 0.5 um/sec. In the absence of kinesin, they do not bind to acid-cleaned glass. As kinesin concentration is increased, binding precedes movement and there is a sharp transition, above which all microtubules move at the limiting velocity of 0.5 um/sec. In the transition range microtubules are either immobile or moving at the limiting velocity. The energy per working stroke available from ATP hydrolysis is about 5x10-13 ergs. The work required to overcome hydrodynamic drag and move microtubules at the observed rates can be calculated to be about 10-15 ergs for distances on the order of 10 nm, the displacement per working stroke typical of other motile proteins. We, therefore, infer that most of the work done by kinesin contributes to breaking microtubule-glass attachments rather than to overcoming hydrodynamic drag. The fact that intermediate velocities are not observed in the transition region may imply that each kinesin generates force through most of its duty cycle. Dependance of microtubule movement on ATP concentration in an excess of kinesin fits Michaelis-Menten kinetics with a constant of 50 uM. It is of interest that the dependance of movement of myosin-coated beads on ATP takes an identical form (J Cell Biol,99:1867,1984). At very low concentrations of ATP, the variance in microtubule displacement during 10 second time intervals increases significantly. Since most of the available energy is apparently used to break attachments, it is unlikely that this variance is due to Brownian drift. Consequently, these variations have potential significance in extracting information about force-generation parameters.

W-PM-B3 MOTILITY RECONSTITUTED FROM PURIFIED PROTEINS: ATP-DEPENDENT MOVEMENT OF ACTIN FILAMENTS ALONG MYOSIN FIXED TO A SUBSTRATUM. S.J. Kron and J.A. Spudich. Department of Cell Biology, Stanford University School of Medicine, Stanford, CA 94305.

In previous work, Sheetz and Spudich (1983, **Nature 303**:31-35) measured the directed movement of myosin-coated microspheres over polar arrays of actin fibers from the alga Nitella. Myosin beads have since been observed to move on a biochemically defined actin array produced from purified actin and the protein severin (Spudich et al., 1985, **Nature 315**:584-586). In each system, myosins moved at speeds characteristic for different myosin types (4 μm/s for skeletal muscle myosin and 1 μm/s for nonmuscle myosin from D. discoideum). We have now progressed to a system consisting only of myosin, actin and fluorescent phalloidin (a specific actin label which stabilizes actin filaments). We have inverted the geometry of the system to observe single actin filaments moving over immobilized myosin thick filaments. Actin filaments move across the myosin substratum at speeds characteristic of the myosin type. The speeds were similar to those observed with myosin-coated beads moving on fixed actin filaments. The actin filaments do not reverse their direction of movement, but individual filaments move in different directions along the randomly oriented thick filaments. Single movements continue for distances ranging from a few microns (the approximate length of a thick filament) up to 50 μm.

W-PM-B4 ELONGATION OF ACTIN FILAMENTS IS A DIFFUSION-LIMITED PROCESS AT THE BARBED END BUT NOT THE POINTED END. Detlev Drenckhahn and Thomas D. Pollard, Dept. of Cell Biology and Anatomy, Johns Hopkins Medical School, Baltimore, MD and the Dept. of Anatomy, University of Marburg, West Germany.

We used the dependence of the rate of nucleated polymerization of pyrene-labeled actin upon the actin monomer concentration to determine the rate constants for elongation in a number of different solvents. The absolute values of the rate constants were determined by electron microscopy. Using either glycerol, sucrose or ethylene glycol to vary the solution viscosity, the association rate constant (k_+) was equal to 10^7 $M^{-1} \cdot s^{-1}$/viscosity (in centipoise). Consequently plots of k_+^{-1} vs viscosity are linear and extrapolate through the origin as expected for a diffusion limited reaction where the rate constant is infinite at zero viscosity. By electron microscopy we found that the inhibitory effect of glycerol is almost entirely at the fast growing, barbed end. For the pointed end plots of k_+^{-1} vs viscosity do not extrapolate through zero, so the reaction is not limited by diffusion. In contrast to these small molecules, polyethylene glycol, dextran and ovalbumin all cause a concentration (and therefore viscosity) dependent increase in k_+. At any given viscosity their effects are similar to each other. For example, at 3.5 centipoise $k_+ = 2.5 \times 10^7 M^{-1} s^{-1}$. We presume that this is due to the influence of these macromolecules on water structure. If the proteins in the cytoplasmic matrix have a similar effect, the association reactions may be much faster than expected from experiments done in dilute buffers. Supported by Research Grants from the Muscular Dystrophy Association of America and the National Institutes of Health.

W-PM-B5 Ca^{2+} AND THE N-TERMINAL STRUCTURE OF G-ACTIN. Kunihiko Konno (sponsored by Manuel F. Morales) CVRI, UCSF, San Francisco, CA 94143.

Previously we showed that the reactivity of thiols 10 and 257 of actin was a function of $[Ca^{2+}]$, with a half completion value at $10^{-8.2}$ M (Konno & Morales, PNAS, in press, 1985). We have now found that in 10^{-3} M Ca chymotrypsinolysis produces, as is well known (Jacobson & Rosenbush, PNAS, 73: 2742, 1976), a 33 kDa fragment and smaller pieces (collectively, "9 kDa"). However, we have found that one of these pieces (5-6 kDa in mass, and containing Cys-10) is tightly complexed with 33 kDa. This complex is isolatable on DE-52 and Sephacryl S-200. In this complex Cys-10 is now accessible. Release of the 5-6 kDa piece, as well as reagent access to Cys-257, increase as a function of $[Ca^{2+}]$, with half completion at $10^{-7.5}$ M.

Research supported by an AHA fellowship and CI-8, and by NHLBI-HL-16683.

W-PM-B6 ACTIN MONOMERS WITHIN F-ACTIN FILAMENTS EXCHANGE WITH BIOTIN-LABELED G-ACTIN. C.G. dos Remedios, J.E. Dennis, J.D. Pardee, A.D. Saad and D.A. Fischman. Department of Cell Biology and Anatomy, Cornell University Medical College, New York, NY 10021.

Addition of monomers to the "barbed" end of F-actin and removal from the "pointed" end is well known. This "treadmilling" is considered to be the major mechanism for the incorporation of protomers into F-actin. Recently, Oosawa (in Actin Structure and Function in Muscle and Nonmuscle Cells, Acad. Press, 1982, p. 69) observed the motion of fluorescently labeled F-actin in the light microscope. These observations included the fracture and reannealing of F-actin during Brownian motion. This spontaneous rejoining of the fractured ends suggests that protomers may incorporate into non-terminal sites on F-actin but there has been little support for such internal addition, principally because of technical difficulties. Here we report that protomers can be exchanged into F-actin. F-actin was stoichiometrically labeled via its highly-reactive cysteine (Cys-374) using an iodoacetamide derivative of biotin (Vector Labs). Biotin is smaller than commonly-used fluorescent probes (e.g. 5-IAF or 1,5-IAEDANS) and its reaction with Cys-374 does not seem to impair the ability of actin to reversibly polymerize. Biotin-labeled sites were visualized in the electron microscope by their reaction with avidin linked to ferritin. We have incubated biotin-labeled monomers with actin filaments under a variety of experimental conditions. Using this technique we can demonstrate the incorporation of a single actin monomer into an unlabeled filament. Given the time-course of this incorporation, we conclude that there is significant incorporation of actin monomers directly into F-actin, compatible with the fracture-reannealing phenomenon. Supported by NIH AM 32147 and GM 32458.

W-PM-B7 MECHANISM OF ACTIN DEPOLYMERIZATION STUDIED WITH ERYTHROCYTE SPECTRIN AND BAND 4.1.

Diane C. Lin and Shin Lin, Dept. of Biophysics, Johns Hopkins Univ., Baltimore, MD 21218

The actin in spectrin-4.1-actin complexes extracted from erythrocyte membranes is in the form of stabilized oligomers. In this study, we explore the possibility that such complexes can add on to both ends of actin filaments, stabilizing them against depolymerizing conditions. Pyrene-labelled F-actin (0.23 mg/ml) was induced to depolymerize by a 20-fold dilution into F- or G-actin buffer (monitored spectrofluorometrically). Addition of microgram quantities of complex at any point after the dilution step resulted in a decrease in the rate of depolymerization. This protective effect was dose-dependent, producing filaments that remained stable for days. The effect was counteracted by filament fragmentation caused by sonication. These results differed with those produced by cytochalasin D, which slowed down, but did not eliminate depolymerization even at high concentrations, presumably because it could prevent monomer loss at only one end of the filaments. Purified spectrin dimers plus band 4.1 also significantly inhibited actin depolymerization at molar ratios as low as 1:1:100 G-actins, while spectrin by itself had no appreciable effect. This study suggests that actin disassembly under depolymerizing conditions does not involve significant fragmentation of filaments, and the loss of monomers at the ends of the filaments can be inhibited by spectrin and band 4.1. (Supported by NIH grant GM-22289).

W-PM-B8 Ca^{++} BINDING AT THE HIGH AFFINITY SITE OF ACTIN IS IN THE NANOMOLAR RANGE

Lewis C. Gershman, Lynn A. Selden and James E. Estes, Research and Medical Services, Veterans Administration Medical Center, Albany, and Departments of Physiology and Medicine, Albany Medical College, Albany, New York 12208

Actin has been long known to have one high affinity Ca^{++} binding site per molecule. It is presently accepted, on the basis of equilibrium dialysis experiments (Martinosi et al., JBC 239:1057-1064, 1964) and on indirect fluorescence studies (Frieden et al., JBC 255: 8991-8993, 1980), that the dissociation constant for this site is about 10 μM. It is also well known that actin is easily denatured upon removal of bound cation and/or bound nucleotide, and this complicates the measurement of the affinity of actin for Ca^{++}. We have measured the Ca^{++}-binding to actin using the new fluorescent Ca^{++}-chelator Quin2 (K=60 nM) to adjust the free $[Ca^{++}]$ and to measure that dissociated from actin. The Scatchard plots are linear at higher free $[Ca^{++}]$ with some curvature at lower free $[Ca^{++}]$, which is likely due to denaturation. We estimate the dissociation constant for the actin high affinity site to be about 2 nM. Kinetic analyses of the dissociation reaction indicate that the dissociation rate constant (k_-) is on the order of 0.02 s^{-1} and that the association rate constant (k_+) is about 10^7 $M^{-1}s^{-1}$. We have confirmed the findings of others that the high affinity binding of Ca^{++} is about 4 times stronger than the binding of Mg^{++}. On the basis of our newly measured value for Ca^{++} affinity, actin may well be the strongest Ca^{++} binding protein known. This tight binding has implications for the stability of the monomer tertiary structure.

Supported by the Veterans Administration and NIH 1R01 GM-32007 01A1

W-PM-B9 CONSTRUCTION AND PERIODICITY OF THE INNER AND OUTER DYNEIN ARMS OF CHLAMYDOMONAS: NEW CONSIDERATIONS.

Jock Avolio, Stuart Arden and Peter Satir. Department of Anatomy and Structural Biology, Albert Einstein College of Medicine, Bronx, N.Y. 10461.

We have previously presented a description of doublet microtubules from Tetrahymena axonemes and a computer model derived from this data that incorporates subunit construction of the outer and inner dynein arms (Avolio et al. J. Mol. Biol. (1984), 173, 389). To generalize this description, we have observed doublet microtubules isolated from axonemes of wildtype (wt) and mutant strains of Chlamydomonas reinhardtii under improved conditions of negative staining in the presence of ATP and AMP-PCP. Wt doublet microtubules treated with 50μM AMP-PCP possess dynein arms that reveal the head, body and cape subunits previously described for Tetrahymena. Furthermore, the trans configuration of dynein arm-subfiber B attachment critical for the mechanochemical cycle is observed. Wt doublets actively move apart when membraneless axonemes are treated with trypsin and 50μM ATP so that outer and inner rows of dynein arms may be observed with respect to the 2-membered radial spoke groups. Both outer and inner arms have a periodicity ca. 24nm. To confirm this, we have observed the flagella of two mutants of Chlamydomonas lacking either the outer (pf-13A) or the inner (pf-23) rows of arms. Inner arms on pf-13A doublet microtubules have the same general subunit construction and the same periodicity as outer or inner arms of wt doublets. Likewise, the outer arms seen on pf-23 doublet microtubules have the same periodicity and subunit construction as either wt or pf-13A arms. We conclude that for Chlamydomonas both the outer and inner dynein arms are structurally similiar. As in Tetrahymena, outer and inner arms occur in a 1:1 ratio without stagger. Supported by USPHS.

W-PM-B10 ANALYSIS OF TUBULIN-CONTAINING CILIARY MEMBRANES BY REVERSE-PHASE HPLC. R. E. Stephens, Marine Biological Laboratory, Woods Hole, Massachusetts 02543.

Ciliary membranes from scallop gill contain a hydrophobic tubulin as the major protein component (Biochemistry 20:4716). Such tubulin and most other membrane proteins can be reconstituted through several cycles with little change in either protein or lipid composition (J. Cell Biol. 100:1082). Membranes solubilized in Triton X-114 can be delipidated by detergent condensation, producing a soluble protein-detergent complex (BBA, in press). This complex is isoelectrically precipitated and redissolved in 0.5% trifluoroacetic acid (TFA); alternatively, either the detergent-protein complex or chloroform/methanol-delipidated ciliary membrane proteins, are dissociated by dialysis against 6M guanidine hydrochloride-10 mM DTT, then TFA is added to 0.5%. The sample is analyzed on a Waters C_{18} μBondapak column (3.9 x 300 mm) by elution with 30%-60% acetonitrile-0.2% TFA. A typical linear gradient consists of 30-36% acetonitrile over 5 minutes, followed by 36-60% for 45 minutes, then 60% for 10 minutes, all at a flow rate of 1 ml/min and 40°C. Identified by SDS-PAGE, a major 40 kDa protein elutes at 34.3 min, β-tubulin at 36.1 min, and α-tubulin at 38.7 min, these being the most hydrophobic major protein constituents. Triton X-114 elutes at 50 min. The use of large sample volumes containing excess detergent causes specific loss of the tubulin subunits by retention on the column; a 1 ml pulse of DMSO, followed by the normal gradient, results in elution of the bound tubulins at their normal retention times. In spite of non-polar amino acid substitutions between membrane and axonemal tubulin subunits, the homologous polypeptide chains co-elute. Whatever hydrophobic domains determine the unique properties of membrane tubulin, they are not reflected as significant differences in HPLC retention time. -Supported by NIH Grant GM 20,644.

W-PM-B11 SPECTRAL ANALYSIS OF SPERM MOTION KINEMATICS

R. O. Davis and D. F. Katz
Division of Environmental Studies and Department of Obstetrics and Gynecology
University of California, Davis 95616

Sperm motion is the manifestation of a number of intra- and intercellular processes, including metabolic activity, membrane transport, cytoskeletal architecture and activity, and fluid dynamics. As such, it reflects sperm cell maturity, viability, and fertility. Micrographic analysis of sperm motion has provided valuable biological insights for over 30 years. However, analysis of kinematics has been limited primarily to the determination of average movement characteristics in the time domain. Little attention has been devoted to transient behavior or, especially, to periodic motion or frequency-domain analysis. In the present study, human spermatozoa were video recorded at 200-1000 fields/sec using Spinn Physics and NAC high-speed video cameras. Video images were digitized, and successive sperm positions were automatically determined, using a Motion Analysis Corporation ExpertVision system. Resulting instantaneous linear and angular velocities of individual spermatozoa were analyzed using a Spectrum Engineering Personal Acoustics Lab signal processing system (PAL). Results show that the spectral properties of sperm motion in semen are not stationary. Amplitude and frequency are modulated, usually over a 50-100 msec period. Strong fundamental frequencies resulting from the periodic flagellar beat are seen from 10-40 Hz. Numerous harmonics extend to 70-80 Hz, and are indicative of the complex motion of the flagellum. Despite large variability within and between spectra, frequency domain feature extraction may allow us to partition variability into classes of movement. Linear models are now being investigated. (Supported in part by NIH HD12971)

W-PM-B12 *A PLAUSIBLE MECHANISM FOR FLAGELLAR ROTATION IN BACTERIA.* *Terence Wagenknecht, Wadsworth Center for Laboratories and Research, New York State Department of Health, Albany, New York 12201.*

Flagellated bacteria swim by rotating their helically-shaped flagellar filaments thereby generating a thrust in a propeller-like manner. The mechanism which produces such rotational motion is unknown. The flagellar basal body, a system of coaxial rings and a central shaft embedded in the cell wall and connected to the filament, evidently forms, at least in part, the energy-transducing rotary motor. A proton-motive force (PMF) is the immediate energy source for the motor in most bacteria. I propose a mechanism for the motor in which rotation is generated when a multisubunit component of the basal body, one of the rings or rods, undergoes a change in quaternary structure such that a net twist is introduced between the two ends of the structure; I call this component the "twistor". There are many documented examples of such structural transitions, for example, the contractile tails of some bacteriophages. By postulating a cyclic series of ligand-binding interactions between the twistor in its two conformations and protons and immobile components of the motor (stators), it is possible to generate continuous rotational motion powered by the PMF. The model readily accounts for the ability of flagella to rotate both clockwise and counterclockwise, a troublesome point for most other proposed mechanisms. Formally, the model I propose is similar to currently popular theories of active transport and muscle contraction. *Supported by NIH grant 1R01 GM29169.*

W-PM-B13 MORPHOGENETIC SEQUENCES IN PARTICLE SUSPENSIONS. N.S. Jaikaria and S.A. Newman, Department of Anatomy, New York Medical College, Valhalla, NY 10595 (Intr. by Lawrence Herman)

Matrix-driven translocation (MDT) is a biophysical process by which cells and nonliving particles are conveyed selectively from one region to another of a compositionally nonuniform collagen-fibronectin matrix [Newman, S.A. et al., Science 288, 885 (1985)]. We have now determined that MDT is a special case of a more general morphogenetic property of particle suspensions. A droplet of a suspension of 6 μm polystyrene latex beads in a physiological buffer is placed contiguous with a droplet of the same buffer lacking beads. Within seconds a coherent front of suspended beads enters the vacant fluid. This is the first of a succession of spatial patterns attained by the beads over a period of 90 minutes before they achieve a time-independent configuration within the confluent droplets. The rate and form of this morphogenetic progression is influenced by both bead concentration and pH of the medium, suggesting that the driving force for the changes is interfacial tension. If type I collagen is present in the initial droplets, the sequence of pattern changes occurs as in the absence of collagen, but is arrested at a nonequilibrium intermediate state because of gelling that results from collagen fibrillogenesis. The arrest in pattern occurs earlier in the sequence the greater the collagen concentration. At a collagen concentration of 1.7 mg/ml the system enters a "biological" regime: the initial movement of the bead front becomes absolutely dependent on an interaction between heparin-like components of the particle surface and the NH_2-terminal heparin binding domain of fibronectin, which must now be present in the fluid droplet that initially lacks particles. Under these conditions the system exhibits MDT.

W-PM-B14 MAMMALIAN CELL SPREADING AT OIL-WATER INTERFACES. **Charles R. Keese and Ivar Giaever, General Electric Research and Development Center, P.O. Box 8, Schenectady, NY 12301**

Anchorage-dependent mammalian cells can be cultured using as a substrate the protein layer that spontaneously forms at the liquid-liquid interface between fluorocarbon fluids and tissue culture medium. A protein film, sufficiently strong to support cell growth, does not occur on purified fluorocarbon fluids but requires the presence of trace amounts of polar, surface active compounds. By the addition of varying quantities of pentafluorobenzoyl chloride to alumina-treated fluorocarbon fluids, interfacial substrates have been produced that differ in their ability to support cell spreading as determined by measurement of the projection areas of cells using a Zeiss IBAS image analysis system. We have produced a variety of interfacial substrates that range from those indistinguishable from conventional solid tissue culture supports to those unable to support any measurable spreading of 3T3 fibroblasts. The surface shear moduli and surface fracture points of these adsorbed protein layers have been directly measured using a modified surface viscometer. Together, these studies have allowed us to define the minimal mechanical properties required of a substrate to support the forces involved in cell spreading.

W-PM-C1 FROZEN, UNSTAINED ACTIN AND THIN FILAMENTS HAVE ANGULAR DISORDER. David L. Stokes and David J. DeRosier, Rosenstiel Center, Brandeis University, Waltham, MA 02254.

Single actin filaments contain helical disorder, which gives rise to a 12° RMS deviation (<d>) in the angular positions of individual actin subunits. This disorder, termed cumulative angular disorder, is present in negatively stained single filaments both of actin and of actin + troponin (Tn) + tropomyosin (Tm) (<d>=15°). The disorder is absent in filaments frayed from the acrosomal process of Limulus sperm, and in filaments of actin + the S1 fragment of myosin. Since adsorption to a carbon film, negative stain and air drying are all possible sources of structural artifacts, we have studied filaments prepared by alternate methods. First, we studied Pt/C replicas of actin filaments that had been rapidly frozen and etched (courtesy of J. Heuser); this technique eliminates the effects both of negative stain and of room temperature drying. Angular disorder measured in freeze-etched actin (<d>=12°) agrees quite well with that in negative stain. The results both from negatively stained and from freeze-etched filaments were obtained by measuring layer line intensity ratios (1st:6th) as a function of filament length. Next we studied filaments both of actin and of actin+Tn+Tm in the frozen-hydrated state (courtesy of P. Flicker). This technique eliminates the effects of film adsorption, of negative stain, and of air drying. The low electron dose used to photograph frozen-hydrated filaments, however, results in a low signal-to-noise ratio along the layer lines. So, rather than measuring layer line intensities, we used layer line positions to calculate the helical symmetry of individual filaments of approximately equal length. The statistical spread in these symmetries is proportional to <d>. Measurements from 20 actin filaments indicate <d>=9°; those from 18 actin+Tn+Tm filaments indicate <d>=13°. These results confirm the hypothesis that angular disorder is intrinsic to the structure of actin. (NIH GM26357)

W-PM-C2 HIGH RESOLUTION COLOR GRAPHICS SIMULATION OF MUSCLE CONTRACTION. Max Schaible, Lillian Goodman, Richard Ludescher, Joel Neisen, Carl Polnaszek, and David D. Thomas, Departments of Chemistry and Biochemistry and University Computer Center, University of Minnesota, Minneapolis, MN 55455.

We have used the program MOVIE.BYU running on a Cray-1 supercomputer to simulate the three dimensional structure and lattice architecture of the muscle proteins. Given geometries of initial and final structures, this program can generate intermediate forms. It can therefore be used to generate a dynamic picture of the motion of individual proteins and protein assemblies. Using geometric data from X-ray diffraction and electron microscopy and dynamic data from EPR and phosphorescence anisotropy, the simulation presents dynamic models of several aspects of muscle contraction: the motion of individual crossbridges on a myosin filament, the steric blocking model for muscle activation, and several current models for the force generating crossbridge power stroke. The computer generated pictures have been photographed and collected into a short film which will be presented. Although the primary value of the film is educational, the development of accurate three dimensional computer simulations for each of the current models of force generation may prove helpful in formulating the essential distinguishing features of each.

W-PM-C3 THREE-DIMENSIONAL RECONSTRUCTION OF RIGOR INSECT FLIGHT MUSCLE USING THIN, OBLIQUE, TRANSVERSE SECTIONS. Taylor, K. A.[1], Reedy, M. C.[1], Reedy, M. K.[1] and Crowther, R. A.[2] [1]Anatomy Dept., Duke Univ. Med. Center, Durham, NC 27710, U. S. A. and [2]MRC Lab. of Molecular Biology, Cambridge, U. K.

The oblique section 3-D image reconstruction method (Crowther, Ultramicros. 13, 295 (1984)) offers advantages over more conventional methods combining multiple tilted views, in that a complete reconstruction is possible with a single image, the reconstruction is unaffected by section thinning due to electron irradiation, and the missing cone problem is overcome. Its major limitation is that sections must be thin relative to the unit cell dimension normal to the section plane. We have used this technique to analyze thin (~15nm thick) sections of insect flight muscle in the rigor state. The oblique angle of sectioning ranged between 1.5 and 6.7 from exactly transverse. The reconstructions are in general agreement with the 3-D reconstruction of the thin longitudinal section MYAC layer (Taylor et al., Nature 310, 285 (1984)) as well as an unpublished MYAC layer reconstruction which included data derived from thick sections to fill in the missing cone. Two classes of rigor crossbridge are observed. The lead bridge is somewhat triangularly shaped with a vertex on the thick filament and one edge in contact with the actin filament. The rear bridge is smaller, somewhat more uniform in shape and less angled than the lead bridge. Supported by NIH grants GM30598-03F1 and AM14317. KAT is an Established Investigator of the American Heart Association.

W-PM-C4 EVIDENCE FOR A PHYSIOLOGICAL ROLE OF TITIN AND NEBULIN IN SKELETAL MUSCLE

R. Horowits, E.S. Kempner, M.E. Bisher and R.J. Podolsky, NIADDK, NIH, Bethesda, MD 20892

Passive and active tension generation in skinned rabbit psoas muscle were studied by radiation inactivation and target analysis. This technique consists of exposing frozen biological material to ionizing radiation and observing the dose-dependent decay of biological function. For simple systems this decay is exponential, and the size of the functional unit, or target, is directly proportional to the rate of exponential decay. In skinned fibers that have absorbed 1 Mrad of radiation, resting tension and maximum calcium-activated force were both less than 20% of their control values. Target analysis yielded molecular weights of 3.2×10^6 for active tension and 3.4×10^6 for passive tension. The similarity of these target sizes suggests that common structural elements are involved in active and passive force generation. Gel electrophoresis of homogenates from irradiated skinned bundles revealed that the large proteins titin and nebulin are almost completely degraded by 1 Mrad of radiation, the two proteins disappearing with target sizes of 5.7×10^6 and 1.7×10^6 Da, respectively. In contrast, myosin heavy chain, actin and α-actinin suffer only minor degradation at this dose. H-zones are generally well defined in electron micrographs of fibers stretched and fixed after absorbing 1 Mrad of radiation, indicating that the thin filaments and Z-discs are largely intact. However, in irradiated fibers the thick filaments are no longer in register at the center of the sarcomere. This disorder is markedly amplified by Ca^{++} activation, leading to almost complete disappearance of the I-band. Together, these observations suggest that a megadalton structure containing titin and/or nebulin provides axial continuity for the production of resting tension upon stretch and also keeps the thick filaments centered within the sarcomere during generation of active force.

W-PM-C5 BIREFRINGENCE OF MECHANICALLY SKINNED FROG FIBRES IN RELAXING AND RIGOR SOLUTION. M. Peckham & M. Irving. Department of Biophysics Kings College London 26-29 Drury Lane LONDON WC2B 5RL

Single fibres were placed between crossed polarisers and a 20μm spot in the centre of the fibre was illuminated. Optical retardation (birefringence x optical path length) was measured by a null method using a Babinet-Soleil compensator. Path length was measured simultaneously by collecting scattered light from the side with a second microscope. In relaxing solution (sarcomere length 2.3μm 8°C), birefringence was $1.46 \pm 0.02 \times 10^{-3}$ (mean ± SEM, n=6). This is lower than the value for intact fibres ($2.2 \pm 0.04 \times 10^{-3}$, n=12). The difference is mainly due to the inverse dependence of birefringence on fibre volume as can be demonstrated by osmotic compression of the filament lattice of skinned fibres with Dextran.

In rigor solution, the birefringence increased to $1.72 \pm 0.03 \times 10^{-3}$ but fibre volume was only 81.4% ± 1.1% of that in relaxing solution. This change in volume would itself produce a birefringence increase. Assuming that a given concentration (g/l) of Dextran T-500 and PVP-40 have the same osmotic pressure (Maughan & Godt, Biophys.J. 28, 391, 1979), fibres in relaxing solution with 30g/l Dextran have the same lattice spacing as those in rigor solution (Matsubara. Goldman & Simmons, J.Mol.Biol. 173, 15, 1984). The birefringence of relaxed skinned fibres in the presence of 30g/l Dextran was $1.87 \pm 0.03 \times 10^{-3}$. Comparing values for which the lattice spacing is the same, there is about an 8% decrease in birefringence for a relaxed to rigor transition. This data is consistent with the long axis of crossbridge heads being more parallel to the thick filament backbone in relaxed than in rigor muscle. This research was carried out during the tenure of a Postdoctoral Fellowship by M. Peckham from the Muscular Dystrophy Association.

W-PM-C6 LINEAR DICHROISM OF SKELETAL MUSCLE FIBERS DURING ISOMETRIC CONTRACTION.

Alfred F. Leung, Department of Physics, The Chinese University of Hong Kong, Hong Kong.

A laser light diffractometer with 1 ms time resolution has been developed to measure directly changes in linear dichroism of single skeletal muscle fibers of frog during fixed-end twitches. Active tension, sarcomere length and diffraction intensity during the twitch are also measured. After the fiber is stimulated with an electrical pulse, the dichorism rises quickly and reaches a maximum near the midpoint of shortening of the fiber. It then decreases to a minimum which is below that of the resting fiber. The minimum occurs near the peak of shortening. The difference between the maximum dichorism of the active fiber and the dichorism of the resting fiber decreases with sarcomere length. The difference becomes zero when sarcomere length is around 3.6 um. The dichoric signal of the active fiber can be explained by molecular conformational changes and the movement of heavy meromyosin toward actin. The increase in dichorism during the early phase of shortening is interpreted to be largely due to molecular conformational changes associated with filament activation. The decrease in dichorism near the peak of shortening might be attributed to the position of heavy meromyosin because conformational changes are expected to be small near the peak of shortening.

W-PM-C7 OPTICALLY DISTINCT PHASES OF LATENCY RELAXATION IN ISOLATED FIBERS OF SKELETAL MUSCLE. Mark Sharnoff, University of Delaware. The optical concomitants of the processes which become active when a skeletal fiber is stimulated can be imaged holographically. Two phases can be distinguished according to the intensity with which they appear in the differential images. The latency interval is marked by weak images whose gradually increasing intensities reflect primarily submicroscopic motions within the fiber. The onset of active tension is heralded by a sudden intensity increase which announces that the displacements are becoming large enough to be resolved in the microscope. The depth of latency relaxation is maximal in fibers stretched to striation spacing of 2.7-3.1 μm, and at these lengths a third optical phase interposes: there is a sudden and brief drop to nearly zero image intensity at the end of the latency interval, and the filamentary pattern which prevails during the other two phases is momentarily replaced by speckle. Initially this phase was noticed in frog semitendinosus fibers, whose lengths are ≈10 times the diameter of the microscope's field of view. It was not easy to dismiss the possibility that this phase was an artefact of momentary cancellation, while active contraction was overcoming latency elongation, of small displacements unnoticeably transmitted from portions of the fiber beyond the field of view. Recent experiments performed on frog toe muscle fibers short enough to fit entirely within the field of view eliminate such possibility, but still reveal the third phase.

W-PM-C8 EFFECTS OF DECREASED MUSCLE ACTIVITY ON THE VELOCITY OF SHORTENING AND MYOSIN ISOZYME COMPOSITION OF SINGLE FIBERS FROM MAMMALIAN FAST AND SLOW MUSCLES. P.J. Reiser, C.E. Kasper* and R.L. Moss, Schools of Medicine and Nursing*, Univ. of Wisconsin, Madison, WI 53706.

To study the effects of a decrease in normal muscle activity (hypokinesia) on the properties of mammalian skeletal muscles, adult rats were subjected to 28 days of hindlimb suspension (HS). We examined the velocity of shortening (V_{max}), myosin isozyme composition, and fiber type using myosin ATPase histochemistry in a total of 120 single fibers from hypokinetic and age-matched, non-suspended, control slow-twitch soleus (SOL) and fast-twitch plantaris (PL) muscles. Hyokinesia was accompanied by decreases of 15% in mean body mass, 45% in mean SOL muscle mass and 15% in mean PL muscle mass (all significant at $P < .005$) compared to control values. The mean V_{max} was 31% faster ($P < .025$) for the hypokinetic compared to the control SOL fibers. V_{max} was not different between the hypokinetic and control PL fibers. The myosin isozyme composition was examined using SDS-PAGE. The fibers from each group of hypokinetic and control SOL and PL muscles which had high V_{max} values also contained the fast type MHC while the slower fibers in each group contained exclusively the slow type MHC. There was a marked increase in the synthesis of fast type myosin heavy chains (MHC) in fiber bundles from hypokinetic SOL compared to control SOL. The MHC composition of bundles from hypokinetic PL and control PL were the same except for a slight decrease in the amount of slow type MHC in the hypokinetic bundles. The results demonstrate that (1) hypokinesia induced by 28 days of HS selectively affects the SOL compared to the PL muscles, and (2) following HS the SOL fibers have a greater mean V_{max} and an increased fast type MHC content. Supported by grants from NIH.

W-PM-C9 EVIDENCE FOR THIN FILAMENT-LINKED REGULATION OF MAXIMUM SHORTENING VELOCITY (V_{MAX}) IN SKINNED SKELETAL MUSCLE FIBERS. R.L. Moss, J.D. Allen and M.L. Greaser, University of Wisconsin, Madison, WI 53706.

The effect of Ca^{2+} upon V_{max} has been investigated in skinned single fibers from rabbit psoas muscle. Slack test data obtained during maximal activation at pCa 4.50 fit a single straight line and yielded a mean V_{max} of 4.44 ± 0.15 muscle length/s (ML/s). However, at lower levels of Ca^{2+} activation, these plots were biphasic, containing a high velocity phase for shortening less than 60-80 nm/half-sarcomere and a low velocity phase for greater extents of shortening. V_{max} during the high velocity phase was little changed when pCa was increased to 6.00 but decreased when Ca^{2+} was lowered further. V_{max} during the low velocity phase decreased as Ca^{2+} was lowered within the entire range of pCa's studied, to a minimum of 0.35 ± 0.09 ML/s at pCa 6.2. The degree of thin filament activation at a given pCa was also varied by partial extraction of troponin-C (TnC) such that isometric tension at pCa 4.50 was about 65% of control values. Partial extraction of TnC altered the plots of slack test data obtained at pCa 4.50 to the biphasic form. V_{max} during the high and low velocity phases of shortening was reduced at each pCa < 4.5. When plotted versus steady isometric tension (as percent maximum control tension, P_o), V_{max} values obtained in the control and extracted fibres were in good agreement. Fibers were also activated in the absence of Ca^{2+} by partial removal of whole Tn complexes. At pCa 9.0, these fibers developed steady tensions less than 30% P_o and underwent biphasic shortening, indicating that this phenomenon cannot be the result of shortening-induced dissociation of Ca^{2+} from TnC. Thus, Ca^{2+} has been found to have a marked effect upon V_{max}, and the magnitude of this effect varies depending on the extent of prior shortening. (Supported by NIH and AHA).

W-PM-C10 CALCIUM SEQUESTRATION IN FROG SARTORIUS MUSCLE AT 0°C CORRELATED WITH UNEXPLAINED ENTHALPY REVERSAL. AN ELECTRON PROBE MICROANALYSIS STUDY. John McD. Tormey and Earl Homsher, Dept. of Physiology, School of Medicine, UCLA, Los Angeles, CA 90024.

It has been postulated that Ca binding to troponin and parvalbumin are the source of the unexplained enthalpy (UE) that is measured during tetanus and recovery. We have tested this hypothesis by using electron probe x-ray microanalysis (EPMA) to measure the time course of Ca sequestration during recovery from a 6 sec tetanus, and by correlating the results with those from a companion study in which time course of UE reversal was measured. If the hypothesis is correct, and if there are no other Ca binding sites involved, Ca sequestration and UE reversal should have the same time course. Sartorius muscles were obtained from the same batch of Rana temporaria used for the UE measurements, and all experiments were carried out at 0°C. Muscles were frozen either at rest, 5 secs into the tetanus, or 2, 8, 16 or 30 secs after ceasing stimulation. EPMA measured the total concentrations of Ca and other elements in different regions, namely, sarcoplasm as a whole, I bands, H bands, and AI overlap regions. Total Ca concentrations increased markedly within each of the myofibrillar regions during tetanus. When muscle tension had just returned to rest level (2 sec after last stimulus), one-third of the Ca released had been sequestered. This initial rate of sequestration is sufficient to account for relaxation without having to invoke a role for parvalbumin as an soluble relaxing factor. At later time periods progressively larger amounts were sequestered, until at 30 secs sequestration was virtually complete. This correlates well with the 30 sec time course of UE reversal (E. Homsher et al., Biophys. J. 47:293a, 1985). (Supported by MDA and by NIH HL31249 and AM30988).

W-PM-C11 CALCIUM-DEPENDENT TENSION DEVELOPMENT IN THE TnC-EXTRACTED FIBERS IN LOW IONIC STRENGTH (LIS): EVIDENCE FOR MYOSIN LINKED REGULATION IN VERTEBRATE MUSCLE.
J. Gulati and A. Babu, Department of Medicine, Albert Einstein College of Medicine, Bronx NY 10461

The dominant role of the thin-filament based regulation for the tension control under physiological conditions in vertebrate muscle is well established, but the question still remains whether a second myosin-linked regulation is also present. In this study we give evidence for such a second system in low ionic strength (LIS). Psoas fibers from Syrian Golden hamsters were used. The skinned fibers are maximally activated with pCa5-4 in 180mM ionic strength. They also made force in LIS (40mM ionic strength) even in the absence of Ca and this Ca-free force was abolished in high Mg (Gulati: Biophys. J., V. 43, 1983; also, Gulati and Babu: Biophys. J. V. 47, 25a, 1985). On extracting the TnC, the fibers remained relaxed in pCa4 in 180mM ionic strength. This is expected since Ca-binding to TnC is presumably the initial step in the physiological mechanism of thin filament regulation. Ca-sensitivity was recovered in the fiber after restoration with exogenous TnC (Babu & Gulati, this volume). We find that the Mg-dependent force in LIS was also blocked after TnC extraction, which indicates that TnC was required for the Ca-free activation as well. This suggests that the mechanism for Ca-free activation also utilizes the thin filament based regulatory system. Surprisingly, however, the TnC extracted fiber still showed sensitivity to Ca in the LIS solution and gave force with pCa5-4. In contrast with the Ca-free force in LIS in normal fibers, the Ca-sensitive force in the TnC-extracted fibers was insensitive to Mg. Since the thin filament based regulation system is locked in the 'off' state (by the TnC removal), our findings raise the possibility that an alternative, myosin-based, regulatory system then controls the activation of the fiber and in the present case requires both LIS and calcium. (Grant Support: NIH AM33736 and HL18824)

W-PM-C12 THE RISE OF UNLOADED SPEED OF SHORTENING FOLLOWING THE END OF LATENCY RELAXATION IN LIVING SINGLE MUSCLE FIBERS. F.J. JULIAN, Department of Anesthesia Research Laboratory, Brigham and Women's Hospital, Boston, MA.

Previous results have shown that the speed of unloaded shortening is already at a near maximum level (V_{max}) early in the rising phase of a contraction (Julian and Sollins, Cold Spring Harbor Sym. Quant. Biol. 37:635-646), subsequently confirmed by others. These results can be taken to indicate that calcium does not influence cross-bridge kinetics. However, recent results from living frog fibers (Close and Lannergren, J. Physiol. 355:323-344, 1984) indicate that the myoplasmic Ca^{2+} signal as indicated by Arsenazo III rises well ahead of the tension signal and reaches the half-maximum level before the development of positive tension following latency relaxation (LR). Experiments are now underway to examine in more detail the early onset of speed of shortening (SOS) in living fibers obtained from the ant. tib. muscle of the frog (R. temporaria). Following electrical stimulation, the experimental aim is to measure SOS while a servo system clamps the force at the initial resting level. Preliminary results have been obtained at temperature 2.5-5°C and average sarcomere length 2.2-2.4 μ. Fully activated V_{max} has been obtained using both the "slack test" technique and extrapolation of a curve fit to steady state force-velocity points. Current servo imperfections have limited the earliest reliable speed measurements to 3-5 ms following the end of LR. Under these conditions, the initial SOS has been high, but has so far been consistently slightly below the fully activated V_{max}. One possible interpretation of these results is that calcium may influence cross-bridge kinetics, but that such an effect is very hard to observe in living fibers due to the extremely rapid rise of activation following stimulation. This work supported by NIH grant HL35032.

W-PM-C13 INFLUENCE OF PARTIAL ACTIVATION ON FORCE-VELOCITY PROPERTIES OF FROG SKINNED MUSCLE FIBERS IN 2 mM MAGNESIUM ION. R.A. Podolin and L.E. Ford. Univ. of Chicago, Chicago, IL 60637

Briefly glycerinated semitendinosis fibers from Rana pipiens were activated rapidly by a short exposure to 2.5 mM free calcium followed by a solution containing calcium buffered with 5 mM EGTA to produce the desired level of force. Steps to isotonic loads were made using a servo motor, usually at 3-5 s after the onset of activation. The relative isotonic forces (P/Po) and velocities were measured for a 15 ms period beginning 20 ms after the step. Contractions obtained under similar circumstances were grouped together and fitted with hyperbolic functions. Solutions contained 6 mM $MgCl_2$, 5 mM ATP, 151 mM K-propionate and 10 mM imidazole buffered to pH 7.2 at 3-5°C. There was no significant difference in the relative force-velocity relations obtained at full activation compared with partial activation when developed force was about 40% of its full value. Control experiments showed that a variety of factors did not influence either the relative force-velocity relations or the finding that partial activation did not change these properties. The factors investigated included the decline in force that occurs with each successive contraction of skinned fibers, the segment length (over a range of 1-3 mm), sarcomere length (over a range of 1.9 - 2.2 μm), the MgATP concentration, the presence of free calcium, and the age of the preparation (up to 30 h). Attempts to repeat earlier experiments showing a dependence of shortening velocity on activation could not be repeated because the low ionic strength used in those experiments caused the fibers to break after a few contractions. The main conclusion, that shortening velocity is independent of the level of activation is consistent with the hypotheses that the cross-bridges act independently and that activating calcium acts only as an all-or-none switch for individual cross-bridge attachment sites, and does not otherwise influence the kinetics of cross-bridge movement.

W-PM-C14 A MOLECULAR MODEL FOR FORCE DEVELOPMENT AND MOTION IN THE ATP-DRIVEN ACTOMYOSIN SYSTEM IN MUSCLE. Neil B. Ingels, Jr., Department of Bioengineering and Physiology, Research Institute, Palo Alto Med. Fdn., Palo Alto, CA 94301

A molecular model is proposed which integrates the structure and biochemistry of the contractile proteins and their assemblies in muscle. The fundamental premise of the model is that the S1 head of each myosin molecule functions as a Coulombic motor consisting of a fixed stator (which binds F-actin and nucleotide) and a movable rotor which is capable of rotating through large angles (up to 135 degrees) with respect to the stator. Force is generated by the Coulombic attraction between two opposite charges buried in a small (6 Angstrom radius), low-dielectric (ε = 6) interior region of the myosin head, one positive charge bound to the stator and one negative charge bound to the rotor. The *net* charge in the vicinity of the stator charge is modulated by the presence or absence of the negatively charged terminal phosphate group (P_γ) of MgATP which binds in the nearby nucleotide binding site. This modulates the torque developed by the rotor with respect to the stator in an all-or-none fashion and thereby regulates the development of contractile force. Force is coupled between the actin and myosin filaments through a spring at the myosin S1/S2 junction which is capable of stretching approximately 100 Angstroms. This coupling is stiffer in tension than in compression due to assumed S2 compressive buckling. The contractile force developed by a single myosin head is a highly nonlinear function of its binding position on F-actin relative to its origin on the myosin filament and has a maximum value of 7.275 pN. The full power stroke of a single myosin head is 205 Angstroms and the maximum work associated with this stroke is 82% of the maximum Gibbs free energy from the hydrolysis of one molecule of ATP. A Monte Carlo simulation of 3650 single-headed myosin molecules interacting with a like number of actin filaments is used to predict the behavior of this model with a 1 msec time resolution and 0.1 Angstrom spatial resolution. Each myosin head is assigned to one of five biochemical states in accordance with a set of probabilistic rules relating to the occupancy of the actin- and nucleotide-binding sites, with two free states and three bound states (one weak-binding and two strong-binding), and two force-generating and three non-force-generating states. The model is shown to fit the data from quick stretch and release experiments, fit the force-velocity relationship at physiological and low concentrations of MgATP, predict the fraction of bridges in three bound states as a function of contraction velocity, fit the relationship between ATP hydrolysis and work (and predict some new features of this relationship), fit the relationship between ATP splitting rate and contraction velocity, and fit the relationship between efficiency and contraction velocity. The model exhibits a maximum thermodynamic efficiency of 48%.

W-PM-D1 SOLVENT AND SEQUENCE INFLUENCE ON THE CONFORMATION AND STABILITY OF A·A AND T·T MISMATCHES IN A DNA OLIGONUCLEOTIDE. F. H. Arnold, S. K. Wolk, P. Cruz, I. Tinoco, Jr., Department of Chemistry, University of California, Berkeley, CA 94720.

The conformations and thermodynamics of the self-complementary dCCCAGGG and dCCCTGGG duplexes containing an A·A and a T·T mismatch, respectively, have been investigated in water and several organic solvents using NMR and UV absorption spectroscopy. The base protons and the H1', H2' and H2" sugar protons in the NMR spectra of the two duplexes have been assigned. 2-D and 1-D Nuclear Overhauser Effect (NOE) experiments have been used to determine the duplex conformations. In water, both mismatched base pairs are incorporated into the double helix. The mismatched bases significantly decrease the stability of the parent dCCCGGG molecule, as determined by optical measurements. The A·A mismatch (T_m~35°C; 10^{-3} M, 0.2 M $NaCl_2$, pH 7.0) destabilizes the duplex to a significantly greater extent than the T·T pair (T_m~49°C; 10^{-3} M, 0.2 M NaCl, pH 7.0). This behavior is in contrast to the results of an earlier study which showed comparable destabilizing effects for A·A and T·T mismatches flanked by A·T base pairs [1]. Organic solvents alter the stabilities of these imperfectly paired DNA oligomers. The influence of the solvent environment on the duplex thermodynamcis and conformations of the mismatches will be discussed.

[1] Aboul-ela, F., D. Koh, I. Tinoco, Jr., Nucl. Acids Res., 13, 4811, 1985.

W-PM-D2 DOUBLE-STRANDED RNA CAN ASSUME TWO DIFFERENT LEFT-HANDED Z-CONFORMATIONS P. Cruz, K. Hall, E. Leonhardt, J. Puglisi, M. O. Trulson, and I. Tinoco, Jr., Department of Chemistry, University of California, Berkeley, CA 94720

In 4M $MgCl_2$ the double-stranded RNA polymer poly[r(G-C)] undergoes a transition to a new form characterized by a circular dichroism (CD) spectrum which closely resembles that of Z-DNA. The distinguishing features of this spectrum are an inversion of the band at 230 nm from negative to positive, a large decrease in the positive band at 265 nm relative to the negative band at 295 nm, and loss of the shoulder at 275 nm, compared to the CD spectrum of the polymer in A-form. This new conformation will be called Z_D-RNA to distinguish it from Z_R-RNA which has previously been observed in high concentrations of $NaClO_4$ or NaBr, and which displays a markedly different CD spectrum. The Raman spectrum of the polymer in 4M $MgCl_2$ shows a diminution of the phosphodiester stretch at 810 cm^{-1}, and a shift in the guanine ring mode from 671 cm^{-1} to 641 cm^{-1}, compared to the A-form. These are the same Raman Z-form markers seen with the Z_R-RNA conformation. The Z_D-RNA and Z_R-RNA Raman spectra differ in several ways, most notably the loss of the band at approximately 1100 cm^{-1}, indicating some structural differences between the two forms. Both proton and phosphorus NMR spectra are also consistent with a left-handed Z-form for the polymer in 4M $MgCl_2$, but again there are some differences between the spectra obtained under Z_D vs. Z_R conditions.

W-PM-D3 STABILIZATION OF LEFT-HANDED Z-RNA AT PHYSIOLOGICAL IONIC STRENGTH. C. C. Hardin*, D. A. Zarling**, J. D. Puglisi*, M. O. Trulson*, and I. Tinoco, Jr.,* Dept. of Chemistry* and the Naval Biosciences Laboratory,** University of California, Berkeley, CA 94720.

Spectroscopic studies have demonstrated that poly[r(C-G)] can exist in three different conformations depending on the solution conditions. In 10 mM sodium phosphate or Tris buffers, the polyribonucleotide adopts a right-handed A-form. However, in 6 M $NaClO_4$ or NaBr buffer at 45°C, circular dichroism (CD), NMR and Raman scattering spectra are consistent with a left-handed Z-RNA (Z_R) structure. In 4 M $MgCl_2$, the polymer has a Z-DNA like (Z_D) CD spectrum. Raman data are consistent with a left-handed structure different from Z_R-RNA. Limited bromination of poly[r(C-G)] results in modification of guanine C8 and cytosine C5, producing a form of the polymer that is stable in the Z_R conformation at much lower ionic strength than the unmodified polynucleotide. Extensive bromination results in stabilization of a form having a Z_D-like CD spectrum in 110mM NaCl or NaBr. Raising the ionic strength to 6M NaBr results in a cooperative reversible CD transition to a spectrum with more Z_R character. Raman scattering, ^{31}P and ^{1}H NMR all provide evidence for a left-handed form of the extensively brominated polymer in 110mM Na^+ buffer. Radioimmunoassays and filter-binding assays were performed to determine the extent of recognition of radiolabeled Br-poly[r(C-G)] by anti-Z-DNA IgGs. Anti-Br-poly[d(C-G)] antibodies specifically recognized one or more cross reacting determinant(s) on left-handed Br-poly[r(C-G)]. Therefore, a Z-DNA-like structural element is present in the left-handed RNA at physiological salt concentration. Thus, these spectroscopic and immunochemical studies demonstrate that under conditions of conformational strain (ie., bromination), Z-RNA can exist at physiological ionic strength.

W-PM-D4 DYNAMICAL STUDIES OF THE CONFORMATION STATES OF RF-ØX174 DNA-BaPDE ADDUCTS.
Hiroko Yoshida*, C.E. Swenberg, Division of Molecular Radiobiology, Armed Forces Radiobiology Research Institute, Bethesda, MD 20814; and N.E. Geacintov, Department of Chemistry, New York University, N.Y. 10003.

Changes in the conformational states of superhelical RF-ØX174 DNA following reactions with Benzo(a)pyrene-diolepoxide (BaPDE) were investigated by time dependence measurements of flow linear dichroism, circular dichroism and gel electrophoresis. Upon the intercalation of BaPDE followed by the formation of covalent binding, superhelical DNA was found to be unwound. The hydrolysis products of BaPDE, Bap tetraols, which also intercalate between the adjacent base pairs of DNA but do not form covalent binding to DNA, produced negligible unwinding. After the covalent modification of DNA with BaPDE a second backward kinetics, presumably rewinding of superhelicity, was observed utilizing flow linear dichroism. The backward kinetic was much slower than the time necessary for covalent binding. Unwinding and rewinding of supercoiled DNA was visualized by agarose gel electrophoresis and a new band between nicked and linear bands appeared as a concentration of BaPDE increased. Results of flow linear dichroism were consistent with circular dichroism measurements. The circular dichroism spectra showed a time dependent increase in the ellipticity at λ = 245 nm during the first five to six hours which subsequently decreased.
(*National Research Council Research Associate.)

W-PM-D5 DIFFERENTIAL CHEMICAL REACTIVITY OF DAUNOMYCIN TOWARD SPIN LABELED SYNTHETIC POLYNUCLEOTIDES. J. C. Ireland, E. V. Bobst, G. T. Pauly, and A. M. Bobst, Department of Chemistry, Cincinnati, OH 45221

Electron spin resonance (ESR) observable interactions of Daunomycin (DM) with site-specifically spin labeled nucleic acid monomers and site-specifically spin labeled single and double stranded synthetic polynucleotides were monitored at relatively high D/P ratios in 0.01 M sodium cacodylate, 0.01 M NaCl and 0.001 M EDTA, pH 7.2. Titration of pls^{4}U, a 4-thiouridylic acid spin labeled in position 4, with DM has no effect on the ESR lineshape and intensity at D/P ratios varying from 0 to 40. However, incorporation of pls^{4}U into the $(C)_n$ lattice to give $(1s^4U,C)_n$ with $1s^4U/C$ ratios of 0.015, 0.03, and 0.07, respectively, results in irreversible destruction of the spin label. Full loss of ESR intensity is determined for the spin labeled single strand RNA $(1s^4U,C)_n$ at a D/P ratio of 1.8 and the ratio does not depend on the amount of incorporated $1s^4U$. The spin labeled single strand DNA $(DUAP, dT)_n$ and the homopolymer DNA duplex $(DUAP, dT)_n(dA)_n$ have both completely lost their ESR signal at the same D/P ratio of 1.3. This suggests that high concentrations of DM readily denature the homopolymer duplex. On the other hand, the alternating copolymer $(DUAP, dT\text{-}dA)_n$ requires a significantly higher D/P ratio (D/P = 3.0) for a full destruction of the ESR signal (for the chemical structure of most spin labeled nucleotides, see Biochemistry 24, 5465 (1985)). It is hypothesized that the full irreversible chemical destruction of the covalently bound spin labels observed at high D/P ratios results from the formation of DM stacks along the single stranded nucleic acid backbone. $(DUAP,dT\text{-}dA)_n$ and $(DUAP,dT)_n(dA)_n$ have both the spin labels in the major groove of the duplex. The higher D/P ratio needed for the destruction of the spin labels in the alternating copolymer as compared to the homopolymer duplex suggests that the DM based destabilization of $(DUAP,dT\text{-}dA)_n$ requires a considerably higher drug concentration than the DM based destabilization of $(DUAP,dT)_n(dA)_n$.

W-PM-D6 OBSERVATION OF A METASTABLE Z CONFORMATION IN POLY(dG-m^{5}dC):POLY(dG-m^{5}dC). Fu-Ming Chen, Department of Chemistry, Tennessee State University, Nashville, Tennessee 37203.

Recent studies reveal that poly(dG-m^{5}dC):poly(dG-m^{5}dC), but not its unmethylated counterpart, exists as Z conformation in solutions containing very low NaCl concentration. A metastable Z conformation that exists in solutions containing low sodium concentrations that would normally favor the B conformation is described in this report. The existence of this metastable Z form further emphasizes the conformational lability of poly(dG-m^{5}dC):poly(dG-m^{5}dC). This metastable Z state is reached by an acid-base titration of a B-poly(dG-m^{5}dC):poly(dG-m^{5}dC) solution and is thermally very stable with direct melting into single strands at approximately 110 ^{o}C. In contrast, the B form DNA, initially in solutions of the same ionic strength (10 mM NaCl), but without exposure to acidic pH, exhibits a biphasic melting profile, with conversion into the Z form at about 52 ^{o}C and an eventual denaturation into single strands at around 110 ^{o}C. The metastable Z form binds ethidium more weakly than its B counterpart, and the ethidium induced Z to B conversion occurs in a step-wise fashion (converting about 7 base pairs for each drug bound) without the requirement of a threshold concentration. The metastable Z conformation is reversed by the addition of EDTA, suggesting the involvement of trace amounts of multi-valent metal ions.

W-PM-D7 CIRCULAR DICHROISM OF POLY(dG-dC).POLY(dG-dC) CHEMICALLY MODIFIED BY N-2-ACETYLAMINOFLUORENE [AAF] AND MITOMYCIN C [MC]*

John Sutherland[a], JoAnn Mugavero[a], Regina Santella[b], and Maria Tomasz[c]
[a]Biology Department, Brookhaven National Laboratory, Upton, NY 11973
[b]Institute of Cancer Research, Columbia University, New York, NY 10032
[c]Dept. of Chemistry, Hunter College of the City University of New York, New York, NY 10021

The CD of poly(dG-dC).poly(dG-dC) between 230 and 320 nm is approximately inverted when the polymer is covalently modified by both AAF and MC. These results have been interpreted as indicating that both AAF and MC cause poly(dG-dC).poly(dG-dC) to adopt the left-handed Z conformation. Independent data suggest that AAF can but MC cannot induce the Z conformation. We have extended measurements of the CD of poly(dG-dC).poly(dG-dC) modified by AAF (41% of the bases) and MC (24% of the bases) to 175 nm. For other molecules the CD below 200 nm has been a better indicator of double helical conformation than the longer wavelength CD. For the AAF modified polymer, we find a negative band at 195 nm, a feature characteristic of the Z form of poly(dG-dC).poly(dG-dC). In contrast, for the MC modified polymer, we find a large positive band at 187 nm, the feature characteristic of right-handed double helical structures of nucleic acids. Hence the CD below 200 nm, which is ten times greater in magnitude and hence less subject to interference of the CD of the AAF and MC chromophores, indicates the AAF complex is a left-handed and the MC complex is a right-handed double helix in agreement with the other types of data.

*Supported by the Dept. of Energy and the National Institutes of Health.

W-PM-D8 TWO-DIMENSIONAL NMR STUDIES OF CONFORMATIONS OF ALTERNATING AND HOMO POLYDEOXYNUCLEOTIDES IN SOLUTION. Babul Borah, Siddhartha Roy, Frank B.Howard, H.Todd Miles and Jack S.Cohen, CPB/NCI and LCP/NIADDK, National Institutes of Health, Bethesda, MD, 20892.

Proton two-dimensional nuclear Overhauser enhancement (2D-NOE) spectroscopy has been used to investigate the secondary structures of alternating and homo polydeoxynucleotide duplexes in solution. The effect of $2NH_2$ and 5-halogen substitution on a possible B-Z transition was investigated for double stranded poly (d2NH_2A-dT), poly(d2NH_2A-d5BrU) and poly(d2NH_2A-d5IU). The alternating polymers form a structure in high salt which is clearly distinct from the B-form present in the low salt conditions. The observed pattern of cross peaks in the 2D-NOE spectra indicate that the conformation of the high salt form is not left handed Z. The presence of significant base proton (H8,H6)-H3' cross peaks indicate a C3'-endo sugar conformation and anti glycosidic torsion for both components of the co-polymers. Correlations of observed 2D-NOE cross peaks and estimated inter-proton distances of the common DNA conformations are consistent only with an A form or closely related structure. This interpretation is also consistent with the negative CD band observed in the high salt form of the polymers and in A-form ribo-homopolymer helices containing $2NH_2$A.

2D-NOE spectra of the homopolymer poly(dA).poly(dT) in low salt show a relatively strong H8-H1' cross peak and differ in this respect from other B form homo and alternating polymers. Quantitative distance measurements however reveal that this homopolymer also adopts a B-like structure in solution with short internucleotide H8-H1' connectivities.

W-PM-D9 ARRANGEMENT OF PACKAGED BACTERIOPHAGE DNA. Philip Serwer, Department of Biochemistry, The University of Texas Health Science Center, San Antonio, Texas 78284.

Double-stranded DNA bacteriophages consist of an outer capsid of protein that contains the DNA genome within a volume twice that of the DNA. During assembly, a DNA-free capsid binds and packages the DNA. Toroidal winding of DNA in the capsid has previously been proposed (1,2). However, toroidal winding requires one rotation of the capsid relative to the DNA for every toroidal turn of the DNA, and also introduces the possibility of tangling, during both packaging and injection. To avoid these problems it is proposed that DNA is packaged in segments separated by 180° folds (kinks). The segments are continuously bent to follow the inner edge of the capsid, and there is one kink for every 360° turn. High affinity binding sites for ethidium bromide, present in the unrelated bacteriophages T7 and P22 (3,4), are candidates for kinks. The above hypothesis is consistent with the number of high affinity binding sites observed. This hypothesis is also consistent with: (a) the circular patterns of intraphage DNA observed by electron microscopy, (b) the x-ray diffraction data, (c) the observation that packaged segments of DNA increase their separation in deletion mutants and (d) the observation that all regions of bacteriophage λ DNA can be crosslinked to the λ capsid (2). Two segments and their mutual kink topologically resemble a loop such as those believed to occur in eukaryotic chromatin.

1. Harrison, S.C. (1983) J. Mol. Biol. 171, 577-580.
2. Widom, J. and Baldwin, R.L. (1983) J. Mol. Biol. 171, 419-437.
3. Griess, G.A., Serwer, P. and Horowitz, P.M. (1985) Biopolymers 24,1635-1646.
4. Griess, G.A., Serwer, P., Kaushal, V. and Horowitz, P.M. (1985) Biophys, J., in press.

W-PM-D10 HYDROPHOBIC INTERACTIONS AND SOLVENT INFLUENCES ON DNA CONFORMATIONS. R.L. Jernigan*, A. Sarai*, K.-L. Ting* and R. Nussinov† *NCI, NIH, Bethesda, MD 20205, † Permanent Address, Institute of Molecular Medicine, Sackler Faculty of Medicine, Tel Aviv University, Ramat Aviv, Israel

We have considered solvent effects on overall DNA conformations by looking at the surface exposures of polar and non-polar atoms in various forms. In addition we have explored possibilities of sequence dependent local conformation variations. In particular such effects can be both electrostatic and hydrophobic in origin and lead to a variety of conformers. In the case of hydrophobic interactions, we considered interactions among aliphatic hydrocarbon groups in A/T sequences. The slightly overwound sequences $(T)_n \cdot (A)_n$ yield structures with small bends and tightly stacked methyl groups along one side of the major groove. The sequence TTAA may yield a sharp bend by folding together the two pairs of stacked methyls on the opposite sides of the major groove. Thus a sequence can affect the formation of either a smooth bend or a sharp kink. The origin of the dipole moment along the helix axis is also being studied. These sequence dependent local conformations may be related to a number of biological results.

W-PM-D11 THEORETICAL STUDIES OF LOCALLY CONSTRAINED STRUCTURES. Nancy L. Marky and Wilma K. Olson, Wright Chemistry Laboratory, Rutgers University, New Brunswick, New Jersey 08903.

Statistical mechanical methods and Monte Carlo techniques have been used to determine the likelihood of occurrence, the thermodynamic stability, and the conformational flexibility of various structural perturbations in helical DNA and RNA. The disturbances include single-stranded hairpin loops, extra helical bulges, non-hydrogen bonded internal loops, and junctions of three or more branched single-stranded chains. These changes are involved in processes such as breathing, transcription, replication, drug intercalation, drug binding and others. Chain statistics, developed and applied on the sugar-phosphate backbone parameters, have been accompanied by a treatment focusing on base morphology. This last approach has been designed to treat the spatial dislocation of a base from an orderly helical structure. In some cases, base sequence dependence has been included. Configurational averages, density distributions, including higher order moments of parameters, and free energies of these structures have been obtained as a function of the occurrence of these perturbations along the chain. (Supported by U.S.P.H.S. Grant GM-20861 and GM-34809-01).

W-PM-D12 A UNIQUE MODEL OF FOUR-STRANDED DNA SYNAPSIS DURING HOMOLOGOUS RECOMBINATION
R. C. Hopkins, University of Houston - Clear Lake, Houston, Texas 77058

The recent results of Griffith & Nash [1] using products from an in vitro recombination system from bacteriophage λ have far-reaching implications for the detailed topology of the synaptic intermediate involved. Two models of four-stranded synapsis between homologous segments from two DNA duplexes have appeared as likely candidates for this intermediate: 1.) the association of two homologous Watson-Crick (Configuration I) duplexes across their major grooves [2], and 2.) the association of two homologous Watson-Crick duplexes across their minor grooves followed by melting and reannealing to produce a region of heteroduplex DNA [3]. Significantly, the topological results [1] are consistent only with the relative strand orientations (5' → 3' chain directions) of the second model. There is, however, a third model which is also consistent with these results: 3.) the association of two homologous Configuration II duplexes across their major grooves [4] as shown below. In this latter model, specific hydrogen bond pairing between identical base pairs provides a mechanism by which homology in the two duplexes can be recognized.

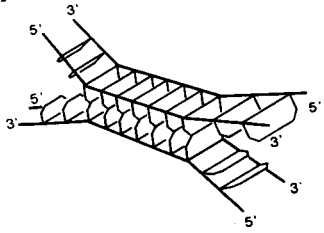

Supported by grant E-889, Robert A. Welch Foundation.

1. Griffith, J.D. & H.A. Nash (1985) PNAS 82, 3124.
2. McGavin, S. (1971) J. Mol. Biol. 55, 293.
3. Wilson, J.H. (1979) PNAS 76, 3641.
4. Hopkins, R.C. (1984) Comments Mol. Cell. Biophys. 2, 153;
(1985) Prog. Clin. Biol. Res. 172, 299.

W-PM-E1 FORMYL-METHIONYL-LEUCYL-PHENYLALANINE (fMet-Leu-Phe) RECEPTOR-COUPLED CALCIUM TRANSPORT IN HUMAN NEUTROPHILS: IDENTIFICATION OF DIHYDROPYRIDINE RECEPTORS. Kim C. Williamson, Alfred I. Tauber and Javier Navarro. Depts. of Physiology, Medicine & Biochemistry, Boston Univ. School of Medicine, Boston MA 02118.

Employing a Dowex column procedure, we have found that chemotactic agent, formyl-methionyl-leucyl-phenylalanine (fMet-Leu-Phe) stimulated calcium uptake in human neutrophils. The calcium uptake was linearly proportional with time and cell density. The uptake of calcium by fMet-Leu-Phe stimulated human neutrophils consists of at least two components, one of which is sensitive to dihydropyridine derivatives. Inhibition by dihydropyridine derivatives showed the rank order of nisoldepine$\rangle$nitrendipine$\rangle$nimodepine$\gg$Bay K 8644. The nisoldepine sensitive calcium uptake exhibited an ID_{50} of 1.5 μM and maximal inhibition was observed at 5 μM. Neither calcium efflux or [^{3}H] fMet-Leu-Phe binding was affected by nisoldepine up to 10 μM. The inhibition by nisoldepine was inversely proportional to the extracellular calcium concentration. Dihydropyridine receptors have been identified in intact neutrophils by employing the dihydropyridine radioligand [^{3}H] methyl-PN 200-110. The specific binding of [^{3}H] methyl-PN 200-110 was saturable and reversible, and the Scatchard plot of the specific binding revealed a nonlinear pattern. Assuming a two-site binding model, we have estimated a high affinity component with a Kd_1 of 21.4 nM and a low affinity component with a Kd_2 of 890 nM. The latter component appears to be in good agreement with the ID_{50} for the inhibition of the fMet-Leu-Phe receptor activated calcium channels. Our data is consistent with the hypothesis that dihydropyridine receptors in neutrophils are linked to calcium channels activated by the fMet-Leu-Phe receptor. The results also support a functional and structural homology between receptor and voltage-dependent calcium channels.

W-PM-E2 [^{3}H] PN 200-110 RECEPTORS IN CONTRACTING MYOTUBES FROM CHICK EMBRYO PECTORALIS MUSCLE. J. Navarro. Dept. of Physiology, Boston Univ. School of Medicine, Boston, MA 02118.

This work describes the properties of the dihydropyridine receptor in skeletal muscle cells containing functional calcium channels. It employed the new dihydropyridine calcium channel antagonist [^{3}H] PN 200-110 and cultured myotubes obtained from chick embryo pectoralis muscle. The [^{3}H] PN 200-110 binding to myotubes was specific, saturable and reversible. Good agreement was observed in the K_d of the [^{3}H] PN 200-110 receptor complex determined by equilibrium (1.20 nM) and kinetic (1.46 nM) methods and displacement (1.78 nM) with unlabeled PN 200-110. These findings support the concept of ligand binding to a single population of high affinity sites. This K_d value, however, was one order of magnitude higher than the K_d for the binding of [^{3}H] PN 200-110 to isolated t-tubules membranes. PN 200-110 and nisoldepine were 200 times more potent than the dihydropyridine calcium channel agonist Bay K 8644 in the inhibition of [^{3}H] PN 200-110 binding to myotubes. Whereas the apparent Hill coefficient (nH) for PN 200-110, nisoldepine and nitrendipine was near 1, the nH for Bay K 8644 was 0.64. The antiarrhythmic drug verapamil produced partial inhibition of [^{3}H] PN 200-110 binding, whereas diltiazem was without effect. A particularly important finding was that micromolar concentrations of extracellular inorganic calcium channel antagonists Cd^{2+} (5 μM) and Mn^{2+} (32 μM) enhanced the binding of [^{3}H] PN 200-110, suggesting the presence of a metal cation binding site with relatively high affinity at or in the vicinity of the dihydropyridine receptor. The presence or absence of extracellular Ca^{2+} or Mg^{2+} apparently did not affect [^{3}H] PN 200-110 binding. (This work was supported by NSF grant DCB-8511671.)

W-PM-E3 PARTIAL RECOVERY OF CALCIUM CHANNELS FROM THE PURIFIED DIHYDROPYRIDINE-BINDING PREPARATION OF SKELETAL MUSCLE. Roberto Coronado, Jeffrey S. Smith and Susan L. Hamilton. Departments of Pharmacology and Biochemistry, University of North Carolina, Chapel Hill, NC 27514, and Department of Physiology and Biophysics, University of Texas Medical Branch, Galveston, TX 77550.

The purified dihydropyridine-binding protein complex (DHP's) described by Borsotto et al (BBRC 122:1357-1366, 1984) was incorporated into planar bilayers in order to test for the presence of active calcium channels. In our hands the preparation consists of three major bands of apparent MW 165,000; 50,000 (diffuse band); and 40,000; and a number of additional minor bands. Barium-selective channels recovered from purified DHP's are similar to calcium channels previously reported from native t-tubule vesicles (Affolter and Coronado, Biophys. J. 48:341-347, 1985) in a) unitary currents of 0.2 - 1.2 pA in the range of -30 mV to +20 mV in 100 mM Ba; b) a divalent-monovalent selectivity , P_{Ba}/P_{Na} = 25, calculated from reversal of single channel currents; and c) a voltage-dependence that activates the channel with cis-positive potentials (side of DHP's addition). They differ however, in their lack of sensitivity to dihydropyridine antagonists. A complicating factor in this preparation of DHP's is the presence of unacceptably high levels of chloride and potassium-conducting channels that mask the small unitary barium currents. In all likelihood these contaminants copurify with the DHP proteins. Thus, from a functional standpoint this preparation is more heterogeneous than anticipated on the basis of binding activity. Supported by NIH grants GM 32824 and HL 32935. (Abstract Introduc. by Sharmila Gupte)

W-PM-E4 HIGH AFFINITY BLOCK OF OPEN Ca CHANNELS BY NIMODIPINE IN RAT ANTERIOR PITUITARY CELLS. C.J. Cohen and R.T. McCarthy, Miles Inst. Preclin. Pharmacol., New Haven, CT

GH_4C_1 rat anterior pituitary cells have 2 types of Ca channels, called "transient" and "slowly inactivating". Nimodipine blocks only the slowly inactivating channels with high affinity [Cohen and McCarthy, Biophys. J. 47, 513a]. The effect of channel gating on drug binding was studied with the whole cell variation of the patch electrode voltage clamp technique. High affinity block is promoted by long depolarizations. This block is observed even when Ca induced inactivation is minimized and there is little or no inactivation during the control depolarization. A comparison of the voltage dependence of steady-state nimodipine block with the voltage dependence of channel activation indicates that channel block is directly proportional to the number of open channels. The results are accounted for by a model that postulates 1:1 high affinity drug binding only to open Ca channels. The K_d for binding to open channels is 517 pM; the K_d for binding to resting state channels is ≅7 μM. The rate of onset of nimodipine block increases with the test potential, such that the rate of block is proportional to the fraction of open channels. The on rate for binding to open channels is 9.6×10^7 M^{-1} s^{-1}; the off rate is 0.050 s^{-1}. Nimodipine block of the transient Ca channels is also modified by channel gating. 2 μM drug causes little or no resting state block, but approximately doubles the rate of current decay during a test pulse. This suggests that binding is enhanced by channel activation. 100 nM nimodipine has little or no effect on the steady state availability of the transient Ca channels. As inferred by studies of ligand binding and high K induced hormone secretion and ^{45}Ca influx, nimodipine can block Ca channels with high affinity in endocrine cells.

W-PM-E5 SENSITIVITY OF TWO TYPES OF CALCIUM CHANNELS TO INORGANIC AND ORGANIC BLOCKERS IN GUINEA PIG VENTRICULAR MYOCYTES. R. Mitra & M. Morad, Dept. of Physiol.,Univ. of PA, Phila., PA

We have provided whole cell voltage clamp evidence for two types of Ca channels in guinea pig ventricular myocytes based upon activation voltage, inactivation kinetics, and pharmacological sensitivities (Mitra & Morad,J. Gen. Physiol., 86:22a,1985). Single channel data from the same preparation has also been reported (Nilius et al., Nature, 316:443,1985). These two channels can also be distinguished by increasing the stimulation frequency (sf) from 0.2 to 1.0 Hz: the current through the low threshold channel decreases by about 40% while the current through the high threshold channel increases slightly. In this report we investigated the sensitivity of each channel to organic & inorganic blockers: D600,diltiazem,nifedipine, Mn^{2+},Co^{2+},Ni^{2+},Cd^{2+}, Ce^{3+}In experiments with D600 & diltiazem using sf of 0.25 to 0.5 Hz, the membrane was held at -65 mV and pulsed to -30 mV, where the low threshold channel is activated, and +10 mV where the high threshold channel is activated. Both drugs suppressed the high threshold Ca current but had no significant effect on the low threshold current. Nifedipine was rapidly photo-inactivated (morad et al.,Nature, 304:635, 1983) and revealed that only the high threshold current was unblocked. All the inorganic ions tested blocked the high threshold channel in order of potency : $Ce^{3+} \geq Cd^{2+} \gg Ni^{2+} \geq Co^{2+} \geq Mn^{2+}$. At high concentrations both channels could be suppressed. Differential sensitivity of the block by these cations could be shown at lower concentrations. When $(Ca^{2+})_o$ = 15mM, both $Ce^{3+}$and Cd^{2+}(150uM) blocked more than 90% of the high threshold channel, but failed to block the low threshold channel significantly. Higher concentrations of Ni^{2+}, Co^{2+}, and Mn^{2+}were required (5mM) to block the high threshold channel. Only Ni^{2+} appeared to suppress the low threshold channel significantly.

W-PM-E6 PHORBOL ESTER PROMOTES A LARGE CONDUCTANCE CA CHANNEL IN APLYSIA BAG CELL NEURONS. J.A.Strong, A.P.Fox, R.W.Tsien, and L.K.Kaczmarek. Depts. Pharm. & Physiol., Yale Univ. Sch. of Med., New Haven, CT. Protein kinase-C (PK-C), a Ca/phosphatidylserine/diacylglycerol-dependent enzyme found in high concentrations in mammalian brain, is also found in nervous tissue of the mollusc Aplysia. Previous whole-cell voltage clamp experiments demonstrated that activation of PK-C by the phorbol ester TPA (12-O-tetradecanoyl-phorbol-13 acetate) enhanced the magnitude of the calcium current in Aplysia bag cell neurons maintained in primary culture. We now report that TPA promotes the appearance of a new class of inward channel in these neurons. Single channel, cell attached recordings were made using Ba as the inward current carrier. A small (10 pS) inward channel (left panel) was seen in control cells. Cells pretreated with TPA (10–100 nM) contained in addition a larger, more active 23 pS inward channel (right panel). This channel was rare or absent in control cells. Both channels were voltage-dependent and activated near -20 mV, in agreement with whole-cell recordings.

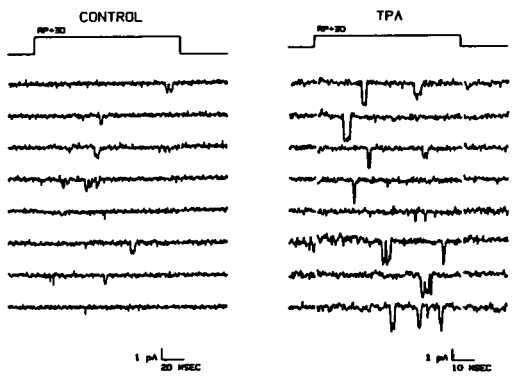

W-PM-E7 PERMEATION AND GATING OF CARDIAC AND SKELETAL MUSCLE Ca CHANNELS IN LIPID BILAYERS
R.L. Rosenberg*, P. Hess*, H. Smilowitz+, J.P. Reeves# and R.W. Tsien*. *Dept. of Physiology, Yale Univ., +Dept. of Biochemistry, Univ. of Connecticut-Farmington, #Roche Inst. of Molecular Biology.

We have incorporated Ca channels from bovine cardiac sarcolemma into planar lipid bilayers (PE:PS, 1:1) and have found single channel activity very similar to that seen in intact cells. In the presence of 1 μM Bay K 8644, depolarization to +10 mV evoked inward unitary Ba currents of ~1.2 pA and ~16 ms mean open time (Fig). The average current showed characteristic time- and voltage-dependent activation and inactivation. Openings were abolished by 6 μM nimodipine. External Cd produced flickery block (K_i ~30 μM). Under matched ionic conditions, I-V curves from bilayers agreed closely with those from cell-attached patches (Fig). Large outward K currents gave rise to an inflected, asymmetric I-V curve. With 100 mM Ba plus 50 mM Na on both sides, the I-V was linear between -60 mV and +140 mV with a slope of 23 pS. Under identical conditions, Ca channels from rabbit skeletal muscle T-tubules had conductances of only 11 pS. We conclude that (1) in the cell-free environment cardiac L-type Ca channels can activate and inactivate normally, (2) in symmetric solutions the Ca pore is functionally symmetric, and (3) cardiac and skeletal Ca channels have different unitary conductances despite common dihydropyridine sensitivity.

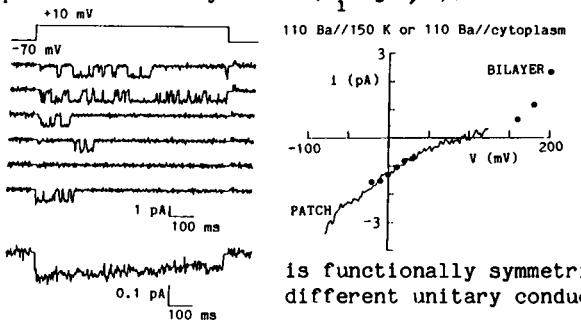

W-PM-E8 THE PEPTIDE TOXIN wCgTX BLOCKS PARTICULAR TYPES OF NEURONAL CA CHANNELS. E.W. McCleskey+, A.P. Fox+, D. Feldman*, B.M. Olivera*, R.W. Tsien+ & D. Yoshikami* *Dept. of Biology, University of Utah and +Dept. of Physiology, Yale University.

The effects of wCgTX, a 27-amino acid peptide from Conus geographicus venom, were tested on three types of Ca channels in chick dorsal root ganglion neurons. Voltage protocols evoked pure T current (a), pure L current (c), or a combination of T, N, and L currents (b). Brief application of toxin (*) produced persistent block of L current (c), N current (b) but not T current (a). The block of L and N current lasts at least an hour whereas T currents are only weakly and transiently reduced. The toxin also blocked some but not all Ca current in rat hippocampal cells but failed to produce persistent block of Ca currents in Aplysia bag cells, guinea pig and frog heart cells, and chick skeletal myotubes; wCgTX distinguished between L-type Ca channels in heart cells and neurons with otherwise similar kinetic and pharmacological properties. A cytoplasmic second messenger mechanism or internal site of action is unlikely since channels isolated in cell-attached patches were protected from block by toxin applied to the rest of the cell. Block of unitary currents was seen with external wCgTX application to outside-out patches. Since block is rapid, persistent, external and selective, wCgTX might be a useful ligand for purification and localization of particular types of neuronal Ca channels.

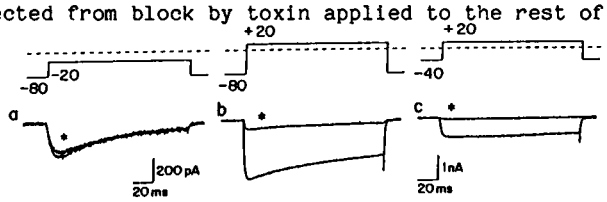

W-PM-E9 INHIBITION OF CALCIUM CHANNELS FROM PARAMECIUM CILIA BY ANALOGUES OF W-7. B.E. Ehrlich, M. Forte*, A.R. Jacobson+, L.M. Sayre+. Department of Physiology, Albert Einstein College, Bronx, NY, Department of *Biology and +Chemistry, Case Western Reserve University, Cleveland, OH.

Calcium (Ca) channels from Paramecium are similar to one class of metazoan Ca channels in that the protozoan channels are insensitive to the organic Ca channel blockers dihydropyridines, verapamil, and diltiazem. Recently it was shown that W-7, an anti-calmodulin agent, blocks the Ca-dependent avoiding behavior and Ca currents in intact Paramecium (Hennessy and Kung, J. Exp. Biol., 110:169 (1984)). We have found that W-7 also blocks Paramecium Ca channels that have been incorporated into planar lipid bilayers. Complete block is obtained with 100 uM W-7 in bilayer experiments and in intact cells. With the goal of finding more potent blocking agents, we synthesized analogues of W-7 (see figure). The effectiveness of the analogues was assayed from behavioral and bilayer experiments. As shown previously, removal of the chlorine decreases the sensitivity 5 fold. However, by increasing the chain length from 6 to 12 (at arrow) the concentration needed to completely block the channels returns to 100 uM. In addition, we found that increasing the chain length to 12 and exchanging the chlorine for bromine increases the potency 100 fold. Most likely this effect of W-7 is not via calmodulin, since blockade is obtained in the absence of calmodulin.

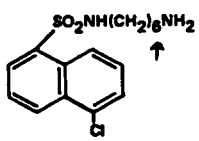

Supported by NSF grant DCB83-09110, American Heart Association grant 83990 and a NY Heart Association Grant-in-Aid. BEE is a NY Heart Association Young Investigator.

W-PM-E10 THE ENANTIOMERS OF BAY K 8644 HAVE DIFFERENT EFFECTS ON Ca CHANNEL GATING IN RAT ANTERIOR PITUITARY CELLS. R.T. McCarthy and C.J. Cohen, Miles Inst. Preclin. Pharm., New Haven, CT

BAY K 8644 has multiple effects on Ca channel gating in myocardial cells, so that Ca currents and twitch tension are either increased or decreased, depending upon the pattern of electrical activity. Analysis of the drug channel interaction was simplified in two ways: 1) each enantiomer was studied separately, since they have different effects on tension and APD in ventricular cells [Frankowiak et al., Eur. J. Pharmacol. 114:223]; 2) effects on activation were separated from those on inactivation by studying Ba currents in GH3 rat anterior pituitary cells: GH3 cells have two types of Ca channels; only one type binds dihydropyridines with high affinity and Ba currents through these channels inactivate very little or not at all. The (-)-(4S) isomer of BAY K 8644 (a positive inotropic agent) preferentially affects the slowly inactivating Ca channels. The voltage dependence of channel activation is shifted to more negative potentials and the rates of channel activation and deactivation are slowed. While the racemic mixture decreases slowly inactivating Ca channel currents during long lasting strong depolarizations, the (-) isomer alone does not. The (+)-(4R) isomer has effects on the slowly inactivating Ca channels similar to those of nimodipine (see accompanying abstract). The rates of channel activation and deactivation are not affected. Channel block is greatest during long lasting depolarizations. The results are accounted for by preferential binding to open channels, with a K_d of $\cong$4 nM for the open state and >1 μM for the resting state. The (+) isomer also blocks the transient Ca channels. Block of these channels is enhanced by channel inactivation. The K_d for binding to channels in the inactivated state is $\cong$50 nM, but >1 μM for channels in the resting state.

W-PM-E11 MULTIPLE TYPES OF CALCIUM CHANNELS IN ACUTELY-EXPOSED NEURONS FROM ADULT HIPPOCAMPUS. Rick Gray and Dan Johnston. Neuroscience Program, Baylor Col. Med., Houston, TX

We have been studying macroscopic calcium currents and their modulation by β-adrenergic agonists in exposed neurons from guinea pig hippocampal slices (Gray & Johnston, Biophys. J. 47:66a, 1985). During these investigations, we have observed that inward currents were detectable only during step commands from -100 mV to potentials more positive than about -35 mV. Also, the whole-cell calcium currents appeared to inactivate partially, even with 10 mM EGTA inside the cell and with Ba as the charge carrier, suggesting that some component of the current is transient. In light of these observations and the recent report of multiple types of Ca channels with different gating characteristics in cultured neurons (Nowycky, Fox & Tsien, Nature 316:440, 1985), we have begun to measure single-channel currents in our system.

Acutely-exposed neurons were prepared as described elsewhere (Gray & Johnston, J. Neurophysiol. 54:134 1985) and were patch-clamped in the cell-attached configuration with 110 mM $BaCl_2$ in the pipette and 140 mM K-aspartate in the bath. Patches were held at -90 mV and depolarizing command pulses applied. The amplitudes of unitary currents at different command potentials were used to construct single-channel I-V plots. We have observed single channels with three slope conductances: 7-8 pS; 13-15 pS and, in one patch, 27 pS. The 7-8 pS channel appeared more transient in nature than the others, with openings clustered near the onset of the step. Individual patches generally contained only one type of channel, although some patches contained multiple channels of the same type. Future experiments will be directed at finding which of these channels are modulated by β-adrenergic receptors. (Supported by NS11535, NS15772, and AFOSR 85-0178).

W-PM-E12 IDENTIFICATION OF SEVERAL TYPES OF VOLTAGE AND/OR Ca ACTIVATED CHANNELS IN A PANCREATIC BETA CELL LINE. D.R. Matteson and F.M. Matschinsky, University of Pennsylvania, Philadelphia, PA.

We have performed voltage-clamp experiments, utilizing the patch clamp technique, on a clonal line of pancreatic beta cells, the HIT cell line which was previously developed from SV-40 transformed hamster pancreatic islet cells. The whole-cell variation of the patch clamp technique was used to identify voltage-dependent channels. Inward currents, isolated by filling patch electrodes with n-methyl glucamine or cesium, are carried by Ca and Na channels. Ca current, studied in the presence of TTX, was found in nearly all cells. When 2 mM MgATP was included in the pipette, Ca current magnitude was stable for up to 45 min, while in the absence of ATP the current declined rapidly within a few min. Ca current is largest during steps to +10 mV, where it averaged 0.24 nA in 11 cells bathed in 10 mM Ca. Some HIT cells had a TTX sensitive transient inward current which was due to the activity of Na channels. Activation threshold for Na channels is near -40 mV and the channels are half maximally activated at -5 mV. Voltage-dependent K currents were studied using patch pipettes filled with (in mM) 105 Kglutamate, 25 KF, 10 KCl, 10 EGTA and 10 Hepes. After K channel activation, using 400 ms steps to positive potentials (40 to 80 mV), the current remained stable throughout the step, indicating that the channels do not inactivate. These K channels were blocked either by external TEA or quinine. In addition to these voltage-dependent channels, we have also identified a large conductance voltage- and Ca-activated K channel in HIT cells, using isolated inside-out patches. With 145 mM K on both sides of the patch, this channel has a single channel conductance of about 250 pS. The activity of the channel was nearly abolished by decreasing the Ca concentration at the intracellular surface of the patch to 10^{-8}M.

W-PM-E13 **H^+ IONS BLOCK AND SHIFT GATING OF CA^{+2} CHANNELS IN RAT VENTRICULAR MYOCYTES.**
D.S. Krafte and R.S. Kass, Dept. of Physiology, Univ. of Rochester, Rochester, NY 14642.

We measured the influence of external pH on Ca^{+2} channel current in isolated rat ventricular myocytes using whole cell patch clamp techniques. Ca^{+2} channel currents were isolated by using intra- and extracellular Cs^+ solutions, TTX, and choice of holding potentials. Intracellular Ca^{+2} and H^+ were buffered with EGTA and HEPES. Decreasing extracellular pH(pH_o) resulted in a decrease in the magnitude of Ca^{+2} channel currents, consistent with previous studies, while extracellular alkalinization increased current magnitude. This alkalinization-induced increase indicates there may be H^+ inhibition of Ca^{+2} channels at pH of 7.4. The reduction in current was due in part to a gating shift which was examined over a pH range of 10.0 to 5.2. We found the maximum shift in gating, approximately 20 mV, saturated near pH 5.5. Gating shifts, however, were not sufficient to completely account for the depression of current as pH_o was lowered because acidification beyond pH 5.5 reduced currents in excess of that predicted by shifts in gating. Changes in selectivity were not a significant factor. This reduction in current appeared to be due to actual block of the channel, and inward current appeared to be blocked more effectively than outward current. Different sites may be involved in gating shifts and block.

W-PM-E14 Ca CHANNELS IN RAT PITUITARY CELLS: KINETIC PROPERTIES AND 'WASHOUT' UNDER WHOLE-CELL RECORDING.
Gabriel Cota and Clay M. Armstrong, Department of Physiology, University of Pennsylvania, School of Medicine, Philadelphia, PA 19104.

Cells were dispersed from the pars intermedia of adult male rats, and kept 1-8 days in culture. Na, K and Ca channels are present in these cells (Cota & Armstrong 1985, Biol. Bull., vol. 169). Ca currents were studied at 20°C using whole-cell recording with patch pipettes (holding potential -80 mV). The external//internal recording solutions contained (mM) 115 NaCl, 25 TEA-Cl, 10 $CaCl_2$ and 1-5 μM-TTX//80 Cs-Glu, 30 NMG-Glu, 20 CsCl, 20 CsF, 2 $MgCl_2$ and 10 EGTA (pH 7.30). As in GH_3 cells (Armstrong & Matteson 1985, Science, vol. 227), two main populations of Ca channels, FD and SD, were distinguished. These two populations differed in apparent activation level (-40 mV, SD; -10 mV, FD), half-maximal activation level (+7 mV; +23 mV), half-time of activation at +20 mV (2-3 ms; 1.0-1.5 ms), time course and degree of inactivation at +20 mV (fast, full; slow, partial) and closing time constant at -80 mV (1.5-2.0 ms; 0.10-0.15 ms).

Functional FD channels were almost completely lost within 20-25 min after breaking into the cell, while SD channels remained practically unmodified. Surprisingly, the FD tail current after steps to +70 mV decreased by 55-75% within 10 min under whole-cell recording while it only decreased by about 20% after steps to +10 mV. This suggests that the activation curve for FD channels may shift towards more negative membrane potentials as a function of time. If so, the same basic mechanism (probably a dephosphorylation process) may explain the loss of functional FD channels and the shift in their activation curve since both effects were prevented by the addition of 3 mM Mg-ATP and 40 μM-GTP to the internal solution. Alternatively, the 'voltage dependence' in the rate of washout may be due to the presence of more than one type of FD channel.